Boundary renormalisation group flows in supersymmetric conformal minimal models

Doktori értekezés

Kormos Márton

ELTE Fizika Doktori Iskola /vez.: Horváth Zalán/
Részecskefizika és csillagászat program /vez.: Csikor Ferenc/

Témavezető: Takács Gábor, Ph.D.
tudományos főmunkatárs

ELTE Elméleti Fizikai Intézet

2007. május

First I would like to thank my family for their encouragement and continual help. I am also grateful to the ELTE Theoretical Physics Department for the many things I have learnt and for the familiar and friendly atmosphere. I am very thankful to my supervisor, Gábor Takács, for his attentive leading and for the interesting and inspiring discussions.

Contents

Chapter 1

Introduction

The field of two dimensional quantum field theories is an important research area of theoretical physics. One reason for this is that they can serve as a model for many phenomena occurring in realistic quantum field theories which are difficult to study in the original theory due to the strength of the interaction. They are also useful in investigating conceptual problems and testing various computational methods. There are models in two dimensions, called integrable models, that are exactly solvable, but there exist powerful methods for investigating non-integrable models as well.

Beyond their role as toy models, two dimensional field theories also have important direct applications. They play a central role in formulating string theory: they describe the dynamics of the string on the world sheet. From this point of view the models with boundary are especially interesting, since these are important in the study of non-perturbative objects of string theory, the D-branes [AS02].

Apart from their applications in string theory there are many problems in condensed matter physics that can be described using two dimensional quantum field theories. Some important examples are the Kondo effect [Aff95, FLS96] and the effect of impurities on transport processes in general [Sal98, Sal00, CSS02, CSS03], behaviour of the edge states in the fractional quantum Hall effect, problems concerning spin chains, polymers, carbon nanotubes etc.

Conformal field theory offers an important class of integrable theories in which in principle all the correlation functions are known. Furthermore, it establishes an important link between quantum field theory and statistical mechanics. Two dimensional critical systems undergoing a second order phase transition are described by conformal field theories. In addition, there exist powerful techniques for investigating systems away from the critical point. In many cases these can be thought of as perturbed conformal field theories when some kind of perturbation breaks conformal invariance by introducing a mass scale and inducing a renormalisation group flow. Conformal perturbation theory is a possible approach to this problem. There is an important class of perturbations that leave the model integrable. In this case exact non-perturbative analysis can be done, for example applying the Thermodynamic Bethe Ansatz method.

This dissertation contributes mainly to the theoretical understanding of the two dimensional quantum field theories, but it is motivated by the applications mentioned above. The main goal is the exploration of the renormalization group flows in supersymmetric theories.

The problem of boundary renormalization group flows can be formulated as follows. We add a local perturbation on the boundary to a conformally invariant (critical) system. Since the system remains critical except for the boundary, the final fixed point of the renormalization group flow will be another critical boundary condition. Our task is to describe and classify these flows in terms of the initial boundary condition and the perturbation, and to give the final critical boundary condition. We focus on the minimal models from the family of the supersymmetric theories.

The investigation of these flows can provide a non-perturbative understanding of the impurity problems. For example, in the Kondo effect the interaction between the electrons and the quantum impurity is renormalised to infinity as temperature goes to zero. Understanding the thermodynamic properties (specific heat, resistance) of the system at low temperatures requires a non-perturbative description of the boundary interaction. In superstring theory the renormalisation group flow generated by a boundary perturbing field corresponds to tachyon condensation and exploring these flows can help in understanding the decay of D-branes [HKM00].

In the investigation of the boundary flows our main tool will be a numerical method, the Truncated Conformal Space Approach (TCSA). The main idea is to diagonalise the exact Hamiltonian on a finite dimensional subspace of the Hilbert space. The generalisation of this approach for perturbed superconformal minimal models is a new result of the author. For integrable flows we will use the Thermodynamic Bethe Ansatz as well.

The thesis is organised as follows. In the next chapter we give a brief summary of the main concepts and techniques of this research area, conformal field theory, superconformal field theory in the presence of boundaries, boundary TCSA and boundary TBA. Chapter 3 deals with the boundary flows of the unitary superconformal minimal models. Based on TCSA results and former theoretical predictions we give the general rules for all flows generated by a certain perturbing operator. In Chapter 4 we investigate and obtain new results on the reflection factors and the boundary flows of a non-unitary superminimal model, the supersymmetric scaling Lee-Yang model.

Chapter 2

Boundary conformal field theory and boundary renormalisation group flows

2.1 Conformal Field Theory

Conformal transformations are mappings $\mathbf{x} \to \mathbf{x}'$ that leave the metric tensor invariant up to a local rescaling:

$$g'_{\mu\nu}(x') = \Omega(x) g_{\mu\nu}(x)\,. \tag{2.1.1}$$

Conformal transformations are locally a combined rescaling and rotation, thus they preserve angles.

The reason why conformal symmetry is so powerful in two dimensions is that the algebra of *local* infinitesimal conformal transformations is infinite dimensional[1]. In general these transformations are not defined on the whole plane.

The two-dimensional plane can be equipped with Minkowski or Euclidean metric. Here we consider flat two-dimensional Euclidean space. It is useful to introduce complex coordinates by identifying the Euclidean space with the conformal plane:

$$z = x + iy\,, \qquad \bar{z} = x - iy\,. \tag{2.1.2}$$

Since analytic functions automatically preserve angles, a general infinitesimal conformal transformation can be written as $z \to z + \varepsilon(z)$ where $\varepsilon(z)$ is an analytic function. The group of global conformal transformations that are well-defined on the entire Riemann sphere are of the form

$$z \to \frac{az+b}{cz+d}\,, \qquad ad - bc = 1\,. \tag{2.1.3}$$

[1] In dimensions greater than two it is finite dimensional.

The group of these transformations is locally isomorphic to the finite dimensional Lie group $\mathrm{SL}(2,\mathbb{C})$.

Every conformal transformation $w = f(z)$ locally looks like a combined rescaling and rotation. In the construction of the CFT those fields which are only sensitive to this local behaviour play a central role. These fields are called *primary* and their transformation properties depend only on the first derivative of f:

$$\phi(z,z^*) \xrightarrow{w=f(z)} f'(z)^h (f'(z)^*)^{\bar{h}} \phi(f(z), f(z)^*) \tag{2.1.4}$$

where h and $\bar{h}$ are called the left and right conformal weight of the primary field $\phi(z,\bar{z})$. In particular, for a combined rotation and rescaling $z \to w(z) = re^{i\theta}z$ this implies

$$\phi(z,z^*) \longrightarrow r^{h+\bar{h}} e^{i\theta(h-\bar{h})} \phi(w(z), w(z)^*)\,, \tag{2.1.5}$$

so the scaling dimension is given by $(h+\bar{h})$ while the spin is $(h-\bar{h})$.

The infinitesimal version of transformation rule (2.1.4) is

$$\delta\phi(z,z^*) = \left[h\varepsilon'(z) + \varepsilon(z)\partial_z + \bar{h}\varepsilon'(z)^* + \varepsilon(z)^*\partial_{\bar{z}}\right]\phi(z,z^*)\,. \tag{2.1.6}$$

Those fields that transform under *global* conformal transformations like the primary fields (2.1.4) are called *quasi-primary*. Every primary field is quasi-primary of course. The one, two and three point correlation functions of these fields are fixed by global conformal invariance:

$$\langle\phi_i(z,\bar{z})\rangle = \delta_{h_i,0}\cdot A_i\,, \tag{2.1.7a}$$

$$\langle\phi_i(z,\bar{z})\phi_j(w,\bar{w})\rangle = \delta_{h_i,h_j}\delta_{\bar{h}_i,\bar{h}_j}\cdot\frac{B_{ij}}{(z-w)^{2h_i}(\bar{z}-\bar{w})^{2\bar{h}_i}}\,, \tag{2.1.7b}$$

$$\begin{aligned}\langle\phi_i(u,\bar{u})\phi_j(v,\bar{v})\phi_j(w,\bar{w})\rangle = C_{ijk}\cdot\frac{1}{(u-v)^{h_{kij}}(u-w)^{h_{jik}}(v-w)^{h_{ijk}}}\\ \cdot\frac{1}{(\bar{u}-\bar{v})^{\bar{h}_{kij}}(\bar{u}-\bar{w})^{\bar{h}_{jik}}(\bar{v}-\bar{w})^{\bar{h}_{ijk}}}\,,\end{aligned} \tag{2.1.7c}$$

where $h_{ijk} = h_i - h_j - h_k$.

2.1.1 The conformal Ward identity

Let us consider the change of correlation functions of primary fields under conformal transformations. If the theory is conformal invariant, then using the path integral formulation we obtain

$$\delta\langle X\rangle = \delta\int \mathrm{D}\Phi X e^{-S[\Phi]} = \int \mathrm{D}\Phi\delta X e^{-S[\Phi]} - \int \mathrm{D}\Phi X\delta S e^{-S[\Phi]} = 0\,, \tag{2.1.8}$$

where X is a collection of fields. The change of the action under an arbitrary coordinate transformation $\varepsilon(x,y)$ can be written as

$$\delta S = -\int \mathrm{d}x\,\mathrm{d}y\,\partial_\mu\varepsilon_\nu(x,y)T^{\mu\nu}(x,y)\,. \tag{2.1.9}$$

Here $T^{\mu\nu}(x,y)$ is the stress energy tensor and this equation can be regarded as its definition.

Now let us specify X to be a collection of primary fields:

$$X = \phi_1(z_1, z_1^*) \dots \phi_N(z_N, z_N^*). \tag{2.1.10}$$

We consider a coordinate transformation $\varepsilon(x,y)$ that is conformal in a small disc around each z_k and otherwise arbitrary in a compact region containing all the discs. Outside this region let $\varepsilon(x,y)$ be zero. Denoting the collection of the discs by D we have $\delta S|_D = 0$. Now using (2.1.8), (2.1.9) and (2.1.6) together we obtain

$$\begin{aligned} &- \int\limits_{\mathbb{R}^2 - D} \mathrm{d}^2x \, \partial_\mu \varepsilon_\nu(x) \langle T^{\mu\nu}(x) \phi_1(z_1, z_1^*) \dots \phi_N(z_N, z_N^*) \rangle \\ &\quad = \sum_{k=1}^{N} \left[h_k \varepsilon'(z_k) + \varepsilon(z_k) \partial_{z_k} + \bar{h}_k \varepsilon'(z_k)^* + \varepsilon(z_k)^* \partial_{\bar{z}_k} \right] \langle \phi_1(z_1, z_1^*) \dots \phi_N(z_N, z_N^*) \rangle \,. \end{aligned} \tag{2.1.11}$$

Using the Gauss theorem the left hand side of the equation becomes

$$\begin{aligned} &- \int\limits_{\partial D} \mathrm{d}^2x \, n_\mu \varepsilon_\nu(x) \langle T^{\mu\nu}(x) \phi_1(z_1, z_1^*) \dots \phi_N(z_N, z_N^*) \rangle \\ &\qquad\qquad + \int\limits_{\mathbb{R}^2 - D} \mathrm{d}^2x \, \varepsilon_\nu(x) \langle \partial_\mu T^{\mu\nu}(x) \phi_1(z_1, z_1^*) \dots \phi_N(z_N, z_N^*) \rangle \,, \end{aligned} \tag{2.1.12}$$

where n_μ is an inward pointing unit vector normal to the boundary of D. The fact that the right hand side is independent of the values of $\varepsilon(x)$ outside the region D implies that $T^{\mu\nu}$ is conserved. Additionally, we assume that due to rotational and scale invariance the stress energy tensor can be made traceless. Now applying the transformation (2.1.2) these properties translate to the following relations in terms of the new tensor components:

$$T_{z\bar{z}} = T_{\bar{z}z} \,, \qquad \partial_{\bar{z}} T_{zz} = 0 \,, \qquad \partial_z T_{\bar{z}\bar{z}} = 0 \,. \tag{2.1.13}$$

The second equation implies that a correlator involving the field $T_{zz}(z,\bar{z})$ is analytic in z on the complex plane except for the insertion points of other fields in the correlator. This is abbreviated by the notations $T(z) = 2\pi T_{zz}(z,\bar{z})$ and $\bar{T}(z) = 2\pi T_{\bar{z}\bar{z}}(z,\bar{z})$. After reformulating (2.1.12) in terms of the complex stress energy tensor we arrive at the following relation, valid when inserted in any correlator:

$$\begin{aligned} &\left(\int\limits_w \frac{\mathrm{d}z}{2\pi i} \varepsilon(z) T(z) - \int\limits_{w^*} \frac{\mathrm{d}\bar{z}}{2\pi i} \varepsilon(\bar{z}) \bar{T}(z^*) \right) \phi(w, w^*) \\ &\qquad = \left(h \varepsilon'(w) + \varepsilon(w) \partial_w + \bar{h} \varepsilon'(w)^* + \varepsilon(w)^* \partial_{\bar{w}} \right) \phi(w, w^*) \,. \end{aligned} \tag{2.1.14}$$

The holomorphic and antiholomorphic parts of this equation can be separated by taking the sum and the difference of this equation and the one for the transformation with $\tilde{\varepsilon} = i\varepsilon$. Then using Cauchy's theorem we arrive at the conformal Ward identity for the correlation functions

$$\begin{aligned}&\langle T(\zeta)\phi_1(z_1,\bar{z}_1)\dots\phi_N(z_N,\bar{z}_N)\rangle \\ &\quad = \sum_{j=1}^{N}\left[\frac{h}{(\zeta-z_j)^2}+\frac{1}{\zeta-z_j}\frac{\partial}{\partial z_j}\right]\langle\phi_1(z_1,\bar{z}_1)\dots\phi_N(z_N,\bar{z}_N)\rangle + \mathrm{reg}(\zeta)\,, \quad (2.1.15)\end{aligned}$$

where $\mathrm{reg}(\zeta)$ is a regular function. A similar relation holds for $\bar{T}(\bar{z})$.

We see that the short distance expansion or operator product expansion (OPE) of the stress energy tensor with a primary field is

$$T(z)\phi(w,\bar{w}) = \left[\frac{h}{(z-w)^2}+\frac{1}{z-w}\frac{\partial}{\partial w}\right]\phi(w,\bar{w}) + \mathrm{reg}(z-w)\,. \quad (2.1.16)$$

$T(z)$ itself is not a primary field. The most general OPE of $T(z)$ consistent with associativity (or Bose symmetry and scale invariance) is

$$T(z)T(w) = \frac{c/2}{(z-w)^4}+\frac{2T(w)}{(z-w)^2}+\frac{\partial T(w)}{(z-w)} + \mathrm{reg}(z-w)\,, \quad (2.1.17)$$

and similarly

$$\bar{T}(\bar{z})\bar{T}(\bar{w}) = \frac{c/2}{(\bar{z}-\bar{w})^4}+\frac{2\bar{T}(\bar{w})}{(\bar{z}-\bar{w})^2}+\frac{\partial\bar{T}(\bar{w})}{(\bar{z}-\bar{w})} + \mathrm{reg}(\bar{z}-\bar{w})\,. \quad (2.1.18)$$

The OPE of T and $\bar{T}$ has no poles. The number c is called central charge and being related to the free energy density, it is one of the characteristic quantities that determine the properties the conformal field theory.

For finite conformal transformations this implies the following transformation rule:

$$T(z) \xrightarrow{z\to f(z)} f'(z)^2 T(w) + \frac{c}{12}\{f;z\}\,, \quad (2.1.19)$$

where $\{f;z\}$ denotes the Schwarzian derivative:

$$\{f;z\} = \frac{f'''(z)}{f'(z)} - \frac{3}{2}\left(\frac{f''(z)}{f'(z)}\right)^2\,. \quad (2.1.20)$$

Note that the Schwarzian derivative vanishes for global conformal transformations (2.1.3), which means that $T(z)$ is quasi-primary with conformal weights $(h,\bar{h}) = (2,0)$ as well as $\bar{T}(\bar{z})$ with weights $(0,2)$.

2.1.2 The operator formalism

The introduction of a Hilbert space in a quantum field theory breaks manifest Lorentz-invariance, because an explicit time direction must be selected. In a Euclidean theory the time direction is somewhat arbitrary and we are free to choose the so-called radial quantisation, which means that time "passes" in the radial direction and equal time spaces are concentric circles around the origin. To make this choice more natural let us consider a line segment with periodic spatial boundary conditions. The corresponding space is an infinite cylinder where time flows along the cylinder and the equal time points form circles. The points of this space can be described by a complex variable $\zeta = t + ix$. By the conformal transformation $\zeta \to z = \exp\left(\frac{2\pi}{R}\zeta\right)$, called the exponential map, we can map the cylinder onto the complex plane. The $t \to -\infty$ points are mapped to the origin and time flows away from it in radial direction. We assume the existence of a vacuum state $|0\rangle$. Then an asymptotic field can be thought of as an operator creating an asymptotic "in" state from the vacuum:

$$|\phi_{\text{in}}\rangle = \lim_{t\to-\infty} \phi(x,t)|0\rangle = \lim_{z,\bar{z}\to 0} \phi(z,\bar{z})|0\rangle\,. \tag{2.1.21}$$

Thus a field inserted at the origin (or at any other point of the complex plane) can be thought of as a state. A remarkable feature of conformal field theory that this correspondence works also in the opposite direction: for every state one can find an operator inserted at an appropriate point (and different operators for different states). In conformal field theory we have full state-field correspondence.

Now we define a hermitian bilinear product on this Hilbert space by defining the hermitian conjugate of an "in" state. In Minkowski space the spacetime coordinates are not affected by conjugation, but in Euclidean space the situation is different. In order that t is unchanged the Euclidean time $\tau = it$ must be reversed: $\tau \to -\tau$. In radial quantization this corresponds to the transformation $z \to 1/z^*$. This leads to the following definition of the hermitian conjugate of a quasi-primary field:

$$\phi(z,\bar{z})^\dagger = \bar{z}^{-2h} z^{-2\bar{h}} \phi(1/\bar{z}, 1/z)\,, \tag{2.1.22}$$

because then the inner product of $|\phi_{\text{in}}\rangle$ and $\langle\phi_{\text{out}}| = |\phi_{\text{in}}\rangle^\dagger = \lim_{z,\bar{z}\to 0}\langle 0|\phi(z,\bar{z})^\dagger$ will be finite and well-defined.

The action of $T(z)$ and $\bar{T}(\bar{z})$ on the Hilbert space is given via their modes which are defined by

$$T(z) = \sum_n L_n z^{-n-2}\,, \qquad \bar{T}(\bar{z}) = \sum_n \bar{L}_n \bar{z}^{-n-2}\,, \tag{2.1.23}$$

or

$$L_m = \frac{1}{2\pi i}\oint_0 \mathrm{d}z\, z^{n+1} T(z)\,, \qquad \bar{L}_m = \frac{1}{2\pi i}\oint_0 \mathrm{d}\bar{z}\, \bar{z}^{n+1} \bar{T}(\bar{z})\,. \tag{2.1.24}$$

Now using the OPE of the stress energy tensor with itself (2.1.17) one can find the commutator of these modes via contour integration:

$$\begin{aligned}[L_n, L_m] &= \oint_0 \frac{\mathrm{d}w}{2\pi i} w^{m+1} \oint_w \frac{\mathrm{d}z}{2\pi i} z^{n+1} T(z)T(w) \\ &= \oint_0 \frac{\mathrm{d}w}{2\pi i} w^{m+1} \oint_w \frac{\mathrm{d}z}{2\pi i} z^{n+1} \left(\frac{c/2}{(z-w)^4} + \frac{2T(w)}{(z-w)^2} + \frac{\partial T(w)}{(z-w)} + \mathrm{reg}(z-w) \right) \\ &= (n-m)L_{n+m} + \delta_{n,-m} \frac{c}{12} n(n^2-1)\,. \end{aligned} \tag{2.1.25}$$

This algebra of the chiral modes L_n is the Virasoro-algebra that we will denote by Vir. An identical result is true for the modes $\bar{L}_n$ and $[L_n, \bar{L}_m] = 0$.

With a similar calculation, now using the OPE (2.1.16), one obtains the following commutation relations:

$$[L_n, \phi(w,\bar{w})] = \left[h(n+1)w^n + w^{n+1}\partial_w \right] \phi(w,\bar{w})\,, \tag{2.1.26a}$$

$$[\bar{L}_n, \phi(w,\bar{w})] = \left[\bar{h}(n+1)\bar{w}^n + \bar{w}^{n+1}\partial_{\bar{w}} \right] \phi(w,\bar{w})\,. \tag{2.1.26b}$$

We want $T(z)|0\rangle$ and $\bar{T}(\bar{z})|0\rangle$ to be well-defined as $z, \bar{z} \to 0$. For this the following must hold:

$$\begin{aligned} L_n|0\rangle &= 0\,, \\ \bar{L}_n|0\rangle &= 0\,. \end{aligned} \qquad (n \geq -1) \tag{2.1.27}$$

In particular this implies that the vacuum state $|0\rangle$ is invariant under global conformal transformations, because it is annihilated by L_{-1}, L_0, L_1 and their antiholomorphic counterparts. It also implies that the vacuum expectation value of the stress energy tensor vanishes:

$$\langle 0|T(z)|0\rangle = \langle 0|\bar{T}(\bar{z})|0\rangle = 0\,. \tag{2.1.28}$$

We emphasize that the $sl(2)$-invariant vacuum $|0\rangle$ may not be the true physical ground state, for example in a non-unitary theory on the cylinder it is not the state with the lowest energy.

The Hilbert space decomposes into highest weight representations of $\mathrm{Vir} \otimes \mathrm{Vir}$. Each module is built on a state $|h,\bar{h}\rangle$ that is created from the conformal vacuum $|0\rangle$ by a primary field:

$$|h,\bar{h}\rangle = \phi_{h,\bar{h}}(0,0)|0\rangle\,. \tag{2.1.29}$$

The module is spanned by vectors, called descendant states, of the form

$$L_{-n_1} L_{-n_2} \ldots \bar{L}_{-m_1} \bar{L}_{-m_2} \ldots |h,\bar{h}\rangle\,, \tag{2.1.30}$$

where all the n_i, m_i are positive. From (2.1.26) it follows that

$$L_0|h,\bar{h}\rangle = h\,|h,\bar{h}\rangle\,, \tag{2.1.31a}$$

$$\bar{L}_0|h,\bar{h}\rangle = \bar{h}\,|h,\bar{h}\rangle\,, \tag{2.1.31b}$$

$$L_n|h,\bar{h}\rangle = \bar{L}_n|h,\bar{h}\rangle = 0 \qquad n > 0\,. \tag{2.1.31c}$$

Using the Virasoro-algebra (2.1.25) we obtain

$$L_0\, L_{-n_1}\dots L_{-n_k}\bar{L}_{-m_1}\dots\bar{L}_{-m_l}|h,\bar{h}\rangle = (h+n_1+\dots+n_k)\cdot \\ L_{-n_1}\dots L_{-n_k}\bar{L}_{-m_1}\dots\bar{L}_{-m_l}|h,\bar{h}\rangle\,, \qquad (2.1.32a)$$

$$\bar{L}_0\, L_{-n_1}\dots L_{-n_k}\bar{L}_{-m_1}\dots\bar{L}_{-m_l}|h,\bar{h}\rangle = (\bar{h}+m_1+\dots+m_l)\cdot \\ L_{-n_1}\dots L_{-n_k}\bar{L}_{-m_1}\dots\bar{L}_{-m_l}|h,\bar{h}\rangle\,, \qquad (2.1.32b)$$

which shows that the modes L_0 and $\bar{L}_0$ act as grading operators. Within a module the state $|h,\bar{h}\rangle$ has the lowest weight, however, with an abuse of terminology, it is called a highest weight state. We see that all states are eigenvectors of L_0 and $\bar{L}_0$ and they are arranged in levels.

A module containing all the descendant states establishes a non-irreducible representation of the Virasoro algebra. In general there are linear combinations of descendant states, $|\psi\rangle$, that satisfy $L_n|\psi\rangle = 0$ for $n > 0$. These are called singular vectors and similarly to a primary state, submodules are built on them by the action of the modes. In order to get an irreducible representation one has to factorise out with these submodules.

By the state-field correspondence descendant fields can be introduced:

$$L_{-n}|h,\bar{h}\rangle \longleftrightarrow (L_{-n}\phi)(w,\bar{w}) = \oint_w \frac{\mathrm{d}z}{2\pi i}(z-w)^{-m+1}T(z)\phi(w,\bar{w})\,. \qquad (2.1.33)$$

The primary field $\phi_{h,\bar{h}}$ with all its descendants is called the conformal family of $\phi_{h,\bar{h}}$.

The hermitian conjugate of a descendant state is simply obtained from the conjugate of the highest weight state and the adjoint of the ladder operators which is found by applying rule (2.1.22) with $(h,\bar{h}) = (2,0)$ for $T(z)$ and $(0,2)$ for $\bar{T}(z)$, yielding

$$L_n^\dagger = L_{-n}\,, \qquad (2.1.34a)$$

$$\bar{L}_n^\dagger = \bar{L}_{-n}\,. \qquad (2.1.34b)$$

The above hermitian conjugation defines a $\mathrm{Vir}\otimes\mathrm{Vir}$ invariant scalar product in the highest weight module. The singular vectors are in the null space of this scalar product, that is they have zero norm and they are orthogonal to every state in the module. This fact offers a possible algorithm for making the representation irreducible.

Since the holomorphic and antiholomorphic part of the algebra decouples, the modules are direct products of chiral modules which are generated only by the modes L_n or $\bar{L}_n$. Thus the Hilbert space can be written formally as the sum

$$\mathcal{H} = \bigoplus_{h,\bar{h}} N_{h,\bar{h}}\, V(c,h)\otimes V(c,\bar{h}) \qquad (2.1.35)$$

where $V(c,h)$ is the chiral module built on the highest weight state with chiral weight h and with central charge c. The positive integer numbers $N_{h,\bar{h}}$ are the multiplicities of the occurrence of the module $V(c,h)\otimes V(c,\bar{h})$ in $\mathcal{H}$.

In the operator product of two primary fields usually conformal families of other primary fields appear. However, the only nontrivial input to the OPE are the coefficients of the primary fields in the expansion, called the structure constants. These are not fixed directly by representation theory of the algebra and they are closely related to the coefficient of the three point function. More precisely,

$$C_{ijk} = \frac{C^i_{jk}}{B_{ii}A_0}\,, \tag{2.1.36}$$

where A_0, B_{ij} and C_{ijk} are the coefficients in (2.1.7)[2].

2.1.3 Partition function and modular invariance

Let us consider a CFT on a cylinder of circumference R constructed from the complex plane by the identification $w \equiv w + iR$ where $w = t + ix$. The Hamiltonian on the cylinder is

$$H_{\text{cyl}} = \int_0^R T_{tt}\mathrm{d}x = \int_0^R \frac{1}{2\pi}(T(w) + \bar{T}(\bar{w}))\mathrm{d}x\,. \tag{2.1.37}$$

Let us map the cylinder onto the plane by the exponential map $z = \exp\left(\frac{2\pi}{R}w\right)$. We get contour integrals in z and $\bar{z}$ and after transforming the integration measure and applying the transformation rule (2.1.19) for the stress energy tensor we arrive at the result

$$H_{\text{cyl}} = \frac{2\pi}{R}\left(L_0 + \bar{L}_0 - \frac{c}{12}\right)\,, \tag{2.1.38}$$

where the term $c/12$ comes from the Schwarzian derivative. Assuming that the vacuum expectation value of $T(z,\bar{z})$ vanishes on the plane, we see that on the cylinder the vacuum energy is non-zero. It is a sort of Casimir energy, generated by the periodic boundary condition. As the macroscopic scale R goes to infinity, this energy vanishes, thus the central charge measures the effect of the macroscopic scales of the theory. Note that the formula for H_{cyl} implies that for the Hamiltonian to be bounded below, the Hilbert space can only consist of highest weight representations of $\mathrm{Vir}\otimes\mathrm{Vir}$.

Now suppose we identify the two ends of the cylinder turning it into a torus of length L. The partition function of the system is

$$\mathcal{Z}(R,L) = \mathrm{tr}\, e^{-LH_{\text{cyl}}} = \mathrm{tr}\, q^{L_0+\bar{L}_0-c/12}\,, \tag{2.1.39}$$

where $q = \exp(-2\pi L/R)$. This can be expressed through the characters of the representations of Vir present in the Hilbert space. They are defined as

$$\chi_{h_i}(q) = q^{-c/24}\mathrm{tr}_i\, q^{L_0}\,, \tag{2.1.40}$$

[2]We assumed that there are only one primary field with conformal weights (0,0) and it is labeled by $i = 0$.

where the trace runs over the highest weight module i. In terms of the characters the partition function reads

$$\mathcal{Z}(R,L) = \sum_{h,\bar{h}} N_{h,\bar{h}} \chi_h(q) \chi_{\bar{h}}(q^*) \,. \tag{2.1.41}$$

If we exchange the role of the Euclidean time and space directions on the cylinder, that is we consider the Hamiltonian

$$\tilde{H}_{\mathrm{cyl}} = \int_0^L T_{xx} \, \mathrm{d}t \tag{2.1.42}$$

and we use the map $\tilde{z} = \exp(2\pi/Lw)$ instead, we arrive at

$$\mathcal{Z}(R,L) = \operatorname{tr} e^{-RH_{\mathrm{cyl}}} = \operatorname{tr} \tilde{q}^{L_0+\bar{L}_0-c/12} = \sum_{h,\bar{h}} N_{h,\bar{h}} \chi_h(\tilde{q}) \chi_{\bar{h}}(\tilde{q}^*) \,, \tag{2.1.43}$$

where $\tilde{q} = \exp(-2\pi R/L)$. The two expressions for the partition function must give the same result, which puts severe constraints on the field content of the theory. More generally a torus is characterized by its two periods on the complex plane. One of them can be chosen to be 1, let us denote the other one by τ. All values of τ that lead to conformally equivalent tori are generated by two operations, called Dehn-twists:

$$T : \tau \to \tau + 1 \,, \tag{2.1.44a}$$

$$S : \tau \to -\frac{1}{\tau} \,. \tag{2.1.44b}$$

The torus partition function must be independent of the parameterisation of the torus and thus it must be invariant under these transformations. This is called modular invariance.

2.2 Superconformal Field Theories

2.2.1 $N = 1$ superconformal algebra

The $N = 1$ superconformal algebra is an extension of the Virasoro algebra where besides $T(z)$ there is a new, fermionic chiral field $G(z)$ in the chiral algebra. It is a quasi-primary field with conformal weight $3/2$. Because of its fermionic character two kinds of boundary conditions are possible for $G(z)$:

$$G(e^{2\pi i}z) = G(z) \qquad \to \text{Neveu–Schwarz sector,} \tag{2.2.1}$$

$$G(e^{2\pi i}z) = -G(z) \qquad \to \text{Ramond sector.} \tag{2.2.2}$$

The mode expansion for $G(z)$ is

$$G(z) = \sum_r G_r z^{-r-3/2}\,, \tag{2.2.3}$$

where according to the boundary conditions for $G(z)$ the indices r, s can take half-integer (Neveu–Schwarz sector) or integer (Ramond sector) values.

Its operator product expansions containing the primary field $\phi_h(z)$ are

$$G(z)\phi(w) = \frac{(\hat{G}_{-1/2}\phi)(w)}{z-w} + \dots\,, \tag{2.2.4a}$$

$$G(z)(\hat{G}_{-1/2}\phi)(w) = \frac{2h\phi(w)}{(z-w)^2} + \frac{\partial\phi(w)}{z-w} + \dots\,, \tag{2.2.4b}$$

where $(\hat{G}_{-1/2}\phi(w))$ is the superpartner of $\phi(w)$ and corresponds to the state $G_{-1/2}\phi(0)|0\rangle$. The operator product expansions of the chiral operators are

$$G(z)G(w) = \frac{c/6}{(z-w)^3} + \frac{1/2T(w)}{z-w} + \dots\,, \tag{2.2.5a}$$

$$T(z)G(w) = \frac{3/2G(w)}{(z-w)^2} + \frac{\partial G(w)}{z-w} + \dots\,. \tag{2.2.5b}$$

Similarly to the derivation of the Virasoro algebra from the $T(z)T(w)$ OPE, from these operator products we can get (anti)commutation relations for the modes, giving the full super Virasoro algebra, SVir:

$$[L_n, L_m] = (n-m)L_{n+m} + \frac{c}{12}n(n^2-1)\delta_{n,-m}\,, \tag{2.2.6a}$$

$$\{G_r, G_s\} = 2L_{r+s} + \frac{c}{3}\left(r^2 - 1/4\right)\delta_{r,-s}\,, \tag{2.2.6b}$$

$$[L_n, G_r] = \left(\frac{n}{2} - r\right)G_{n+r}\,. \tag{2.2.6c}$$

Exploiting the OPE (2.2.4) we can get commutation relations similar to (2.1.26) for the Neveu–Schwarz modes of $G(z)$:

$$G_r\phi(z) = z^{r+1/2}(\hat{G}_{-1/2}\phi)(z) + \eta_\phi\phi(z)G_r\,, \tag{2.2.7a}$$

$$G_r(\hat{G}_{-1/2}\phi)(z) = z^{r-1/2}((2r+1)h + z\partial)\phi(z) - \eta_\phi(\hat{G}_{-1/2}\phi)(z)G_r \tag{2.2.7b}$$

with $\eta_\phi = \pm 1$ for fields of even and odd fermion number, respectively.

The (chiral) highest weight representations of the algebra are defined by highest weight states $|h\rangle$ satisfying

$$L_n|h\rangle = 0 \qquad n > 0\,, \tag{2.2.8a}$$

$$L_0|h\rangle = h\,, \tag{2.2.8b}$$

$$G_r|h\rangle = 0 \qquad r > 0\,. \tag{2.2.8c}$$

The chiral Verma module is generated by operators having a nonpositive index. The vectors

$$L_{n_1}\dots L_{n_k}G_{r_1}\dots G_{r_l}|h\rangle\,, \qquad n_1 \le \dots \le n_k < 0\,,\ \ r_1 < \dots < r_l \le 0 \tag{2.2.9}$$

constitute a generating system for the Verma module. Note that the inequalities for the r_i-s are strict since $G_r^2 = L_{2r} - \frac{c}{12}\,\delta_{r,0}$ by equation (2.2.6b). The Hilbert space consists of the direct sum of direct products of highest weight modules, just like in (2.1.35).

The full operator algebra of the Neveu–Schwarz and Ramond fields is obtained by sewing the left and right chiral parts together. This algebra is non-local in general, however, there exist projections that give local operator algebras. One of them is the so-called fermion model, in which one keeps only the Neveu–Schwarz sector.

Here we consider the so-called spin model which is obtained in the following way. In both sectors a fermion parity operator $(-1)^F$ can be introduced with algebraic relations $[(-1)^F, L_n] = \{(-1)^F, G_r\} = 0$. Thus every level of a Verma module consists of $(-1)^F = \pm 1$ eigenstates. The projection onto the even parity ($(-1)^F = +1$) states in the Neveu–Schwarz sector and onto either the even ($(-1)^F = +1$) or the odd ($(-1)^F = -1$) parity states in the Ramond sector yields a well defined local theory.

The minimal series

The irreducible highest weight representations are the quotients of the Verma modules by their maximal invariant submodules. In this paper we deal with the superconformal minimal models in which the operator product expansions (or fusion of states) close for a *finite number* of primary fields. The Hilbert space contains only a finite number of irreducible representations of the Virasoro algebra. Furthermore, in these models the Verma modules turn out to be highly reducible.

The superconformal minimal models are indexed by two positive integers, p and q (we choose the convention $p < q$). Their central charge is given by

$$c(p,q) = \frac{3}{2}\left(1 - 2\frac{(p-q)^2}{pq}\right), \qquad \left(p\,, \frac{q-p}{2}\right) = 1\,. \tag{2.2.10}$$

Setting $q = p+2$ gives the one parameter family of *unitary* superconformal minimal models.

Within a superconformal minimal model the highest weights are also characterized by two integers, r and s:

$$h(r,s) = \frac{(ps-qr)^2 - (p-q)^2}{8pq} + \frac{1-(-1)^{r+s}}{32}, \qquad 1 \le r \le p-1,\ \ 1 \le s \le q-1\,. \tag{2.2.11}$$

The sum $r+s$ is even for a Neveu–Schwarz state and odd for a Ramond state. The weights can be arranged in a $(p-1)\times(q-1)$ matrix, the super Kac table. Since $h(p-r,q-s) = h(r,s)$ the transformation

$$\left.\begin{aligned} r &\to p-r \\ s &\to q-s \end{aligned}\right\} \tag{2.2.12}$$

is a symmetry of the Kac table which is thus a centrally symmetric matrix. If p and q are both even there is a fixed point of this transformation, the weight $h(\frac{p}{2},\frac{q}{2})$. Apart from this each weight appears twice in the Kac table.

In the Ramond sector the zero mode G_0 commutes with L_0, thus the highest weight states are two-fold degenerate: $|h\rangle$ and $G_0|h\rangle$. From the relation $G_0^2 = L_0 - c/24$ follows that if $h = c/24$ then $G_0|h\rangle$ is a null state. In this case the highest weight state is unique. For the unitary models for even values of p the representation $(\frac{p}{2},\frac{p+2}{2})$ in the middle of the Kac table has weight $c(p,p+2)/24$, so the corresponding highest weight state is unpaired. We shall call this representation "supersymmetric".

One can consider the minimal models on a cylinder of length R and circumference L. The super characters are defined as

$$\chi_i^{\mathrm{NS}}(q) = \mathrm{tr}_i\, q^{L_0-c/24}\,, \qquad i \in \Delta_{\mathrm{NS}}\,, \tag{2.2.13a}$$

$$\chi_i^{\widetilde{\mathrm{NS}}}(q) = \mathrm{tr}_i(-1)^F\, q^{L_0-c/24}\,, \qquad i \in \Delta_{\mathrm{NS}}\,, \tag{2.2.13b}$$

$$\chi_i^{\mathrm{R}}(q) = \mathrm{tr}_i\, q^{L_0-c/24}\,, \qquad i \in \Delta_{\mathrm{R}} \tag{2.2.13c}$$

with $q = e^{-\pi L/R}$, explicit formulae can be found in Appendix A.1. Under the S modular transformation (2.1.44) the characters transform as

$$\chi_i^{\mathrm{NS}}(q) = \sum_{j\in\Delta_{\mathrm{NS}}} S_{ij}^{[\mathrm{NS},\mathrm{NS}]}\chi_j^{\mathrm{NS}}(\tilde{q})\,, \tag{2.2.14a}$$

$$\chi_i^{\widetilde{\mathrm{NS}}}(q) = \sum_{j\in\Delta_{\mathrm{R}}} S_{ij}^{[\widetilde{\mathrm{NS}},\mathrm{R}]}\sqrt{2}\chi_j^{\mathrm{R}}(\tilde{q})\,, \tag{2.2.14b}$$

$$\sqrt{2}\chi_i^{\mathrm{R}}(q) = \sum_{j\in\Delta_{\mathrm{NS}}} S_{ij}^{[\mathrm{R},\widetilde{\mathrm{NS}}]}\chi_j^{\widetilde{\mathrm{NS}}}(\tilde{q})\,, \tag{2.2.14c}$$

where $\tilde{q} = e^{-4\pi R/L}$. For the unitary superconformal minimal models $\mathrm{SM}(p, p+2)$ with p odd the modular S matrices are

$$S^{[\mathrm{NS},\mathrm{NS}]}_{(n,m),(n',m')} = \frac{4}{\sqrt{p(p+2)}} \sin\frac{\pi n n'}{p} \sin\frac{\pi m m'}{p+2}\,, \tag{2.2.15a}$$

$$S^{[\widetilde{\mathrm{NS}},\mathrm{R}]}_{(n,m),(n',m')} = \frac{4}{\sqrt{p(p+2)}} (-1)^{(n-m)/2} \sin\frac{\pi n n'}{p} \sin\frac{\pi m m'}{p+2}\,, \tag{2.2.15b}$$

$$S^{[\mathrm{R},\widetilde{\mathrm{NS}}]}_{(n,m),(n',m')} = \frac{4}{\sqrt{p(p+2)}} (-1)^{(n'-m')/2} \sin\frac{\pi n n'}{p} \sin\frac{\pi m m'}{p+2}\,. \tag{2.2.15c}$$

For even p the character and the matrix elements are different for the supersymmetric representation by some numerical factors.

The modular transformation T (2.1.44) has a much simpler, diagonal action on the characters: under T χ_i gets multiplied by $e^{2\pi(h_i - c/24)}$. In order for the partition function (2.1.41) to be modular invariant, $h - \bar{h}$ must therefore be an integer for every individual tensor product of chiral representations in the direct sum (2.1.35). An obvious solution of this condition is $N_{h,\bar{h}} = \delta_{h,\bar{h}}$ giving the partition function

$$\mathcal{Z} = \sum_i |\chi_i|^2\,, \tag{2.2.16}$$

which is automatically invariant under the S modular transformation as well, thanks to the unitarity of S ($S^2 = 1$). This is called the *diagonal invariant* and we restrict our investigations to this case.

It is an interesting question which primary fields (and their conformal families) appear in the short distance operator product expansion of two primary fields. Let us introduce the fusion coefficient N_{ij}^k that is 1 if the primary field k appears in the fusion of the primary fields i and j and it is 0 if it does not. We can introduce the abstract notion of fusion algebra:

$$\phi_i \times \phi_j = \sum_k N_{ij}^k \phi_k\,, \tag{2.2.17}$$

which for the corresponding highest weight representations gives a rule for fusing different irreducible representations of Vir.

The fusion rule for the diagonal modular invariant supersymmetric minimal models is

$$\phi_{(r_1,s_1)} \otimes \phi_{(r_2,s_2)} = \sum_{r'=|r_1-r_2|+1}^{\min\binom{2p-r_1-r_2-1}{r_1+r_2-1}\prime} \sum_{s'=|s_1-s_2|+1}^{\min\binom{2q-s_1-s_2-1}{s_1+s_2-1}\prime} \phi_{(r',s')}\,, \tag{2.2.18}$$

where the prime on the sums means that r' and s' jump by steps of 2.

Verlinde found a relation [Ver88] between the fusion coefficients N_{ij}^k and the matrix elements S_{ij} describing the transformation of the characters under the modular transformation S, which is the celebrated Verlinde formula:

$$\sum_i S_{ij} N_{kl}^i = \frac{S_{kj} S_{lj}}{S_{0j}}\,. \tag{2.2.19}$$

2.2.2 Coset construction for superminimal models

The SM$(p, p+2)$ unitary superminimal models are realized by the

$$\frac{su(2)_k \otimes su(2)_2}{su(2)_{k+2}} \tag{2.2.20}$$

coset models with $p = k+2$. Let us label the sectors of $su(2)_k$ by $l = 0, 1, \ldots, k$, the sectors of $su(2)_2$ by $m = 0, 1, 2$ and the sectors of $su(2)_{k+2}$ by $l' = 0, 1, \ldots, k+2$. The sectors of the direct product are thus labeled by the pairs (l, m). These sectors split up with respect to the $su(2)_{k+2}$ subalgebra,

$$V_{l,m} = \bigoplus_{l'} W_{l,m,l'} \otimes V_{l'}\,, \tag{2.2.21}$$

where $W_{l,m,l'}$ are the sectors of the coset theory. Only those coset sectors are allowed for which

$$l + m + l' \quad \text{is even.} \tag{2.2.22}$$

Furthermore, there are identifications between these admissible representations:

$$(l, m, l') \cong (k - l, 2 - m, k + 2 - l')\,. \tag{2.2.23}$$

Using the $p = k + 2$ rule and the new variables (the Kac-indices)

$$\begin{aligned} r &= l + 1 \qquad & r &= 1, 2, \ldots, p-1\,, \\ s &= l' + 1 \qquad & s &= 1, 2, \ldots, p+1 \end{aligned}$$

the precise relations with the superminimal fields are [GKO86]:

$$(r, s)_{\mathrm{NS}} = (r-1, 0, s-1) \oplus (r-1, 2, s-1)\,, \tag{2.2.25}$$

$$(r, s)_{\mathrm{R}} \;= (r-1, 1, s-1)\,. \tag{2.2.26}$$

In the Neveu–Schwarz sector the direct sum in (2.2.25) corresponds to the sum of the $(-1)^F$-projected subspaces. The identification (2.2.23) translates to

$$(r, s) \cong (p - r, p + 2 - s)\,, \tag{2.2.27}$$

which is the well-known symmetry relation (2.2.12) of the Kac table of the superminimal models.

In the diagonal superminimal models the boundary conditions α are labeled by triplets (l, m, l') taking values in the same range as the sectors including selection and identification rules. The NS and $\widetilde{\mathrm{NS}}$ boundary conditions correspond to the $m = 0, 2$ choices. The agreement between our results and the predictions for the flows justifies this correspondence.

We will need the fusion of $su(2)_n$ representations which is given by

$$l_1 \times l_2 = |l_1 - l_2| \oplus |l_1 - l_2| + 2 \oplus \cdots \oplus \min(l_1 + l_2, n)\,. \tag{2.2.28}$$

2.3 Boundary SCFT

The upper half plane (UHP) is the prototype of geometries having nontrivial boundaries. The superconformal transformations then have two roles. Firstly they connect the correlation functions on general geometries to those on the UHP. On the other hand the transformations that leave the geometry invariant put constraints on the correlation functions on the UHP.

The study of boundary conformal field theory originates from research on open string theory and boundary critical systems. The seminal paper of Cardy [Car84] led to the unification of methods and to the introduction of important concepts [Car89],[CL91]. In these papers the notions of boundary operator, boundary condition changing operator and boundary states are introduced and a non-trivial equation, the Cardy equation, is deduced as a necessary condition that the conformal invariant boundary states must satisfy. In [BPPZ00] Behrend et al. applied systematically the methods of Cardy and Lewellen to rational conformal field theories and showed, among others, that the complete solutions of the Cardy equation are in one-to-one correspondence with the integer valued matrix representations of the Verlinde algebra (2.2.19).

Having a conformally invariant bulk theory the conformal invariance can be extended to the boundaries. In order for the boundary conditions to be invariant under scale transformations they have to satisfy some conditions and constraints. The conformal Ward identity on the UHP leads to a new constraint on the operators of the chiral algebra. We follow the steps of subsection 2.1.1 but now we choose an infinitesimal transformation characterized by $\varepsilon(x,y)$ so that it leaves the UHP invariant (in particular, $\varepsilon_y(x,0)=0$), it is conformal in a semi-disc D containing all the fields in the correlator, it is arbitrary in a compact domain containing the semi-disc and zero outside this domain. We demand that the boundary condition is conformally invariant, so $\delta S|_D = 0$. Applying the steps we again arrive at equation (2.1.11) where the left hand side, similarly to (2.1.12), is given by

$$-\int\limits_{\partial(K-D)} \mathrm{d}^2x\, n_\mu \varepsilon_\nu(x)\langle T^{\mu\nu}(x)\phi_1(z_1,z_1^*)\dots\phi_N(z_N,z_N^*)\rangle + \int\limits_{K-D} \mathrm{d}^2x\, \varepsilon_\nu(x)\langle \partial_\mu T^{\mu\nu}(x)\phi_1(z_1,z_1^*)\dots\phi_N(z_N,z_N^*)\rangle\,. \quad (2.3.1)$$

From the second term we again conclude that the stress energy tensor is conserved, but the first term gives something new. It contains a portion of the integral which has to be taken along the real axis of the form $\int \varepsilon_x(x,0)\langle T^{xy}(x,y)\dots\rangle \mathrm{d}x$. Demanding this to be independent of $\varepsilon_x(x,0)$ leads to the condition $T_{xy}(x,0)=0$, which means that there is no energy flow across the boundary (the real axis). In complex coordinates this translates to the condition

$$T(z,\bar z) = \bar T(\bar z, z) \qquad \text{for } \mathrm{Re}\, z = 0. \quad (2.3.2)$$

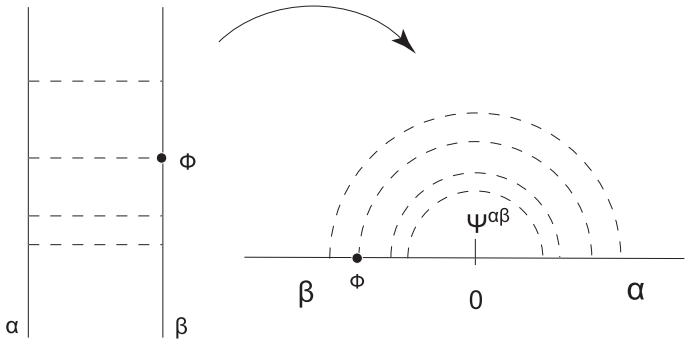

Figure 2.1: Exponential map from the strip onto the UHP (periodic boundary condition in the "time" direction)

A strip of width R with boundary conditions α and β on the left and the right boundary, respectively, can be mapped to the UHP by the exponential mapping $\zeta \to z = \exp\left(\frac{\pi}{R}\zeta\right)$, under which the boundaries of the strip are mapped to the negative and positive part of the real axis (see Fig. 2.1). The conformal boundary conditions on the strip become conformal boundary conditions on the plane. If a bulk field approaches the boundary its correlators display a singular behaviour characteristic to the boundary condition on that part of the real axis. If the boundary condition is different on the negative and positive part of the axis then this singular behaviour will be different for $z \to 0 + \varepsilon$ and $z \to 0 - \varepsilon$. This discontinuity can be described by the insertion of a boundary condition changing field $\psi^{\alpha\beta}$ at the origin. If the boundary condition is the same along the whole real axis then the fields $\psi^{\alpha\alpha}$ can be equally thought of as $\alpha \to \alpha$ boundary condition changing operators or boundary degrees of freedom, fields living on the boundary α. The fields $\psi^{\alpha\beta}$ are in one to one correspondence with the operator content of the theory on the strip.

2.3.1 Physical boundary conditions

Looking at the strip from the side ("closed channel") and letting the time flow in the direction of R the boundary conditions turn into initial and final boundary states (see Fig. 2.2). Then the conformal invariance of the boundary conditions translate to the following condition on these boundary states:

$$(L_n - \bar{L}_{-n})|B\rangle = 0 \qquad (B = \alpha,\ \beta)\,. \tag{2.3.3}$$

For a general chiral field W of spin s one finds

$$(W_n - (-1)^s \bar{W}_{-n})|B\rangle = 0\,, \tag{2.3.4}$$

which in our case $(s = 1/2)$ means

$$(G_r \pm i\bar{G}_{-r})|B\rangle = 0\,. \tag{2.3.5}$$

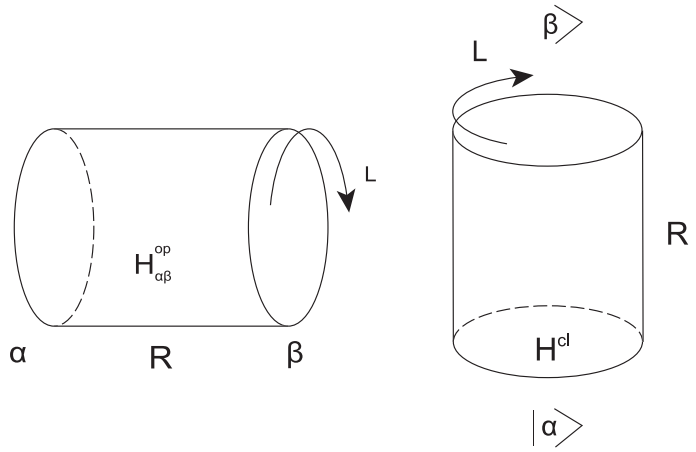

Figure 2.2: The theory on the cylinder: open and closed channel

The sign ambiguity comes from the square root $(-1)^{1/2}$. We see that the left-chiral and right-chiral part of the theory are linked together. Only one copy of the supersymmetric Virasoro algebra remains and all the calculations are chiral.

From now we specialize on the superconformal models and we give the consistent boundary states based on paper [Nep01b].

Apart from the constraints (2.3.3,2.3.5) there are further consistency conditions on the boundary states coming from considering the spin model on a cylinder with boundary conditions α and β:

$$\mathcal{Z}(L,R) = \mathrm{tr}_{\mathrm{NS}}\frac{1}{2}(1+(-1)^F)e^{-LH^{\mathrm{open}}_{\alpha\beta}} + \mathrm{tr}_{\mathrm{R}}\frac{1}{2}(1+(-1)^F)e^{-LH^{\mathrm{open}}_{\alpha\beta}} = \langle\alpha|e^{-RH^{\mathrm{closed}}}|\beta\rangle\,, \tag{2.3.6}$$

where the Hamiltonians are

$$H^{\mathrm{open}}_{\alpha\beta} = \frac{\pi}{R}\left(L_0 - \frac{c}{24}\right)\,, \tag{2.3.7a}$$

$$H^{\mathrm{closed}} = \frac{2\pi}{L}\left(L_0 + \bar{L}_0 - \frac{c}{12}\right)\,. \tag{2.3.7b}$$

H^{open} is obtained from the Hamiltonian on the strip through the exponential map to the UHP.

In [Nep01b] these equations for the boundary states are solved for odd p, when the supersymmetric Ramond representation $(\frac{p}{2},\frac{q}{2})$ is absent. First we introduce the

following coefficients:

$$\mathrm{tr}_{\mathrm{NS}}\, e^{-LH_{\alpha\beta}} = \sum_{i\in\Delta_{\mathrm{NS}}} n^i_{\alpha\beta}\chi^{\mathrm{NS}}_i(q)\,, \tag{2.3.8a}$$

$$\mathrm{tr}_{\mathrm{NS}}\,(-1)^F e^{-LH_{\alpha\beta}} = \sum_{i\in\Delta_{\mathrm{NS}}} \widetilde{n}^i_{\alpha\beta}\chi^{\widetilde{\mathrm{NS}}}_i(q)\,, \tag{2.3.8b}$$

$$\mathrm{tr}_{\mathrm{R}}\, e^{-LH_{\alpha\beta}} = \sum_{i\in\Delta_{\mathrm{R}}} m^i_{\alpha\beta}\chi^{\mathrm{R}}_i(q)\,, \tag{2.3.8c}$$

$$\mathrm{tr}_{\mathrm{R}}\,(-1)^F e^{-LH_{\alpha\beta}} = 0\,. \tag{2.3.8d}$$

Using these relations and the modular transformation properties of the characters (2.2.14), in the open channel picture we get for the partition function

$$\begin{aligned}\mathcal{Z}^{\mathrm{open}}(L,R) &= \frac{1}{2}\sum_{i\in\Delta_{\mathrm{NS}}}\Big(n^i_{\alpha\beta}\chi^{\mathrm{NS}}_i(q) + \widetilde{n}^i_{\alpha\beta}\chi^{\widetilde{\mathrm{NS}}}_i(q)\Big) + \frac{1}{2}\sum_{i\in\Delta_{\mathrm{R}}} m^i_{\alpha\beta}\chi^{\mathrm{R}}_i(q)\\ &= \frac{1}{2}\sum_{i\in\Delta_{\mathrm{NS}}}\left(\sum_{j\in\Delta_{\mathrm{NS}}} n^i_{\alpha\beta}S^{[\mathrm{NS},\mathrm{NS}]}_{ij}\chi^{\mathrm{NS}}_j(\tilde{q}) + \sum_{j\in\Delta_{\mathrm{R}}}\tilde{n}^i_{\alpha\beta}S^{[\widetilde{\mathrm{NS}},\mathrm{R}]}_{ij}\sqrt{2}\chi^{\mathrm{R}}_j(\tilde{q})\right)\\ &\qquad + \sum_{i\in\Delta_{\mathrm{R}}}\sum_{j\in\Delta_{\mathrm{NS}}} m^i_{\alpha\beta}S^{[\mathrm{R},\widetilde{\mathrm{NS}}]}_{ij}\frac{1}{\sqrt{2}}\chi^{\widetilde{\mathrm{NS}}}_j(\tilde{q})\,.\end{aligned} \tag{2.3.9}$$

The closed channel the equations (2.3.3,2.3.5) for the boundary state can be solved in terms of the Ishibashi states:

$$(L_n - \bar{L}_{-n})|j_\pm\rangle\rangle = 0\,, \tag{2.3.10a}$$

$$(G_r \pm i\bar{G}_{-r})|j_\pm\rangle\rangle = 0 \tag{2.3.10b}$$

with parity properties

$$(-1)^F|j^{\mathrm{NS}}_\pm\rangle\rangle = +|j^{\mathrm{NS}}_\pm\rangle\rangle\,, \tag{2.3.11a}$$

$$(-1)^F|j^{\mathrm{R}}_\pm\rangle\rangle = \pm|j^{\mathrm{R}}_\pm\rangle\rangle\,. \tag{2.3.11b}$$

They are of the form:

$$|j_\pm\rangle\rangle = \sum_N |j;N\rangle\otimes U_\pm\overline{|j;N\rangle}\,, \tag{2.3.12}$$

where the vectors $|j;N\rangle$ constitute an orthonormal basis of the representation j and $U_\pm$ are anti-unitary operators with properties

$$U_\pm\overline{|j;0\rangle} = \overline{|j;0\rangle}^*\,, \qquad U_\pm\bar{G}_{-r} = \pm i\bar{G}_{-r}U\,. \tag{2.3.13}$$

It can be shown that these Ishibashi states satisfy equations (2.3.10) by direct computation or by the following argument. The state $|B\rangle$ is an element of the bulk Hilbert space (2.1.35) which is a direct sum of direct products of representations

of SVir. Since the representation spaces are invariant subspaces of L_n and G_r (and their anti-holomorphic counterparts), the mode operators act independently in the modules. Therefore the solutions of (2.3.10) can be looked for in the form $|B\rangle = \sum_i |B_i\rangle$, where $|B_i\rangle \in V(c,h_i) \otimes V(c,\bar{h}_i)$. Thus the states $|B_i\rangle$ can be thought of as $V(c,h_i) \to V(c,\bar{h}_i)$ linear maps (after identifying $V(c,h_i)$ with its dual via Hermitian conjugation). Equations (2.3.10) mean that this map is an intertwiner between two SVir representations. Since the Hilbert space is built from *irreducible* representations, by Schur's lemma $V(c,h_i)$ must be isomorphic to $V(c,\bar{h}_i)$ (in particular, $h_i = \bar{h}_i$) and the sum of these maps is a projector that corresponds to the states (2.3.12)[3].

Now assuming that the Ishibashi states constitute a basis for the boundary states, the right hand side of (2.3.6) can be written in terms of this basis. Using the following relations for the matrix elements:

$$\langle\langle j^{\mathrm{NS}}_{\pm}|e^{-RH^{closed}}|j^{\mathrm{NS}}_{\pm}\rangle\rangle = \chi^{\mathrm{NS}}_j(\tilde{q})\,, \tag{2.3.14a}$$

$$\langle\langle j^{\mathrm{NS}}_{\mp}|e^{-RH^{closed}}|j^{\mathrm{NS}}_{\pm}\rangle\rangle = \chi^{\widetilde{\mathrm{NS}}}_j(\tilde{q})\,, \tag{2.3.14b}$$

$$\langle\langle j^{\mathrm{R}}_{\pm}|e^{-RH^{closed}}|j^{\mathrm{R}}_{\pm}\rangle\rangle = \chi^{\mathrm{R}}_j(\tilde{q})\,, \tag{2.3.14c}$$

$$\langle\langle j^{\mathrm{R}}_{\mp}|e^{-RH^{closed}}|j^{\mathrm{R}}_{\pm}\rangle\rangle = 0\,, \tag{2.3.14d}$$

we obtain

$$\begin{aligned}\mathcal{Z}^{\mathrm{closed}}(L,R) = \sum_{j\in\Delta_{\mathrm{NS}}} \Big[&\left(\langle\alpha|j^{\mathrm{NS}}_+\rangle\rangle\langle\langle j^{\mathrm{NS}}_+|\beta\rangle + \langle\alpha|j^{\mathrm{NS}}_-\rangle\rangle\langle\langle j^{\mathrm{NS}}_-|\beta\rangle\right)\chi^{\mathrm{NS}}_j(\tilde{q}) \\ &+ \left(\langle\alpha|j^{\mathrm{NS}}_-\rangle\rangle\langle\langle j^{\mathrm{NS}}_+|\beta\rangle + \langle\alpha|j^{\mathrm{NS}}_+\rangle\rangle\langle\langle j^{\mathrm{NS}}_-|\beta\rangle\right)\chi^{\widetilde{\mathrm{NS}}}_j(\tilde{q})\Big] \\ &+ \sum_{j\in\Delta_{\mathrm{R}}} \langle\alpha|j^{\mathrm{R}}_+\rangle\rangle\langle\langle j^{\mathrm{R}}_+|\beta\rangle\chi^{\mathrm{R}}_j(\tilde{q})\,. \end{aligned} \tag{2.3.15}$$

Comparing this to the open channel partition function we arrive at the super Cardy equations:

$$\frac{1}{2}\sum_{i\in\Delta_{\mathrm{NS}}} n^i_{\alpha\beta} S^{[\mathrm{NS},\mathrm{NS}]}_{ij} = \langle\alpha|j^{\mathrm{NS}}_+\rangle\rangle\langle\langle j^{\mathrm{NS}}_+|\beta\rangle + \langle\alpha|j^{\mathrm{NS}}_-\rangle\rangle\langle\langle j^{\mathrm{NS}}_-|\beta\rangle\,, \tag{2.3.16a}$$

$$\frac{1}{\sqrt{2}}\sum_{i\in\Delta_{\mathrm{NS}}} \tilde{n}^i_{\alpha\beta} S^{[\widetilde{\mathrm{NS}},\mathrm{R}]}_{ij} = \langle\alpha|j^{\mathrm{R}}_+\rangle\rangle\langle\langle j^{\mathrm{R}}_+|\beta\rangle\,, \tag{2.3.16b}$$

$$\frac{1}{2\sqrt{2}}\sum_{i\in\Delta_{\mathrm{R}}} m^i_{\alpha\beta} S^{[\mathrm{R},\widetilde{\mathrm{NS}}]}_{ij} = \langle\alpha|j^{\mathrm{NS}}_+\rangle\rangle\langle\langle j^{\mathrm{NS}}_-|\beta\rangle + \langle\alpha|j^{\mathrm{NS}}_-\rangle\rangle\langle\langle j^{\mathrm{NS}}_+|\beta\rangle\,. \tag{2.3.16c}$$

These equations are highly non-trivial since the coefficients $n^i_{\alpha\beta}$, $m^i_{\alpha\beta}$ must be positive integers and $\tilde{n}^i_{\alpha\beta}$ are integers, too.

[3]To be precise, the Ishibashi states are only formally elements of the bulk Hilbert space, since they have infinite norm.

The following set of coefficients and boundary states provide a solution for these equations. For every Neveu–Schwarz highest weight representation there are two physical boundary state:

$$|\mathbf{k}^{\mathrm{NS}}\rangle = \frac{1}{\sqrt{2}} \sum_{j\in\Delta_{\mathrm{NS}}} \frac{S_{kj}^{[\mathrm{NS},\mathrm{NS}]}}{\sqrt{S_{0j}^{[\mathrm{NS},\mathrm{NS}]}}} |j_+^{\mathrm{NS}}\rangle\rangle + \frac{1}{\sqrt[4]{2}} \sum_{j\in\Delta_{\mathrm{R}}} \frac{S_{kj}^{[\widetilde{\mathrm{NS}},\mathrm{R}]}}{\sqrt{S_{0j}^{[\widetilde{\mathrm{NS}},\mathrm{R}]}}} |j_+^{\mathrm{R}}\rangle\rangle\,, \tag{2.3.17a}$$

$$|\mathbf{k}^{\widetilde{\mathrm{NS}}}\rangle = \frac{1}{\sqrt{2}} \sum_{j\in\Delta_{\mathrm{NS}}} \frac{S_{kj}^{[\mathrm{NS},\mathrm{NS}]}}{\sqrt{S_{0j}^{[\mathrm{NS},\mathrm{NS}]}}} |j_+^{\mathrm{NS}}\rangle\rangle - \frac{1}{\sqrt[4]{2}} \sum_{j\in\Delta_{\mathrm{R}}} \frac{S_{kj}^{[\widetilde{\mathrm{NS}},\mathrm{R}]}}{\sqrt{S_{0j}^{[\widetilde{\mathrm{NS}},\mathrm{R}]}}} |j_+^{\mathrm{R}}\rangle\rangle \tag{2.3.17b}$$

with

$$n^i_{\mathbf{0}^{\mathrm{NS}}\mathbf{k}^{\mathrm{NS}}} = \widetilde{n}^i_{\mathbf{0}^{\mathrm{NS}}\mathbf{k}^{\mathrm{NS}}} = \delta^i_k\,, \qquad m^i_{\mathbf{0}^{\mathrm{NS}}\mathbf{k}^{\mathrm{NS}}} = 0\,, \tag{2.3.18a}$$

$$n^i_{\mathbf{0}^{\mathrm{NS}}\mathbf{k}^{\widetilde{\mathrm{NS}}}} = -\widetilde{n}^i_{\mathbf{0}^{\mathrm{NS}}\mathbf{k}^{\widetilde{\mathrm{NS}}}} = \delta^i_k\,, \qquad m^i_{\mathbf{0}^{\mathrm{NS}}\mathbf{k}^{\widetilde{\mathrm{NS}}}} = 0\,. \tag{2.3.18b}$$

In the Ramond sector there is a one-to-one correspondence between the physical boundary states and the highest weight representations:

$$|\mathbf{k}^{\mathrm{R}}\rangle = \sum_{j\in\Delta_{\mathrm{NS}}} \frac{S_{kj}^{[\mathrm{R},\widetilde{\mathrm{NS}}]}}{\sqrt{S_{0j}^{[\mathrm{NS},\mathrm{NS}]}}} |j_-^{\mathrm{NS}}\rangle\rangle \tag{2.3.19}$$

with

$$n^i_{\mathbf{0}^{\mathrm{NS}}\mathbf{k}^{\mathrm{R}}} = \widetilde{n}^i_{\mathbf{0}^{\mathrm{NS}}\mathbf{k}^{\mathrm{R}}} = 0\,, \qquad m^i_{\mathbf{0}^{\mathrm{NS}}\mathbf{k}^{\mathrm{R}}} = 2\delta^i_k\,. \tag{2.3.20}$$

The coefficients in general can be expressed in terms of the modular S matrix. These relations can be regarded as generalisations of the ordinary Verlinde formula (2.2.19) (see Appendix A.2).

At this point it is still a question whether these boundary states, as solutions of the super Cardy equations, correspond to physical boundary conditions in terms of the fields. In [RP02] the authors provide an integrable lattice realisation for the boundary states derived above. They found boundary conditions on the lattice except for the supersymmetric representation $(\frac{p}{2}, \frac{p+2}{2})$ when p is even.

Setting the boundary condition to the identity one ($\mathbf{k} = 0$) at one of the boundaries yields a very simple Hilbert space. If we choose β corresponding to $|\mathbf{0}^{\mathrm{NS}}\rangle$ and α to $|\mathbf{k}^{\mathrm{NS}}\rangle$ (or $|\mathbf{0}^{\widetilde{\mathrm{NS}}}\rangle$ and $|\mathbf{k}^{\widetilde{\mathrm{NS}}}\rangle$) then from (2.3.9) and (2.3.18,2.3.20) we get

$$\mathcal{Z} = \frac{1}{2}\left(\chi_k^{\mathrm{NS}}(q) + \chi_k^{\widetilde{\mathrm{NS}}}(q))\right) = \mathrm{tr}_k^{\mathrm{NS}} \frac{1}{2}(1 + (-1)^F)\, q^{L_0 - c/24}\,. \tag{2.3.21}$$

Choosing β to be the boundary condition corresponding to $|\mathbf{0}^{\mathrm{NS}}\rangle$ and α to $|\mathbf{k}^{\widetilde{\mathrm{NS}}}\rangle$ (or $|\mathbf{0}^{\widetilde{\mathrm{NS}}}\rangle$ and $|\mathbf{k}^{\mathrm{NS}}\rangle$) we obtain

$$\mathcal{Z} = \frac{1}{2}\left(\chi_k^{\mathrm{NS}}(q) - \chi_k^{\widetilde{\mathrm{NS}}}(q))\right) = \mathrm{tr}_k^{\mathrm{NS}} \frac{1}{2}(1 - (-1)^F)\, q^{L_0 - c/24}\,. \tag{2.3.22}$$

Finally, if we choose β corresponding to $|\mathbf{0}^{\mathrm{NS}}\rangle$ (or $|\mathbf{0}^{\widetilde{\mathrm{NS}}}\rangle$) and α to $|\mathbf{k}^{\mathrm{R}}\rangle$ the result is

$$\mathcal{Z} = \chi_k^{\mathrm{R}}(q)\,. \tag{2.3.23}$$

Thus the Hilbert space consists of the *bosonic levels* of the corresponding module *if the boundary conditions are both of NS or $\widetilde{NS}$ type* and of the *fermionic levels* of this module *if they are different*. For a bosonic primary field the bosonic levels are the integer levels and for a fermionic primary field they are the half-integer levels. Finally, the Hilbert space is the module itself if exactly one of the boundary conditions is of R type.

The case of even p is more complicated due to the special supersymmetric representation $(\frac{p}{2}, \frac{p+2}{2})$.

2.4 Boundary flows

For each boundary condition there is a set of boundary fields that can exist on the boundary. An operator ψ living on the boundary of the strip is mapped under the exponential map to an operator living on the real axis. We want this operator to leave the boundary condition unchanged along the axis, which means that the coefficients in (2.3.8) for $\alpha = \beta$ should be nonzero. Since they can be related to the fusion coefficients this means that the representation ϕ_α should appear in the fusion of ϕ_α with ψ.[4]

Once we know the possible boundary conditions and the corresponding set of boundary fields we can consider boundary perturbations of conformal models, with the general action

$$S = S_{\mathrm{BCFT}} + \sum_i \lambda_i \int\limits_{\partial M} \phi_i(l)\mathrm{d}l\,. \tag{2.4.1}$$

Here the bulk part of the action S_{BCFT} depends on the boundary conditions and ∂M denotes the boundary.

If the scaling dimension of ϕ_i is h_i then the coupling λ_i has mass dimension $1-h_i$. Under scale transformations it has the β-function

$$\dot{\lambda}_i = \beta_i = (1-h_i)\lambda_i + \ldots \tag{2.4.2}$$

The boundary perturbation introduces a mass scale and breaks conformal invariance and thus it induces a renormalisation group flow under scale transformations. If there is no bulk perturbation this flow will take place in the space of boundary conditions of the same bulk universality class. In this space the fixed points are the conformal boundary conditions (see Fig. 2.3).

[4] The coefficients $\widetilde{n}^i_{\alpha\beta}$ are not fusion coefficients themselves, but this does not change the argument essentially.

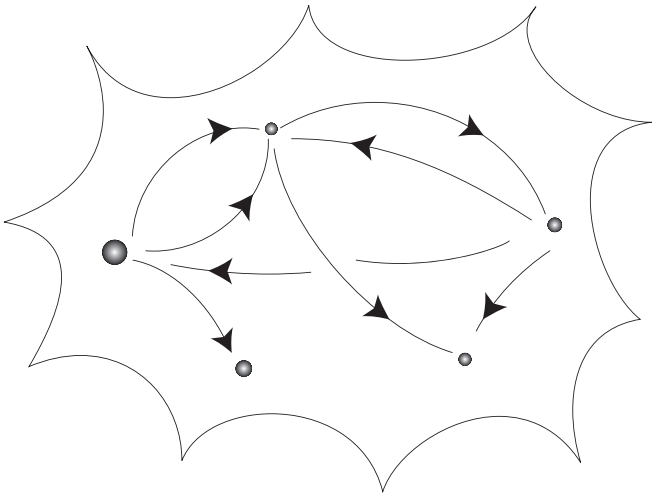

Figure 2.3: Space of flows

Relevant perturbations are realized by fields with $h_i < 1$ since according to (2.4.2) then we flow out from an UV fixed point. For $h_i > 1$ we flow into an IR fixed point, these are the irrelevant perturbations. The case of naively marginal perturbations, i. e. when $h_i = 0$, requires further investigation.

The situation is similar in the supersymmetric case if the boundary perturbation preserves supersymmetry: the RG flow takes place in the space of possible supersymmetric boundary conditions in which the fixed points are the superconformal ones. Here we consider superconformal minimal models on a cylinder perturbed by a single boundary operator at one of the boundaries.

The Hamiltonian of the perturbed superconformal field theory takes the form

$$H = H_{\mathrm{CFT}} + H_{\mathrm{pert}}\,, \tag{2.4.3}$$

where H_{CFT} is the Hamiltonian of the unperturbed theory

$$H_{\mathrm{CFT}} = H_{\alpha 0} = \frac{\pi}{L}(L_0 - \frac{c}{24}) \tag{2.4.4}$$

and H_{pert} comes from the perturbation on the strip:

$$H_{\mathrm{pert}}^{\mathrm{strip}} = \lambda\, \phi_{\mathrm{pert}}(0,0)\,. \tag{2.4.5}$$

The location of the left boundary is at $x = 0$ and we are free to choose $t = 0$ for calculating the spectrum. By the exponential map this becomes on the z-plane

$$H_{\mathrm{pert}} = \lambda \left(\frac{\pi}{L}\right)^{h_{\mathrm{pert}}} \phi_{\mathrm{pert}}(1)_z\,. \tag{2.4.6}$$

Thus the complete Hamiltonian on the plane can be written as

$$H = \frac{\pi}{L}\left[L_0 - \frac{c}{24} + \lambda \left(\frac{L}{\pi}\right)^{1-h_{\mathrm{pert}}} \phi_{\mathrm{pert}}(1)\right]\,. \tag{2.4.7}$$

2.4.1 g-functions

For flows induced by bulk perturbations Zamolodchikov's c-theorem [Zam87] brings order to the space of flows. The theorem states that there is a function which is decreasing along the flows and which is equal to the central charge of the corresponding conformal field theory at the fixed points.

A similar theorem for the boundary flows would be very useful for organising the flows. The first step is to give a quantitative estimate for the number of degrees of freedom associated with a boundary condition. Heuristically this number should decrease along the flow, since due to the perturbation some states acquire mass and 'freeze out' from the spectrum at the conformal IR fixed point.

The g-factor was defined by Affleck and Ludwig [AL91] as the constant term in the logarithm of the partition function of a critical system on a cylinder of length R in the $R \to \infty$ limit:

$$\log \mathcal{Z} = \frac{\pi}{6} c \frac{R}{L} + \log g \,. \tag{2.4.8}$$

This constant term can be interpreted as a zero temperature entropy contribution of the boundaries ($g = g_\alpha g_\beta$). Using finite size scaling arguments it can be shown to be universal: it depends only on the bulk universality class and the boundary condition and not on the microscopic details of the system.

Since

$$\mathcal{Z}_{\alpha\beta}(L,R) = \langle \alpha | e^{-RH^{\mathrm{cl}}(L)} | \beta \rangle \xrightarrow[R\to\infty]{} \frac{\langle \alpha|\Omega\rangle\langle\Omega|\beta\rangle}{\langle\Omega|\Omega\rangle} e^{-RE_0^{\mathrm{cl}}} \,, \tag{2.4.9}$$

where Ω is the ground state of the closed channel Hamiltonian, one gets

$$g_\alpha = \frac{\langle \Omega|\alpha\rangle}{\langle\Omega|\Omega\rangle^{1/2}} \,. \tag{2.4.10}$$

For unitary superconformal minimal models the g-factors for the superconformal boundary conditions can be expressed explicitly using the formulae of section 2.3.1 [Nep01b]:

$$g_{\mathbf{k}_{\mathrm{NS}}} = g_{\mathbf{k}_{\widetilde{\mathrm{NS}}}} = \frac{1}{\sqrt{2}} \frac{S_{k0}^{[\mathrm{NS,NS}]}}{\sqrt{S_{00}^{[\mathrm{NS,NS}]}}} \,, \tag{2.4.11a}$$

$$g_{\mathbf{k}_{\mathrm{R}}} = \frac{1}{\sqrt{2}} \frac{S_{k0}^{[\mathrm{R},\widetilde{\mathrm{NS}}]}}{\sqrt{S_{00}^{[\mathrm{NS,NS}]}}} \,. \tag{2.4.11b}$$

The g-factors can be defined off-critically for a theory with characteristic mass scale M yielding a function $g(l)$ ($l = ML$) that takes the conformal values at the fixed points of the renormalisation group flow ($l = 0$ and $l = \infty$). The partition function is now

$$\mathcal{Z}_{\alpha\beta}(M,L,R) = \sum_{n=0}^{\infty} e^{-LE_n^{\mathrm{op}}(M,R)} = \sum_{n=0}^{\infty} G_\alpha^{(n)}(l) G_\beta^{(n)}(l) e^{-RE_n^{\mathrm{cl}}(M,L)} \,, \tag{2.4.12}$$

with

$$G_\alpha^{(n)}(l) = \frac{\langle \alpha | \psi_n \rangle}{\langle \psi_n | \psi_n \rangle^{1/2}} \,. \tag{2.4.13}$$

The g-function is defined as

$$\log g_\alpha = \log G_\alpha^{(0)}(l) + f_\alpha L \,, \tag{2.4.14}$$

where f_α is the boundary free energy per unit length.

Affleck and Ludwig proposed a theorem [AL91] which states that along boundary renormalisation group flows the g-function is strictly decreasing, and $\dot{g} = 0$ only at the fixed points. They present a perturbative proof for the case when the infrared fixed point lies in the perturbative domain of the ultraviolet fixed point. This happens when the conformal weight of the perturbating operator is close to one: $h_{\text{pert}} = 1 - y$, $0 < y \ll 1$. Let the perturbating part of the Hamiltonian be

$$-\lambda \int \mathrm{d}\tau \phi_{\text{pert}}(\tau) \,. \tag{2.4.15}$$

If ϕ_{pert} is quasi-primary its two and three point functions up to normalisation are fixed by global conformal invariance (see (2.1.7)):

$$\langle \phi_{\text{pert}}(\tau_1) \phi_{\text{pert}}(\tau_2) \rangle = |\tau_1 - \tau_2|^{-2(1-y)} \,, \tag{2.4.16a}$$

$$\langle \phi_{\text{pert}}(\tau_1) \phi_{\text{pert}}(\tau_2) \phi_{\text{pert}}(\tau_3) \rangle = -b \, |(\tau_1 - \tau_2)(\tau_2 - \tau_3)(\tau_1 - \tau_3)|^{-(1-y)} \,. \tag{2.4.16b}$$

Here the coefficient in the two point function is set to one and b is real if the model is unitary.

The β-function up to quadratic order in λ is

$$\beta(\lambda) = \frac{\mathrm{d}\lambda(l)}{\mathrm{d}(\log l)} = y\lambda - b\lambda^2 + \dots \tag{2.4.17}$$

which predicts a fixed point at $\lambda^* = y/b$. The g-function in terms of the running coupling turns out to be

$$\log g(\lambda(l)) = \log \left(g(0) \right) - \lambda(l)^2 y \pi^2 + \frac{2}{3} \lambda(l)^3 \pi^2 b + \mathcal{O}(\lambda^4) \,, \tag{2.4.18}$$

which at the fixed point takes the value

$$\log g(\lambda^*) = \log g_{\text{IR}} = \log g_{\text{UV}} - \frac{1}{3} \pi^2 \frac{y^3}{b^2} \,. \tag{2.4.19}$$

Since b is real this means that $g_{\text{IR}} < g_{\text{UV}}$. We know the fixed point values for minimal models and thus this simple inequality brings some order into the space of boundary flows.

The fixed point in the other direction, i. e. for $\lambda < 0$ is non-perturbative as can easily be seen from the β-function. Friedan and Konechny presented a non-perturbative proof for a version of the g-theorem [FK04]. With their notations

$\log g(\mu L)$ is a function of L and some renormalisation scale μ. They define the boundary entropy as

$$s(\mu L) = (1 - L\partial/\partial L) \log g \tag{2.4.20}$$

which is another interpolating function between the fixed point g-factors. Then they prove the gradient formula

$$g_{ab}(\lambda)\beta^b(\lambda) = -\frac{\partial s}{\partial \lambda^a} \tag{2.4.21}$$

where λ^a form a complete set of boundary conditions, g_{ab} is a certain metric on the space of boundary conditions and $\beta^a(\lambda) = \partial\lambda^a/\partial\mu$ are another kind of β-functions. From the gradient formula it follows directly that

$$\mu\frac{\partial s}{\partial \mu} = \beta^a \frac{\partial s}{\partial \lambda^a} = -g_{ab}\beta^a\beta^b\,, \tag{2.4.22}$$

so s decreases along the renormalisation group flow except at the critical points where $\beta^a = 0$.

It would be very useful to find other non-perturbative ways to calculate the g-function. As we shall see in the next sections, boundary TCSA and boundary TBA are possible approaches for this purpose.

2.5 Truncated Conformal Space Approach

The so-called truncated conformal space approach or TCSA is a numerical method for calculating the spectrum of the theory. In this approach the infinite dimensional Hilbert space is truncated to a finite dimensional vector space by using only those states whose energy is not greater than a threshold value, E_{cut}. This is equivalent to truncating the Hilbert space at a given level. The Hamiltonian is then diagonalised on this truncated space. One can think of this procedure as being equivalent to the variational method: the Ansatzes for the energy eigenstates of the perturbed Hamiltonian are finite linear combinations of the eigenstates of the conformal Hamiltonian. The original idea was proposed in [YZ90], it was applied for the first time for boundary problems in [DPTW98] and in a supersymmetric theory in [BDP$^+$04]. The method used here is based on the techniques of [KTW97], modified for superconformal minimal models for the first time in [Kor06].

The Hamiltonian is given by (2.4.7). Since a numerical calculation requires dimensionless quantities we have to introduce some mass scale, μ and measure the volume (R) and the energies in units of μ. For massive theories μ can be the mass of the lightest particle. In other words, we use the dimensionless quantities $r = \mu R$, $\varepsilon = E/\mu$, $\kappa = \lambda/\mu^{1-h_{\text{pert}}}$ and $\hat{h} = \hat{H}/\mu$:

$$\hat{h} = \frac{\pi}{r}\left[L_0 - \frac{c}{24} + \kappa\left(\frac{r}{\pi}\right)^{1-h_{\text{pert}}}(\hat{G}_{-1/2}\phi_{\text{pert}})(1)\right]\,. \tag{2.5.1}$$

There are two ways for determining the eigenvalues of the total Hamiltonian. The first is to use an orthonormal basis for calculating the matrix elements, which

requires an orthogonalisation process. We can avoid this by choosing the second way, in which the basis is not orthogonal. But then the numerical matrix to be diagonalised is

$$h_{ij} = \langle f_i | h | e_j \rangle \,, \tag{2.5.2}$$

where $\{f_i\}$ are the elements of the reciprocal basis, that is

$$\langle f_i | e_j \rangle = \delta_{ij} \,. \tag{2.5.3}$$

This amounts to calculating the matrix element

$$h_{ij} = (M^{-1})_{ik} \langle e_k | h | e_j \rangle \,, \tag{2.5.4}$$

where M is the inner product matrix:

$$M_{ij} = \langle e_i | e_j \rangle \,. \tag{2.5.5}$$

Using the notation

$$B_{ij} = \langle e_i | \phi_{\mathrm{pert}}(1) | e_j \rangle \tag{2.5.6}$$

it can be expressed as

$$h_{ij} = \frac{\pi}{r} \left[(h_i - \frac{c}{24}) \delta_{ij} + \kappa \left(\frac{r}{\pi} \right)^{1-h_{\mathrm{pert}}} (M^{-1} B)_{ij} \right] . \tag{2.5.7}$$

Here we made use of the fact that the basis elements $\{e_i\}$ are of the form (2.2.9) and thus are eigenvectors of H_0.

Everything we want to know is encoded into the spectrum. For example, from the degeneracy pattern of the energy eigenvalues it is possible to determine the fixed points of the boundary renormalisation group flows. The g-function can also be extracted from the scaling region of $\log \mathcal{Z}$, where $\mathcal{Z}$ is approximated by a finite sum over the TCSA eigenvalues.

The renormalisation group flow can be implemented by varying the volume r while keeping the coupling constant κ fixed. Equivalently – and we choose this way – one can keep r fixed and vary κ on some interval. Starting from $\kappa = 0$, which is the ultraviolet (UV) limit, the matrix h can be diagonalised at different positive and negative values of κ. In both directions the flow approaches a fixed point, that is a new supersymmetric conformal boundary condition. By (2.3.9) we should observe the eigenstates rearranging themselves into a direct sum of representation modules (see the figures in the Appendix). Since by (2.3.18,2.3.20) the coefficients in this sum can only take values 0 and 1, we expect a simple sum of modules at the end of the flows. From the degeneracy pattern of the eigenvalues we can identify the modules (the boundary conditions) using the characters and weight differences of the supersymmetric minimal model in question.

It is important that the errors of the TCSA diagonalisation cannot be handled easily. For example, it may happen that before the flow reaches the scaling region the truncation errors start to dominate. This behaviour can be excluded using various

cuts and checking that the the flow picture does not change essentially, only the precision of the result gets higher with higher cuts.

Establishing the endpoint of the renormalisation group flow by TCSA cannot be regarded as a conclusive proof. What one can see is that the flow goes in the vicinity of some superconformal boundary condition. The exact infrared fixed point can never be reached by TCSA because of the truncation (this can be observed in figure A.3(a)). We are looking for the range where the TCSA trajectory is closest to the fixed point.

2.5.1 Computing the matrix elements of the perturbing field between descendant states

The main part of the work in the TCSA method, apart from the diagonalisation itself, is the calculation of the matrices M and B defined in (2.5.5,2.5.6). Once this is done we have to determine the eigenvalues of the resulting matrix h. The Hilbert space consists of the (half of the) representation corresponding to ϕ_α (see (2.3.21,2.3.22,2.3.23)) and as mentioned above, we choose the following basis elements:

$$L_{n_1}\dots L_{n_k}G_{r_1}\dots G_{r_l}|h\rangle\,, \qquad n_1\le\dots\le n_k<0\,,\;\; r_1<\dots<r_l\le 0\,. \tag{2.5.8}$$

Due to the singular vectors, not all of these are linearly independent. One can obtain a basis for the irreducible submodule by requiring the non-singularity of the inner product matrix level by level. In the Ramond sector we only kept the states which had even number of G_r operators. Choosing the odd parity sector instead gives exactly the same result: the spectrum of the Hamiltonian falls into two identical copies.

The calculation of h is now a question of algebraic manipulations. We use the basic algebraic relations (2.2.6), (2.2.8) and the definition of adjoint operators

$$L_n^\dagger = L_{-n}\,, \tag{2.5.9}$$

$$G_n^\dagger = G_{-n}\,. \tag{2.5.10}$$

In the Ramond case during the calculation of the inner product matrix M we also demand that $\langle\alpha|G_0|\alpha\rangle = 0$ (α is primary), because the inner product of states with opposite fermion parity must vanish.

The calculation of the matrix B is more difficult because it requires some commutation rules to reduce the matrix elements. However, these commutation rules and the applied method for the reduction are different for the Ramond and the Neveu–Schwarz case, therefore we deal with the two cases separately [Kor06].

Neveu–Schwarz case

In the Neveu–Schwarz case we can derive the rules for reducing the three point functions using contour integration technique. From

$$\begin{aligned}\langle L_n A(\infty)|B(0)\rangle = \langle A(\infty)|L_{-n}B(0)\rangle &= \langle A(\infty)|\oint_0 \frac{dz}{2\pi i} z^{-n+1}T(z)B(0)\rangle \\ &= \langle -\oint_\infty \frac{dz}{2\pi i} z^{-n+1}T(z)A(\infty)|B(0)\rangle \quad (2.5.11)\end{aligned}$$

we obtain

$$L_n\Phi(\infty) = -\oint_\infty \frac{dz}{2\pi i} z^{-n+1}T(z)\Phi(\infty)\,. \quad (2.5.12)$$

For a three point function:

$$\begin{aligned}\langle L_{-n}A(\infty)|B(1)|C(0)\rangle &= -\oint_\infty \frac{dz}{2\pi i} z^{n+1}\langle T(z)A(\infty)|B(1)|C(0)\rangle \\ &= \oint_1 \frac{dz}{2\pi i}\sum_{k=-1}^{n}\binom{n+1}{k+1}(z-1)^{k+1}\langle A(\infty)|T(z)B(1)|C(0)\rangle \\ &\qquad + \oint_0 \frac{dz}{2\pi i} z^{n+1}\langle A(\infty)|B(1)|T(z)C(0)\rangle \\ &= \langle A(\infty)|B(1)|L_nC(0)\rangle + \sum_{k=-1}^{n}\binom{n+1}{k+1}\langle A(\infty)|L_kB(1)|C(0)\rangle\,. \quad (2.5.13)\end{aligned}$$

With similar manipulations one can obtain rules for the remaining two initial positions of L_{-n} and their counterparts for the modes G_{-r}. These formulae can be obtained from the algebraic commutation relations (2.1.26,2.2.7) as well. Now they can be applied iteratively to the three point function in the following manner.

First we throw all operators from the first field to the others:

$$\langle L_{-n}A|B(1)|C\rangle = \langle A|B(1)|L_nC\rangle + \sum_{k=-1}^{n}\binom{n+1}{k+1}\langle A|L_kB(1)|C\rangle\,, \quad (2.5.14a)$$

$$\langle G_{-n}A|B(1)|C\rangle = \eta_B\langle A|B(1)|G_nC\rangle + \sum_{k=-1/2}^{n}\binom{n+\frac{1}{2}}{k+\frac{1}{2}}\langle A|G_kB(1)|C\rangle\,. \quad (2.5.14b)$$

Then, exploiting that A is now primary we throw everything from the rightmost

field to the middle one:

$$\langle A|B(1)|L_{-n}C\rangle = -\sum_{k=-1}^{\infty}\binom{-n+1}{k+1}\langle A|L_kB(1)|C\rangle\,, \tag{2.5.15a}$$

$$\langle A|B(1)|G_{-n}C\rangle = -\eta_B\sum_{k=-1/2}^{\infty}\binom{-n+\frac{1}{2}}{k+\frac{1}{2}}\langle A|G_kB(1)|C\rangle\,. \tag{2.5.15b}$$

Note that the infinite sums always truncate at the level of B. Finally we eliminate the operators from the field B (A and C are now primary):

$$\langle A|L_{-n}B(1)|C\rangle = (-1)^n\langle A|B(1)|L_{-1}C\rangle + (-1)^n(n-1)\langle A|B(1)|L_0C\rangle\,, \tag{2.5.16a}$$

$$\langle A|G_{-n}B(1)|C\rangle = \eta_B(-1)^{n+1/2}\langle A|B(1)|G_{-1/2}C\rangle\,. \tag{2.5.16b}$$

Now we can throw L_{-1} and $G_{-1/2}$ back onto the middle field using (2.5.15) and repeat step (2.5.16). Since $G_{-1/2}^{\,2} = L_{-1}$, eventually some L_{-1} and possibly one $G_{-1/2}$ can accumulate on the middle field. The effect of operators L_{-1} is simply differentiating. Since conformal symmetry determines the functional form of the three point function of quasi-primary fields we obtain:

$$\begin{aligned}\langle A|L_{-1}^mB(1)|C\rangle = (h_A-h_B-h_C)(h_A-h_B-h_C-1)\ldots\\ \ldots(h_A-h_B-h_C-m+1)\langle A|B(1)|C\rangle\,.\end{aligned} \tag{2.5.17}$$

In the end we end up with a linear combinations of matrix elements

$$\langle\alpha|(\hat{G}_{-1/2}\phi_{1,3})(1)|\alpha\rangle, \tag{2.5.18a}$$

$$\langle\alpha|\phi_{1,3}(1)|\alpha\rangle, \tag{2.5.18b}$$

that are given by independent structure constants. Depending on the fermion parity of ϕ only one of them is nonzero. So we found that every matrix element can be reduced to a single structure constant. However, we do not need the numerical value of it, because it can be absorbed into the coupling constant κ. The value of κ is related to the physical scale where the crossover takes place (and to the mass scale μ). Since we are interested only in the asymptotic behaviour of the flows (the fixed points), we do not need to fix the real physical scale.

Ramond case

There is a cut in the operator product of $G(z)$ with a Ramond field, which turns the contour integration technique essentially unusable. For this reason we must find another method in the Ramond sector, based on formal commutation relations of the fields.

For the modes of L_n we have the commutation rule (2.1.26). Combining the rule for $n = m$ and $n = 0$ we can get rid of the derivative term, obtaining

$$L_m\phi(z) = z^mL_0\phi(z) + \phi(z)(mhz^m - z^mL_0 + L_m)\,, \tag{2.5.19a}$$

$$\phi(z)L_m = z^m\phi(z)L_0 + (-mhz^m - z^mL_0 + L_m)\phi(z)\,. \tag{2.5.19b}$$

Similarly, since $(\hat{G}_{-1/2}\phi)(z)$ is primary from the point of view of $T(z)$:

$$L_m(\hat{G}_{-1/2}\phi)(z) = z^m L_0(\hat{G}_{-1/2}\phi)(z) + (\hat{G}_{-1/2}\phi)(z)(m(h+1/2)z^m - z^m L_0 + L_m)\,, \quad (2.5.20a)$$

$$(\hat{G}_{-1/2}\phi)(z)L_m = z^m(\hat{G}_{-1/2}\phi)(z)L_0 + (-m(h+1/2)z^m - z^m L_0 + L_m)(\hat{G}_{-1/2}\phi)(z)\,. \quad (2.5.20b)$$

We make use of these formulae in reducing the three point functions. Here is an example of the application of rule (2.5.19a):

$$\begin{aligned}\langle L_{-n}\mathcal{O}_1\alpha|\phi_{1,3}(1)|\mathcal{O}_2\alpha\rangle &= \langle\mathcal{O}_1\alpha|L_n\phi_{1,3}(1)|\mathcal{O}_2\alpha\rangle \\ &= (h_\alpha + nh_{1,3} - h_\alpha)\langle\mathcal{O}_1\alpha|\phi_{1,3}(1)|\mathcal{O}_2\alpha\rangle + \langle\mathcal{O}_1\alpha|\phi_{1,3}(1)|L_n\mathcal{O}_2\alpha\rangle\,, \quad (2.5.21)\end{aligned}$$

where $\mathcal{O}_1$ and $\mathcal{O}_2$ are arbitrary strings of lowering operators.

Because of the cut in the operator product of $G(z)$ and a Ramond field, a Ramond field changes the moding of $G(z)$ from integral to half-integral and vice versa. So it is impossible to obtain a commutation relation of G_r with a Ramond field for fixed r. Fortunately, we can avoid using any (anti)commutation relation for Ramond fields in our calculations. All we need is formally generalising relations (2.2.7) for integral r. From the first rule (2.2.7a) we have

$$G_r\phi(z) = z^{r+1/2}(\hat{G}_{-1/2}\phi)(z) + \eta_\phi\phi(z)G_r\,, \quad (2.5.22a)$$

$$\phi(z)G_r = -\eta_\phi z^{r+1/2}(\hat{G}_{-1/2}\phi)(z) + \eta_\phi G_r\phi(z)\,. \quad (2.5.22b)$$

The relation (2.2.7b) contains an unpleasant derivative term. But just like in the Virasoro case, combining the (2.2.7b) equations for $r = m$ and $r = 0$ yields

$$G_m(\hat{G}_{-1/2}\phi)(z) = z^m G_0(\hat{G}_{-1/2}\phi)(z) + 2mhz^{m-1/2}\phi(z) + \eta_\phi(\hat{G}_{-1/2}\phi)(z)(z^m G_0 - G_m)\,, \quad (2.5.23a)$$

$$(\hat{G}_{-1/2}\phi)(z)G_m = z^m(\hat{G}_{-1/2}\phi)(z)G_0 + \eta_\phi 2mhz^{m-1/2}\phi(z) + \eta_\phi(z^m G_0 - G_m)(\hat{G}_{-1/2}\phi)(z)\,. \quad (2.5.23b)$$

These rules can be used in a similar way to (2.5.21), but only if ϕ_α is a Ramond field ($G_0\phi_\alpha$ is not defined for Neveu–Schwarz fields). Iteratively applying the rules (2.5.20) and (2.5.22), (2.5.23) to a matrix element leads to a linear combination of the following correlation functions:

$$\langle\alpha|(\hat{G}_{-1/2}\phi_{\text{pert}})(1)|\alpha\rangle, \quad (2.5.24a)$$

$$\langle\alpha|\phi_{\text{pert}}(1)|\alpha\rangle, \quad (2.5.24b)$$

$$\langle G_0\alpha|\phi_{\text{pert}}(1)|\alpha\rangle, \quad (2.5.24c)$$

$$\langle\alpha|\phi_{\text{pert}}(1)|G_0\alpha\rangle. \quad (2.5.24d)$$

Here we will apply this method for perturbating operator $\phi_{\text{pert}} = \phi_{1,3}$ which is always a fermion-like operator, so $\eta_{\phi_{1,3}} = -1$. This means that the second one of these four possibilities is zero. Furthermore, due to (2.5.22a)

$$\langle G_0\alpha|\phi_{1,3}(1)|\alpha\rangle = \langle\alpha|(\hat{G}_{-1/2}\phi_{1,3})(1)|\alpha\rangle + \eta_\phi\langle\alpha|\phi_{1,3}(1)|G_0\alpha\rangle. \tag{2.5.25}$$

Since $G_0^\dagger = G_0$

$$\langle G_0\alpha|\phi_{1,3}(1)|\alpha\rangle = \langle\alpha|\phi_{1,3}(1)|G_0\alpha\rangle, \tag{2.5.26}$$

which implies that for $\eta_{\phi_{1,3}} = -1$

$$\langle G_0\alpha|\phi_{1,3}(1)|\alpha\rangle = \frac{1}{2}\langle\alpha|(\hat{G}_{-1/2}\phi_{1,3})(1)|\alpha\rangle. \tag{2.5.27}$$

We see that all matrix elements can be reduced to the three point function

$$\langle\alpha|(\hat{G}_{-1/2}\phi_{1,3})(1)|\alpha\rangle\,, \tag{2.5.28}$$

which is a single structure constant, like in the Neveu–Schwarz case.

It is interesting to note that albeit $G_0\phi_\alpha$ is not really well-defined for ϕ_α being a Neveu–Schwarz field, the Ramond method still works when α is a Neveu–Schwarz field and gives the same result as the contour integral method.

2.6 Boundary Thermodynamic Bethe Ansatz

The Thermodynamical Bethe Ansatz is based on the quantisation of the energy levels using the S-matrices and the reflection factors of the model. Let us imagine that we have several particles with diagonal scattering on a line segment of length R with boundary conditions α and β and we take a particle to the right boundary, to the left boundary and then back to its place. When we pass another particle the wave function of the multi-particle state gets multiplied by the corresponding S-matrix and similarly, at the boundaries it gets multiplied by the reflection factors. While our particle travels around the wave function acquires also the phase e^{ip2R}, but when the original situation is restored, the wave function should be the same:

$$e^{2im_iR\sinh\theta_i}\left(\prod_{j\neq i}S^{ij}(\theta_i-\theta_j)S^{ij}(\theta_i+\theta_j)\right)R^i_\alpha(\theta_i)R^i_\beta(\theta_i) = 1\,, \tag{2.6.1}$$

where all the rapidities are positive. These are the Bethe–Yang equations in the boundary case for diagonal scattering and reflection[5]. They correspond to a tree-level approximation of the quantum field theory and the momenta or energies obtained from these equations are subject to exponential ($\sim e^{-mR}$) corrections.

[5] A more precise derivation is based on comparing different asymptotics of the multi-particle wave function.

For the massless case there is no such derivation for the Bethe–Yang equations, since the corrections are power-like in principle. However, according to experience, they give good and consistent results in the massless case, too. The formal massless limit of equations (2.6.1) is obtained by setting $m = \mu n$, $\theta = \theta_0 + \hat{\theta}$ and taking the joint limit

$$n \to 0 \quad \theta_0 \to \infty \quad ne^{\theta_0} = 1\,. \tag{2.6.2}$$

The momentum and energy become $E = p = \frac{1}{2}\mu e^{\hat{\theta}}$. The reflection factors also may contain some boundary parameter which should be scaled in a proper way while taking the massless limit. So the equations (2.6.1) become

$$e^{2iR\frac{\mu_i}{2}e^{\hat{\theta}_i}} \prod_{j\neq i} S^{ij}(\hat{\theta}_i - \hat{\theta}_j) S^{ij}(\infty) \hat{R}^i_\alpha(\hat{\theta}_i) \hat{R}^i_\beta(\hat{\theta}_i) = 1\,, \tag{2.6.3}$$

where $\hat{R}^i(\hat{\theta})$ are the massless limits of the reflection factors. The left-right scattering becomes trivial for massless particles since $S^{ij}(\infty)$ are constant. Now all positive and negative pseudo-rapidities are allowed. Taking the logarithm we get

$$2iR\frac{\mu_i}{2}e^{\hat{\theta}_i} + \sum_{j\neq i} \Big(\log S^{ij}(\hat{\theta}_i - \hat{\theta}_j) + \log S^{ij}(\infty)\Big) + \log\Big(\hat{R}^i_\alpha(\hat{\theta}_i)\hat{R}^i_\beta(\hat{\theta}_i)\Big) = 2n_i\pi\, i\,, \quad n_i \in \mathbb{Z}\,. \tag{2.6.4}$$

In the following we will drop the hat in the notation of the pseudo-rapidity. In the thermodynamic limit we introduce the density of rapidities. Let $2R\rho_a(\theta)\mathrm{d}\theta$ be the number of particles of type a with rapidities between θ and $\theta + \mathrm{d}\theta$. Similarly, we denote the number of allowed rapidities in this interval, i. e. the rapidities that solve equation (2.6.4) by $2RP_a(\theta)\mathrm{d}\theta$. Those solutions that are not realized by the particles are called 'holes'. Taking the derivative of (2.6.4) we arrive at

$$2\pi P_a(\theta) = \frac{\mu_a}{2}e^{\theta} + \sum_b \int_{-\infty}^{\infty} \mathrm{d}\theta' \rho_b(\theta')\Phi^{ab}(\theta - \theta') + \frac{\Psi^a_{\alpha\beta}(\theta)}{2R}\,, \tag{2.6.5}$$

where

$$\Phi^{ab}(\theta) = \frac{1}{i}\frac{\mathrm{d}}{\mathrm{d}\theta}\log S^{ab}(\theta)\,, \tag{2.6.6a}$$

$$\Psi^a_{\alpha\beta}(\theta) = \frac{1}{i}\frac{\mathrm{d}}{\mathrm{d}\theta}\log\Big(\hat{R}^a_\alpha(\theta)\hat{R}^a_\beta(\theta)\Big)\,. \tag{2.6.6b}$$

Several microscopic n_i sets lead to the same macroscopic $\rho(\theta)$, $P(\theta)$ densities. It does not make any difference how the rapidities within a $\mathrm{d}\theta$ interval are distributed between the particle and the holes, which means

$$\mathrm{d}N = \frac{[P(\theta)\mathrm{d}\theta]!}{[P(\theta)\mathrm{d}\theta]![(P(\theta) - \rho(\theta))\mathrm{d}\theta]!} \tag{2.6.7}$$

possibilities. The corresponding contribution to the entropy is

$$\mathrm{d}S = \log \mathrm{d}N = \log(P(\theta)\mathrm{d}\theta)! - \log(\rho(\theta)\mathrm{d}\theta)! - \log((P(\theta) - \rho(\theta))\mathrm{d}\theta)! \tag{2.6.8}$$

The factorials can be approximated by the Stirling formula:

$$\log n! \approx \frac{1}{2}\log 2\pi - (n+1) + (n+\frac{1}{2})\log(n+1) \approx -n + n\log n\,, \tag{2.6.9}$$

which leads to

$$S = \sum_a \int \mathrm{d}S_a = 2R\sum_a \int_{-\infty}^{\infty} \mathrm{d}\theta \Big\{ P_a(\theta)\log P_a(\theta) - \rho_a(\theta)\log\rho_a(\theta) - \\ \big(P_a(\theta)-\rho_a(\theta)\big)\log\big(P_a(\theta)-\rho_a(\theta)\big)\Big\}\,. \tag{2.6.10}$$

The energy is given by

$$E = 2R\sum_a \int_{-\infty}^{\infty} \mathrm{d}\theta \rho_a(\theta)\frac{\mu_a}{2}e^{\theta}\,. \tag{2.6.11}$$

In the saddle-point approximation for the partition function we minimize the free energy, $F = E - TS$ over the rapidity distribution. The variation of the entropy is given by

$$\delta S = 2R\sum_a \int_{-\infty}^{\infty} \mathrm{d}\theta \left\{ \delta P_a(\theta)\log\frac{P_a(\theta)}{P_a(\theta)-\rho_a(\theta)} - \delta\rho_a(\theta)\log\frac{\rho_a(\theta)}{P_a(\theta)-\rho_a(\theta)}\right\}\,. \tag{2.6.12}$$

We know from (2.6.5) that

$$\delta P_a(\theta) = \sum_b \frac{1}{2\pi}\int_{-\infty}^{\infty}\mathrm{d}\theta' \Phi^{ab}(\theta-\theta')\delta\rho_b(\theta') = \sum_b (\Phi^{ab}\star\delta\rho_b)(\theta)\,, \tag{2.6.13}$$

where we introduced the usual $\star$ notation for the convolution. It proves to be useful to introduce the so-called pseudo-energy functions:

$$e^{-\varepsilon_a(\theta)} = \frac{\rho_a(\theta)}{P_a(\theta)-\rho_a(\theta)}\,. \tag{2.6.14}$$

Now the variation of the free energy is

$$\delta F = \sum_a \int_{-\infty}^{\infty}\mathrm{d}\theta\Big\{\delta\rho_a(\theta)\frac{\mu_a}{2}e^{\theta} - T\sum_b(\Phi^{ab}\star\delta\rho_b)(\theta)L_a(\theta) - T\varepsilon_a(\theta)\delta\rho_a(\theta)\Big\}\,, \tag{2.6.15}$$

where

$$L_a(\theta) = \log(1+e^{-\varepsilon_a(\theta)})\,. \tag{2.6.16}$$

Exploiting the fact that $\Phi^{ab}(\theta)$ are even functions because of the unitarity of the S-matrices (see (A.6.1)), the order of the integrations can be changed in the integral of the convolution:

$$\int_{-\infty}^{\infty} \mathrm{d}\theta (\Phi^{ab} \star \delta\rho_b)(\theta) L_a(\theta) = \int_{-\infty}^{\infty} \mathrm{d}\theta (\Phi^{ab} \star L_a)(\theta) \delta\rho_b(\theta)\,. \tag{2.6.17}$$

We arrive at the condition for the extremum of the free energy ($\delta F = 0$) known as the TBA equations:

$$\varepsilon_a(\theta) = \frac{\mu_a}{T}\frac{e^\theta}{2} - \sum_b \int_{-\infty}^{\infty} \mathrm{d}\theta' \Phi^{ab}(\theta - \theta') \log(1 + e^{-\varepsilon_a(\theta)})\,. \tag{2.6.18}$$

It is interesting to note that in the TBA equation there is no term or parameter that depends on the boundaries. In fact this equation is the bulk TBA equation, that is the TBA equation for periodic boundary condition.

Now the minimal free energy can be written with the following steps. First we substitute for the e^θ term using the TBA equation:

$$\frac{F}{T} = \sum_a \int_{-\infty}^{\infty} \mathrm{d}\theta \rho_a(\theta) \Big\{ \varepsilon_a(\theta) + \sum_b (\Phi^{ab} \star L_a)(\theta) - e^{\varepsilon_a(\theta)} L_a(\theta) - \log(1 + e^{\varepsilon_a(\theta)}) \Big\}\,, \tag{2.6.19}$$

then we change back the convolution using (2.6.17) and substitute $\sum_b (\Phi^{ab} \star \rho_b)(\theta)$ using equation (2.6.5) to arrive at

$$-\frac{F}{T} = \frac{1}{2\pi} \sum_a \int_{-\infty}^{\infty} \mathrm{d}\theta \big(\mu_a R e^\theta + \Psi^a_{\alpha\beta}(\theta) \big) \log(1 + e^{-\varepsilon_a(\theta)})\,. \tag{2.6.20}$$

The left hand side is nothing else than $\log \mathcal{Z}_{\alpha\beta}$ and comparing the result with (2.4.8) or (2.4.12) we conclude that

$$\log(g_\alpha g_\beta) = \frac{1}{2\pi} \sum_a \int_{-\infty}^{\infty} \mathrm{d}\theta\, \Psi^a_{\alpha\beta}(\theta) \log(1 + e^{-\varepsilon_a(\theta)})\,. \tag{2.6.21}$$

For the sake of completeness we cite here the corresponding result for the massive case, which is [LMSS95]

$$\log(g_\alpha g_\beta) = \frac{1}{4\pi} \sum_a \int_{-\infty}^{\infty} \mathrm{d}\theta \left(\Psi^a_{\alpha\beta}(\theta) - 2\Phi^{aa}(2\theta) - \delta(\theta) \right) \log(1 + e^{-\varepsilon_a(\theta)})\,. \tag{2.6.22}$$

However, this TBA formula for the g-function turned out to be incorrect. This is not surprising, since we used a saddle-point approximation in the calculation of

a subleading term. It was observed that for massive models it predicted a wrong T-dependence, but the ratios of g-functions for different boundary conditions were correct. This suggested that a boundary condition independent extra term which is zero in massless models was missing from the formula. It was found in [DFRT04].

The case is much more difficult if the S-matrix of the theory is non-diagonal. Now when a particle takes a round trip it scatters non-diagonally with all the others and at the boundaries. The multiparticle wavefunction should be an eigenfunction of the product of the S and R-matrices. Thus one has to diagonalise the transfer matrix:

$$\begin{aligned} T^{e_1 e_2 \dots e_N}_{a_1 a_2 \dots a_N}(\theta|\theta_1,\dots,\theta_N) = \\ \sum_{\{b_i\},\{c_i\},\{d_i\}} S^{b_1 c_1}_{\alpha a_1}(\theta-\theta_1) S^{b_2 c_2}_{b_1 a_2}(\theta-\theta_2)\dots S^{b_N c_N}_{b_{N-1} a_N}(\theta-\theta_N) R^{d_0}_{b_N}(\theta) \\ S^{d_1 e_1}_{d_0 c_N}(\theta+\theta_N) S^{d_2 e_2}_{d_1 c_{N-1}}(\theta+\theta_{N-1})\dots S^{d_N e_N}_{d_{N-1} c_1}(\theta+\theta_1) R^{\alpha}_{d_N}(\theta)\,, \end{aligned} \quad (2.6.23)$$

which is a very difficult task in general. The particular properties and symmetries of the scattering and reflection matrices can simplify the problem by making some diagonalising techniques applicable. We will mention one of them in section 4.4.

Chapter 3

Boundary renormalisation group flows of unitary superconformal models

In this chapter we try to find general rules for the boundary renormalisation group flows of the unitary supersymmetric conformal minimal models using TCSA [Kor06].

Many papers appeared in the literature about boundary perturbations and the corresponding renormalisation flows of unitary minimal models [RRS00, DRTW00, LSS98, GRW01, GRW00]. Up to now, a systematic charting of the boundary flows of the unitary *superconformal* minimal models has been missing. Although there may be flows within the perturbative domain, for a general study a non-perturbative tool is necessary. We choose the Truncated Conformal Space Approach (TCSA), originally proposed in the paper [YZ90] and applied to boundary problems in [DPTW98] and [GRW01]. The essence of the TCSA is to diagonalise the Hamiltonian of the system on a subspace of the infinite dimensional Hilbert space.

3.1 Hilbert space and the Hamiltonian

To study flows starting from a Cardy boundary condition it is convenient to choose the boundary condition on one of the edges of the strip to correspond to the $h = 0$ primary field, that is $\beta \sim |\mathbf{0}^{\mathrm{NS}}\rangle$ or $|\mathbf{0}^{\widetilde{\mathrm{NS}}}\rangle$. Then (2.3.21) implies that if α and β are both NS or $\widetilde{\mathrm{NS}}$ type boundary conditions, the Hilbert space contains only the bosonic half of a single Neveu–Schwarz module, the one corresponding to α. Similarly, according to (2.3.22), if α is a NS type and β is a $\widetilde{\mathrm{NS}}$ type boundary condition (or vice versa), the Hilbert space consists of the fermionic half of a single α module. Finally, as (2.3.23) shows, if α is a R type boundary condition, the Hilbert space contains a single Ramond module.

At the endpoint of the flow the final boundary condition can be read off in a similar way simply from the spectrum of the Hamiltonian. Since the boundary

condition β does not change along the flow (it is not perturbed), if we start with the bosonic half of a NS module (NS–NS or $\widetilde{\text{NS}}$–$\widetilde{\text{NS}}$) and at the end of the flow we find bosonic part(s) of module(s) then this is a NS→NS (or $\widetilde{\text{NS}} \to \widetilde{\text{NS}}$) type flow. Similarly, if we identify fermionic part(s) then this indicates a NS→ $\widetilde{\text{NS}}$ (or $\widetilde{\text{NS}}$ →NS) type flow.

We have to choose the perturbing field on the boundary α. We would like a perturbation that preserves supersymmetry off-critically. Ramond operators do not spoil supersymmetry but they are boundary condition changing operators, so they cannot live on a boundary. Neveu–Schwarz fields of the form $(\hat{G}_{-1/2}\phi_{\text{pert}})$ also preserve supersymmetry and they can be located on the boundary, so we choose this kind of perturbation. The perturbing operator should be relevant, that is its scaling dimension must be less than one. Finally, since the Hamiltonian is bosonic, ϕ_{pert} must be fermionic. The choice $\phi_{\text{pert}} = \phi_{1,3}$ satisfy all these conditions. $(\hat{G}_{-1/2}\phi_{1,3})$ has conformal weight $p/q < 1$ and $\phi_{1,3}$ is fermionic. The latter can be seen from the fact that in the free fermion limit $p, q \to \infty$ $(q - p = \text{const.})$ $h_{1,3} \to 1/2$.

Our choice also has the advantage that this operator can live on every boundary that has supersymmetric relevant perturbations. This can be seen from the following. Every field appears in its fusion with $\phi_{1,3}$ except for the ones in the first and the last column of the superconformal Kac table $(\phi_{(1,s)}, \phi_{(p-1,s)})$, but the corresponding boundaries do not have any relevant supersymmetric perturbations at all. Also note that being a bosonic field, the fusion with $(\hat{G}_{-1/2}\phi_{1,3})$ maps the GSO-projected subspaces onto themselves. The perturbation $(\hat{G}_{-1/2}\phi_{1,3})$ is an integrable one [Mat90], but we shall not use this property in our analysis.

The Hamiltonian on the plane has the form (see (2.4.7)):

$$H = \frac{\pi}{L}\left[L_0 - \frac{c}{24} + \lambda\left(\frac{L}{\pi}\right)^{1/2-h_{1,3}}\phi_{1,3}(1)\right]. \tag{3.1.1}$$

Using the dimensionless quantities $r = \mu R$, $\varepsilon = E/\mu$, $\kappa = \lambda/\mu^{1-h_{1,3}}$ the dimensionless Hamiltonian $\hat{h} = \hat{H}/\mu$ is:

$$\hat{h} = \frac{\pi}{r}\left[L_0 - \frac{c}{24} + \kappa\left(\frac{r}{\pi}\right)^{1/2-h_{1,3}}(\hat{G}_{-1/2}\phi_{1,3})(1)\right], \tag{3.1.2}$$

where κ characterizes the relation between the boundary coupling and the chosen mass scale μ, thus it is not fixed to any preferred value yet. As it is explained in section 2.5, in the TCSA approach we diagonalize the matrix

$$h_{ij} = \frac{\pi}{r}\left[(h_i - \frac{c}{24})\delta_{ij} + \kappa\left(\frac{r}{\pi}\right)^{1/2-h_{1,3}}(M^{-1}B)_{ij}\right], \tag{3.1.3}$$

where M is the inner product matrix:

$$M_{ij} = \langle e_i | e_j \rangle, \tag{3.1.4}$$

and

$$B_{ij} = \langle e_i | \phi_{1,3}(1) | e_j \rangle \,. \tag{3.1.5}$$

Here the $\{e_i\}$ vectors are of the form (2.2.9) so they are eigenvectors of the conformal Hamiltonian H_0.

3.2 Previous results and expectations

There exist predictions for the boundary flows in the literature [Fre03] in the framework of the coset construction which we summarized in subsection 2.2.2. The boundary flows are predicted in the following way. First we have to find a boundary condition α and a representation S of $su(2)_k \otimes su(2)_2$ so that

$$(0, S|_{su(2)_{k+2}}) \times \alpha = (l, m, l') \,, \qquad (l + m + l' \text{ is even}) \,. \tag{3.2.1}$$

Then a boundary flow is predicted between the following coset boundary configurations:

$$X := (0, S|_{su(2)_{k+2}}) \times \alpha \longrightarrow (S, 0) \times \alpha =: Y \,. \tag{3.2.2}$$

If we want to study flows starting from the boundary condition (l, m, l') with $0 \leq l' \leq k$ we can set $\alpha = (l, m, 0)$ and $S = (l', 0)$. This choice corresponds to the flow

$$(l, m, l') \longrightarrow \bigoplus_J N_{l,l'}^{(k)J} (J, m, 0) \,, \tag{3.2.3}$$

where the $N_{l,l'}^{(k)J}$ are the fusion coefficients in $su(2)_k$.
Similarly, in the case of $2 \leq l' \leq k+2$ the choice $\alpha = (k - l, 2 - m, 0)$ and $S = (k + 2 - l', 0)$ leads to the flow

$$(l, m, l') \longrightarrow \bigoplus_J N_{l,l'-2}^{(k)J} (J, 2 - m, 0) \,. \tag{3.2.4}$$

The boundary conditions which are not covered by these rules are[1] for $l' = k+1$, 1. These correspond to the (r, p) and $(r, 2)$ states. (The boundary conditions $(r, p+1)$ and $(r, 1)$ do not have relevant supersymmetric perturbations.)
For $l' = k + 1$ the suitable choice is $S = (0, 1)$ and $\alpha = (l, m, k + 2)$. Then

$$(l, 0 \text{ or } 2, k + 1) \longrightarrow (l, 1, k + 2) \cong (k - l, 1, 0) \,, \tag{3.2.5a}$$

$$(l, 1, k + 1) \longrightarrow (k - l, 0, 0) \oplus (k - l, 2, 0) \,. \tag{3.2.5b}$$

Finally, for $l' = 1$ one should choose $S = (0, 1)$ and $\alpha = (l, m, 0)$, which yields the flows

$$(l, 0 \text{ or } 2, 1) \longrightarrow (l, 1, 0) \,, \tag{3.2.6a}$$

$$(l, 1, 1) \longrightarrow (l, 0, 0) \oplus (l, 2, 0) \,. \tag{3.2.6b}$$

[1] The author is thankful to S. Fredenhagen for private discussion on these cases.

Let us summarize the $l = 0$ case, when these results give

$$(0, m, l') \longrightarrow (l', m, 0) \qquad 0 \leq l' \leq k\,, \tag{3.2.7a}$$
$$(0, 0\,\text{or}\,2, k+1) \longrightarrow (k, 1, 0) \qquad l' = k+1\,, \tag{3.2.7b}$$
$$(0, 1, k+1) \longrightarrow (k, 0, 0) \oplus (k, 2, 0)\,, \tag{3.2.7c}$$

$$(0, m, l') \longrightarrow (l'-2, 2-m, 0) \qquad 2 \leq l' \leq k+2\,, \tag{3.2.7d}$$
$$(0, 1, 1) \longrightarrow (0, 0, 0) \oplus (0, 2, 0)\,. \tag{3.2.7e}$$

Multiplying both sides of these rules by $(l, 0, 0)$ we get back the rules for general l. In the Kac index language this is the „disorder line rule", discussed in paper [GW04]: if there is a flow between boundary conditions α and β, then there exists a flow between $\alpha \times \gamma$ and $\beta \times \gamma$ where $\times$ denotes the fusion product. For the boundary states of $N = 1$ superminimal models the fusion rule (2.2.18) should be used together with the rules[2]

$$\mathrm{NS} \times \mathrm{NS} = \widetilde{\mathrm{NS}} \times \widetilde{\mathrm{NS}} = \mathrm{NS}\,, \tag{3.2.8a}$$
$$\mathrm{NS} \times \widetilde{\mathrm{NS}} = \widetilde{\mathrm{NS}}\,, \tag{3.2.8b}$$
$$\mathrm{R} \times \mathrm{NS} = \mathrm{R} \times \widetilde{\mathrm{NS}} = \mathrm{R}\,, \tag{3.2.8c}$$
$$\mathrm{R} \times \mathrm{R} = \mathrm{NS} \oplus \widetilde{\mathrm{NS}}\,. \tag{3.2.8d}$$

This means that we only need to determine the flows starting from states in the first row of the Kac table, all the other flows are given by the fusion rules of the operator algebra.

The authors of paper [AR99] have also derived the flows for some Neveu–Schwarz states in the first row of the Kac table, but only for even p.

3.3 TCSA results

We were searching the answers for the following questions.

1. Does our TCSA analysis affirm or disprove the predictions of the Fredenhagen rules?

2. Do all the flows obey the disorder line rule?

3. What happens in the models with p even, where both these rules and the classification of consistent boundary conditions are somewhat uncertain?

[2] These are correct with the choice $m = 0 \iff \mathrm{NS}$ and $m = 2 \iff \widetilde{\mathrm{NS}}$. In case of the other choice a $\mathrm{NS} \leftrightarrow \widetilde{\mathrm{NS}}$ swap is needed.

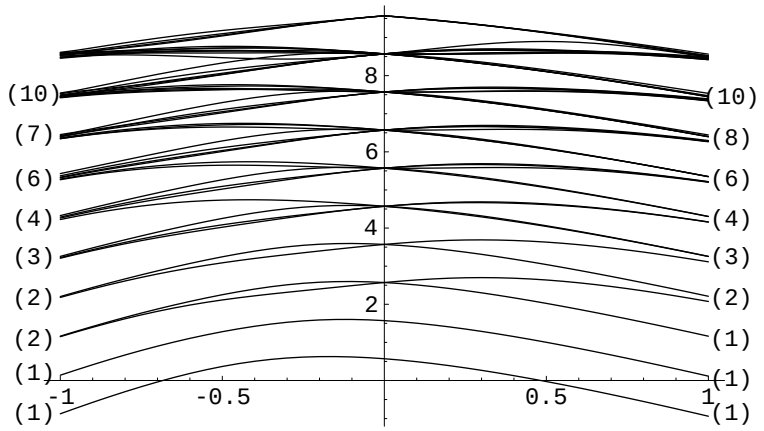

(a) Flows starting from b.c. $(1,3)$ in SM(3,5) (integer levels)

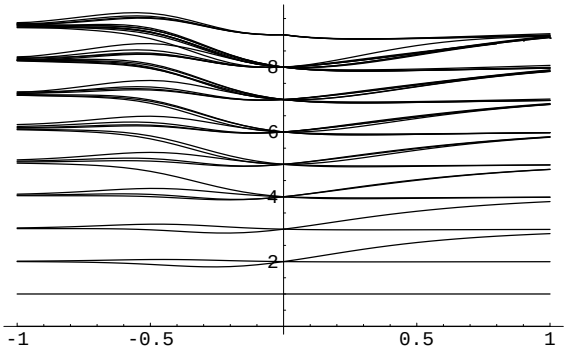

(b) Flows starting from b.c. $(1,3)$ in SM(3,5) (integer levels)

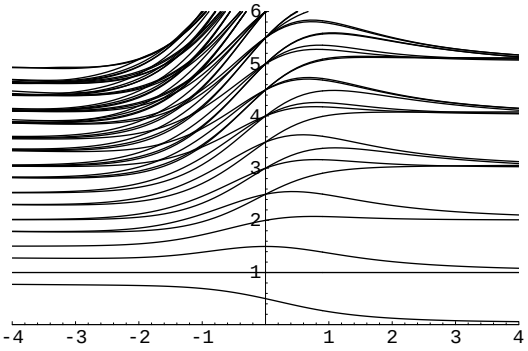

(c) Flows starting from b.c. $(1,3)$ in SM(3,5) (all levels)

Figure 3.1: Flows starting from b.c. $(1,3)$ in SM(3,5)

As it is explained in subsection 2.5, we can read off the IR boundary conditions from the degeneracy pattern of the TCSA spectrum using the characters and weight differences of the minimal model. As an example, let us consider the model SM$(3,5)$ with initial UV boundary conditions $(1,1)$ and $(1,3)$. If both boundary conditions are of NS or $\widetilde{\text{NS}}$ type then the Hilbert space consists of the bosonic levels of the module $(1,3)$ (see (2.3.21)), which are the half-integer levels because of the fermionic nature of $\phi_{1,3}$. The character is

$$\chi_{1,3}(q) = 1+q^{1/2}+q+q^{3/2}+q^2+2q^{5/2}+2q^3+2q^{7/2}+3q^4+4q^{9/2}+4q^{10}+\dots \quad (3.3.1)$$

so the multiplicities of the lowest energy levels of the Hilbert space (from the odd levels) are $(1,1,2,2,4,5,\dots)$. The TCSA energy levels for both signs of κ are plotted in Figure 3.1(a). In Figure 3.1(b) the normalized energy levels, $(\varepsilon-\varepsilon_0)/(\varepsilon_i-\varepsilon_0)$ are shown. The numbers in parentheses are the multiplicities in the IR. Since the

characters for the representations $(1,1)$ and $(1,2)$ are

$$\chi_{1,1}(q) = q^{17/240}(1 + q^{3/2} + q^2 + q^{5/2} + q^3 + 2q^{7/2} + 2q^4 + 2q^{9/2} + 2q^5 + 3q^{11/2} + \dots), \tag{3.3.2}$$

$$\chi_{2,1}(q) = 2q^{49/120}(1 + q + q^2 + 2q^3 + 3q^4 + 4q^5 + 6q^6 + \dots) \tag{3.3.3}$$

we see that we get the half-integer levels of the $(1,1)$ representation and the half of the Ramond module $(2,1)$. The half-integer levels are the fermionic levels in $(1,1)$. Had we started with the fermionic levels of $(1,3)$ we would have got the bosonic levels of $(1,1)$. Thus using again the relations (2.3.21,2.3.22,2.3.23) we conclude that we have found the flows

$$(1,1)_{\widetilde{\rm NS}} \longleftarrow (1,3)_{\rm NS} \longrightarrow (2,1)_{\rm R}\,, \tag{3.3.4}$$

$$(1,1)_{\rm NS} \longleftarrow (1,3)_{\widetilde{\rm NS}} \longrightarrow (2,1)_{\rm R}\,. \tag{3.3.5}$$

In Figure 3.1(c) these flows are plotted together, that is the flows starting from the superponed boundary condition $(1,3)_{\rm NS} \oplus (1,3)_{\widetilde{\rm NS}}$. It can be clearly seen that because the IR fixed point is a NS boundary condition in the negative direction and R in the positive one, the gaps on the positive side are twice as big as those on the negative side.

Our next examples are the flows starting from the boundary condition $(2,2)$ in the minimal model SM$(6,8)$. If we begin with the bosonic (integer) levels of the $(2,2)$ representation we end up in the IR with the multiplicities read off from Figure 3.3.

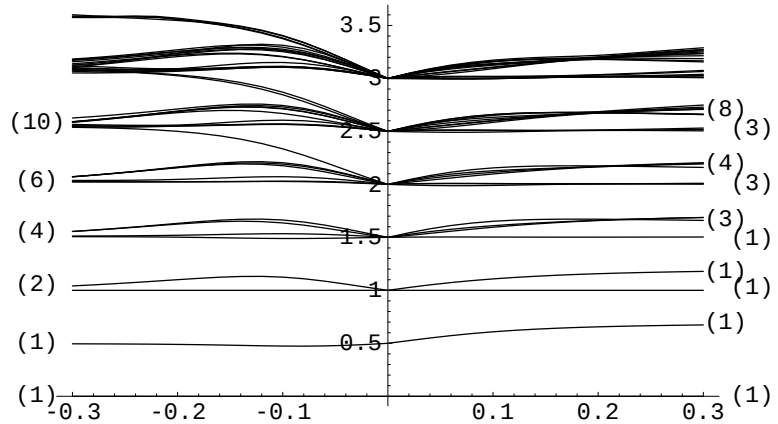

Figure 3.2: Flows starting from b.c. $(2,2)$ in SM(4,6) (integer levels)

In order to identify the corresponding boundary conditions we need the following characters:

$$\chi_{1,1}(q) = q^{-5/96}(1 + q^{3/2} + q^2 + q^{5/2} + q^3 + 2q^{7/2} + 3q^4 + 3q^{9/2} + 3q^5 + 5q^{11/2} + \dots), \tag{3.3.6}$$

$$\chi_{3,1}(q) = q^{25/32}(1 + q^{1/2} + q + q^{3/2} + 2q^2 + 3q^{5/2} + 3q^3 + 4q^{7/2} + 6q^4 + 8q^{9/2} + \dots), \tag{3.3.7}$$

$$\chi_{2,1}(q) = 2q^{25/96}(1 + q + 2q^2 + 4q^3 + 6q^4 + 10q^5 + 16q^6 + \dots)\,. \tag{3.3.8}$$

In the negative direction we clearly see the degeneracy pattern of the Ramond module $(2,1)$. In the positive direction the situation is more complicated: we see the sum of two modules. The integer levels of the module $(1,1)$ and the half-integer levels of $(3,1)$ are mixed together. Note that for both modules the bosonic part is present. Taking into account that $h_{3,1} - h_{1,1} = 5/6$ the order and the distance of the different energy levels coming after each other is fixed and it is indeed what we see from the TCSA spectrum. We conclude that in the IR fixed point a linear combination of Cardy boundary conditions is realized. The corresponding flows are:

$$(2,1)_{\mathrm{R}} \longleftarrow (2,2)_{\mathrm{NS}} \longrightarrow (1,1)_{\mathrm{NS}} \oplus (3,1)_{\mathrm{NS}}\,, \tag{3.3.9}$$

$$(2,1)_{\mathrm{R}} \longleftarrow (2,2)_{\widetilde{\mathrm{NS}}} \longrightarrow (1,1)_{\widetilde{\mathrm{NS}}} \oplus (3,1)_{\widetilde{\mathrm{NS}}}\,. \tag{3.3.10}$$

In the following subsections we summarize the results of the TCSA for the first few unitary models in detail. In the tables the “level” entry indicates the level up to which the agreement between the character and the calculated degeneracy pattern in the IR holds. In the fourth field of every row the dimension of the truncated Hilbert space is shown. The last field contains the number of the corresponding figure that are collected in Appendix A.3.

3.3.1 Flows for $\kappa > 0$

If $2 \leq s \leq p-1$

model	flow	level	dim	fig.
SM$(3,5)$	$(1,2) \to (2,1)$	11	302	A.1(b)
SM$(4,6)$	$(1,3) \to (3,1)$	16	454	A.2(a)
	$(2,2) \to (1,1) \oplus (3,1)$	17,15	536	A.2(b)
	$(1,2) \to (2,1)$	11	414	
SM$(5,7)$	$(1,3) \to (3,1)$	13	388	
	$(2,2) \to (1,1) \oplus (3,1)$	13,11	311	
	$(2,4) \to (3,1)$	12	601	A.3(b)
	$(1,2) \to (2,1)$	11	341	
	$(1,4) \to (4,1)$	7	357	A.3(c)
	$(2,3) \to (2,1) \oplus (4,1)$	8,6	303	A.3(d)
SM$(6,8)$	$(1,3) \to (3,1)$	14	396	
	$(1,5) \to (5,1)$	8	540	A.4(a)
	$(2,2) \to (1,1) \oplus (3,1)$	13,11	316	
	$(2,4) \to (3,1) \oplus (5,1)$	12,8	440	A.4(b)
	$(1,2) \to (2,1)$	10	344	
	$(1,4) \to (4,1)$	7	385	
	$(2,3) \to (2,1) \oplus (4,1)$	8,6	318	
	$(2,5) \to (4,1)$	6	367	A.4(d)
	$(3,2) \to (2,1) \oplus (4,1)$	9,8	317	A.4(e)

For the $(1,s)$ UV boundary conditions the following pattern seems to work:

$$(1,s)_{\mathrm{NS}} \longrightarrow (s,1)_{\mathrm{NS}}\,, \tag{3.3.11a}$$
$$(1,s)_{\widetilde{\mathrm{NS}}} \longrightarrow (s,1)_{\widetilde{\mathrm{NS}}}\,, \tag{3.3.11b}$$
$$(1,s)_{\mathrm{R}} \longrightarrow (s,1)_{\mathrm{R}}\,. \tag{3.3.11c}$$

This agrees with the Fredenhagen result (3.2.7a). In accordance with the disorder line rule we also observe the following pattern for the general UV boundary conditions (cf. (3.2.3)):

$$(r,s) \to (|s-r|+1,1) \oplus (|s-r|+3,1) \oplus \cdots \oplus (\min \tbinom{s+r-1}{2p-(s+r)-1}, 1)\,. \tag{3.3.12}$$

These flows do not change the type of the boundary condition so on the right hand side all boundary conditions are of the same type. Thus, if two of them have different fermion parity, then the half-integer levels of one should combine with the integer levels of the other. That is exactly what we observed.

If $s = p$

model	flow	level	dim	fig.
SM$(3,5)$	$(1,3) \to (2,1)$	6	407	A.1(a)
SM$(4,6)$	$(1,4) \to (3,1)$	18	490	A.2(c)
SM$(5,7)$	$(1,5) \to (4,1)$	7	298	A.3(a)
SM$(6,8)$	$(1,6) \to (5,1)$	14	289	A.4(f)
	$(2,6) \to (4,1)$	7	426	A.4(c)

For the $(1,p)$ boundary conditions we see

$$(1,p)_{\mathrm{NS}} \longrightarrow (p-1,1)_{\mathrm{R}}\,, \tag{3.3.13a}$$
$$(1,p)_{\widetilde{\mathrm{NS}}} \longrightarrow (p-1,1)_{\mathrm{R}}\,, \tag{3.3.13b}$$
$$(1,p)_{\mathrm{R}} \longrightarrow (p-1,1)_{\mathrm{NS}} \oplus (p-1,1)_{\widetilde{\mathrm{NS}}}\,. \tag{3.3.13c}$$

These flows obey the Fredenhagen rules (3.2.7b,3.2.7c). Note that if the initial boundary condition is of Neveu–Schwarz type, then the result of the flow is a Ramond type boundary condition and vice versa. We can also identify the flows related to the flow (3.3.14) by the disorder line rule (corresponding to the rules (3.2.5)):

$$(r,p)_{\mathrm{NS}} \longrightarrow (p-r,1)_{\mathrm{R}}\,, \tag{3.3.14a}$$
$$(r,p)_{\widetilde{\mathrm{NS}}} \longrightarrow (p-r,1)_{\mathrm{R}}\,, \tag{3.3.14b}$$
$$(r,p)_{\mathrm{R}} \longrightarrow (p-r,1)_{\mathrm{NS}} \oplus (p-r,1)_{\widetilde{\mathrm{NS}}}\,. \tag{3.3.14c}$$

3.3.2 If $\kappa < 0$

If $3 \le s \le p$

model	flow	level	dim	fig.
SM$(3,5)$	$(1,3) \to (1,1)$	12	407	A.1(a)
SM$(4,6)$	$(1,3) \to (1,1)$	18	454	A.2(a)
	$(1,4) \to (2,1)$	10	490	A.2(c)
SM$(5,7)$	$(1,3) \to (1,1)$	12	388	
	$(1,5) \to (3,1)$	14	298	A.3(a)
	$(2,4) \to (1,1) \oplus (3,1)$	15,13	601	A.3(b)
	$(1,4) \to (2,1)$	9	357	A.3(c)
	$(2,3) \to (2,1)$	8	303	A.3(d)
SM$(6,8)$	$(1,3) \to (1,1)$	14	396	
	$(1,5) \to (3,1)$	14	540	A.4(a)
	$(2,4) \to (1,1) \oplus (3,1)$	13,11	440	A.4(b)
	$(2,6) \to (3,1) \oplus (5,1)$	17,13	426	A.4(c)
	$(1,6) \to (4,1)$	9	289	A.4(f)
	$(1,4) \to (2,1)$	9	385	
	$(2,3) \to (2,1)$	7	318	
	$(2,5) \to (2,1) \oplus (4,1)$	7,5	367	A.4(d)

For the boundary conditions from the first row of the Kac table we extract the rules

$$(1,s)_{\mathrm{NS}} \longrightarrow (s-2,1)_{\widetilde{\mathrm{NS}}}\,, \tag{3.3.15a}$$
$$(1,s)_{\widetilde{\mathrm{NS}}} \longrightarrow (s-2,1)_{\mathrm{NS}}\,, \tag{3.3.15b}$$
$$(1,s)_{\mathrm{R}} \longrightarrow (s-2,1)_{\mathrm{R}}\,. \tag{3.3.15c}$$

This again gives back the Fredenhagen flow (3.2.7d). We find that the disorder line rule applies: we also identify the flows (c.f. (3.2.4))

$$(r,s) \to (|r-s+2|+1,1) \oplus (|r-s+2|+3,1) \oplus \cdots \oplus (\min \tbinom{s+r-3}{2p-(s+r)+1}, 1)\,. \tag{3.3.16}$$

In the Neveu–Schwarz case these flows, just like their ancestors, change the type of the boundary conditions. The comment given in case 3.3.1 is true here as well.

If $s = 2$

model	flow	level	dim	fig.
SM(3, 5)	$(1,2) \to (1,1)$	9	302	A.1(b)
SM(4, 6)	$(2,2) \to (2,1)$	9	536	A.2(b)
	$(1,2) \to (1,1)$	22	414	
SM(5, 7)	$(2,2) \to (2,1)$	7	311	
	$(1,2) \to (1,1)$	20	341	
SM(6, 8)	$(2,2) \to (2,1)$	7	316	
	$(1,2) \to (1,1)$	20	344	
	$(3,2) \to (3,1)$	16	317	A.4(e)

We found (see also (3.2.7e))

$$(1,2)_{\mathrm{R}} \longrightarrow (1,1)_{\mathrm{NS}} \oplus (1,1)_{\widetilde{\mathrm{NS}}}\,. \tag{3.3.17}$$

This is another example for a flow starting from a Ramond boundary condition running to a Neveu–Schwarz one. The disorder line rule is consistent with the flows (as in (3.2.6)).

$$(r,2)_{\mathrm{NS}} \longrightarrow (r,1)_{\mathrm{R}}\,, \tag{3.3.18a}$$
$$(r,2)_{\widetilde{\mathrm{NS}}} \longrightarrow (r,1)_{\mathrm{R}}\,, \tag{3.3.18b}$$
$$(r,2)_{\mathrm{R}} \longrightarrow (r,1)_{\mathrm{NS}} \oplus (r,1)_{\widetilde{\mathrm{NS}}}\,. \tag{3.3.18c}$$

It is interesting that despite the lack of a complete classification of consistent boundary states for p even, our results indicate the same rules for these cases. The only exception is the boundary condition corresponding to the supersymmetric $(\frac{p}{2}, \frac{p+2}{2})$ representation for which the resulting degeneracy pattern do not correspond to the energy levels of any fixed point Hilbert space. Since our Hamiltonian (3.1.1) was written based on its algebraic properties, every Hamiltonian for physical

boundary conditions is of this form, but it is not guaranteed that every one of our Hamiltonians is physical. Taking into account that no lattice realisation was found for the state $(\frac{p}{2}, \frac{p+2}{2})$ [RP02], it is possible that there is simply no corresponding physical boundary condition for this solution of the Cardy equations.

It is also interesting to note that via the symmetry transformation of the Kac table ($r \to p - r$, $s \to p + 2 - s$) the rules (3.3.12), (3.3.14) are mapped to the rules (3.3.16) and (3.3.18), respectively. This means that the two groups of rules ($\kappa < 0$, $\kappa > 0$) are not independent.

We note that although one can only approach and never reach the fixed point, the endpoints are $(r, 1)$ type boundary conditions that have no relevant supersymmetric perturbations, so it is reasonable to take our observations to be strong indications for the exact result.

Regarding the questions addressed at the beginning of this section we have positive answers for the first two: the TCSA results confirmed the Fredenhagen rules and are consistent with the disorder line rule. For the third question we saw that a natural extension of the rules works in the models with even p.

Chapter 4

Boundary renormalisation group flows in the supersymmetric Lee–Yang model and its extensions

So far we dealt with unitary superconformal models. In this chapter we investigate non-unitary models and mainly their prototype, the supersymmetric Lee–Yang model. We determine the reflection factors and the boundary flows of this model and check them using boundary TCSA and boundary TBA. This chapter is based on paper [Kor07] of the author.

Several papers appeared in the literature that deal with the consistent boundary conditions and reflection factors [Nep01b, Tot04, BPT02, BK03, Nep01a, ANS06], the boundary perturbations and the corresponding renormalisation flows [NA02, FPR03, AN01, Kor06] of two-dimensional supersymmetric field theories.

One of the simplest supersymmetric theory is the supersymmetric Lee–Yang (SLY) model and here we study this model in the presence of boundaries. In a paper [AN01] Ahn and Nepomechie proposed reflection factors for the superconformal boundary conditions and determined a boundary flow using Boundary Thermodynamic Bethe Ansatz (BTBA). Here we argue that both their reflection factor and one of their TBA formulae are mistaken. We propose different reflection factors which we check using Boundary Truncated Conformal Space Approach (BTCSA). We also predict a different boundary flow using BTBA and we compare the fixed points and the change of the boundary entropy again with our BTCSA results.

4.1 The supersymmetric Lee–Yang model

The supersymmetric Lee–Yang model or the superconformal minimal model SM(2,8) is a non-unitary conformal field theory with central charge $c = -\frac{21}{4}$. The super Kac-table with the highest weights of the primary fields is

0	$-\frac{3}{32}$	$-\frac{1}{4}$	$-\frac{7}{32}$	$-\frac{1}{4}$	$-\frac{3}{32}$	0

This model can also be defined as the minimal model M(3,8) with Kac table

0	-7/32	-1/4	-3/32	1/4	25/32	3/2
3/2	25/32	1/4	-3/32	-1/4	-7/32	0

Suitable combinations of the Virasoro representations constitute irreducible representations of the superconformal algebra:

$$\Big(0\Big)_{\text{SVir}} \longleftrightarrow \Big(0\Big)_{\text{Vir}} \oplus \Big(\frac{3}{2}\Big)_{\text{Vir}}, \tag{4.1.1a}$$

$$\Big(-\frac{1}{4}\Big)_{\text{SVir}} \longleftrightarrow \Big(-\frac{1}{4}\Big)_{\text{Vir}} \oplus \Big(\frac{1}{4}\Big)_{\text{Vir}}, \tag{4.1.1b}$$

$$\Big(-\frac{7}{32}\Big)_{\text{SVir}} \longleftrightarrow \Big(-\frac{7}{32}\Big)_{\text{Vir}} \oplus \Big(\frac{25}{32}\Big)_{\text{Vir}}, \tag{4.1.1c}$$

$$\Big(-\frac{3}{32}\Big)_{\text{SVir}} \longleftrightarrow \Big(-\frac{3}{32}\Big)_{\text{Vir}}. \tag{4.1.1d}$$

Since the superprimary fields are also Virasoro primary fields and the g-factors are the same for the NS and $\widetilde{\text{NS}}$ boundaries, the g-factors of the various conformal boundary conditions can be calculated in the Virasoro picture. The matrix elements of the S modular transformation are

$$S_{(r,s),(r',s')} = 2\sqrt{\frac{2}{pq}}(-1)^{rs'+r's+1} \sin\left(rr'\frac{q}{p}\pi\right) \sin\left(ss'\frac{p}{q}\pi\right) \tag{4.1.2}$$

and according to [DRTW00] the g-factors are given by

$$g_{(1,s)} = \frac{S_{\Omega,(1,s)}}{\sqrt{|S_{\Omega,0}|}} \tag{4.1.3}$$

where 0 denotes the conformal vacuum and Ω denotes the state of lowest conformal weight. In our case $0 = (1,1)$ and $\Omega = (1,3)$, so

$$g_{(1,s)} = \frac{(-1)^s}{\sqrt{2}} \frac{\sin\frac{9\pi}{8}s}{\sqrt{\sin\frac{\pi}{8}}}. \tag{4.1.4}$$

As in the case of the unitary models we choose the $\beta = (1,1)$ boundary condition at one of the edges and $\alpha = (1,s)$ at the other one. We have seen that the partition function for Neveu–Schwarz boundary conditions becomes (2.3.21,2.3.22):

$$\mathcal{Z}(L,R) = \text{tr}_{(1,s)} \frac{1 \pm (-1)^F}{2} e^{-\pi\frac{L}{R}(L_0 - c/24)}, \tag{4.1.5}$$

where the sign is "+" if both boundaries are of NS or $\widetilde{\text{NS}}$ type and "−" if they are different. The only Neveu–Schwarz boundary condition that has relevant perturbations is the $(1,3)$ boundary condition, so $s=3$.

Similarly to the unitary case we consider the boundary perturbation of this model defined by the action:

$$\mathcal{A}=\mathcal{A}_{\text{SM}(2,8)+\text{SCBC}(1,3)}+h\int_{-\infty}^{\infty}\mathrm{d}t\,(\hat{G}_{-1/2}\phi_{1,3})(0,t)\,. \tag{4.1.6}$$

4.2 The reflection factor

We will obtain the S-matrix and the reflection factor of our theory as the massless limit of the scaling boundary supersymmetric Lee–Yang model defined by the action

$$\mathcal{A}=\mathcal{A}_{\text{SM}(2,8)+\text{SCBC}(1,3)}+g\int\mathrm{d}x\int_{-\infty}^{\infty}\mathrm{d}t\,(G_{-1/2}\bar{G}_{-1/2}\phi_{1,3})(x,t)+h\int_{-\infty}^{\infty}\mathrm{d}t\,(\hat{G}_{-1/2}\phi_{1,3})(0,t)\,. \tag{4.2.1}$$

This is a massive theory and the mass of the elementary excitation is related to the coupling g:

$$g=\text{const.}\cdot m^{5/2}\,. \tag{4.2.2}$$

The key idea for obtaining the S-matrix and reflection factor is considering this model as a reduction of the supersymmetric sine–Gordon (SSG) model. The idea originates in the work of Smirnov [Smi90] and it was first applied in supersymmetric context for bulk S-matrices in [Ahn91]. The SSG S-matrix was also derived in [Ahn91], the formulae are collected in appendix A.4.

If $\lambda>2$ in the SSG model the pole in the S-matrix describing the scattering of the first breather on itself corresponds to the second breather as a bound state. For $\lambda<2$ only the first breather is in the spectrum and the pole is alternatively explained by the Coleman–Thun mechanism [CT78] which requires the presence of solitons in the theory. However, at the particular value of the coupling constant $\lambda=\frac{3}{2}$ the masses and the S-matrices for the first and the would-be second breathers become equal: $m_1=m_2$ and $S^{1,1}_{\text{SSG}}=S^{1,2}_{\text{SSG}}=S^{2,2}_{\text{SSG}}$, so the pole can be explained by the self fusion of the only breather and the solitons can be projected out consistently from the theory [Ahn91]. Thus the SSG model is reduced to the supersymmetric scaling Lee–Yang model containing only one superdoublet. The S-matrix simplifies to

$$S_{\text{SLY}}(\theta)=S_{\text{LY}}(\theta)S_{\text{SUSY}}(\theta) \tag{4.2.3}$$

where

$$S_{\text{LY}}(\theta)=\frac{\sinh(\theta)+i\sin(\frac{2\pi}{3})}{\sinh(\theta)-i\sin(\frac{2\pi}{3})} \tag{4.2.4}$$

and

$$S_{\mathrm{SUSY}}(\theta) = \tilde{Z}(\theta) \times \begin{pmatrix} 1 + 2i\,\frac{\sin(\frac{\pi}{3})}{\sinh(\theta)} & 0 & 0 & \frac{\sin(\frac{\pi}{3})}{\cosh(\frac{\theta}{2})} \\ 0 & 1 & i\,\frac{\sin(\frac{\pi}{3})}{\sinh(\frac{\theta}{2})} & 0 \\ 0 & i\,\frac{\sin(\frac{\pi}{3})}{\sinh(\frac{\theta}{2})} & 1 & 0 \\ \frac{\sin(\frac{\pi}{3})}{\cosh(\frac{\theta}{2})} & 0 & 0 & -1 + 2i\,\frac{\sin(\frac{\pi}{3})}{\sinh(\theta)} \end{pmatrix}, \tag{4.2.5}$$

$$\tilde{Z}(\theta) = \frac{\sinh(\frac{\theta}{2})}{\sinh(\frac{\theta}{2}) + i\sin(\frac{\pi}{3})} \exp\left\{ \int_0^\infty \frac{\mathrm{d}t}{t} \frac{\sinh(\frac{t}{3})\sinh(\frac{2t}{3})}{\cosh^2(\frac{t}{2})\cosh(t)} \sinh(\frac{it\theta}{\pi}) \right\}. \tag{4.2.6}$$

This is the S-matrix used also by Ahn and Nepomechie in [AN01]. For later convenience we introduce the notation

$$Z(\theta) = S_{\mathrm{LY}}(\theta)\tilde{Z}(\theta)\,. \tag{4.2.7}$$

It is easy to check that this S-matrix satisfies the appropriate unitarity and crossing relations and that the Yang–Baxter equations are also satisfied (cf. A.6).

4.2.1 The "folding"

We have seen that at the particular coupling $\lambda = \frac{3}{2}$ the bulk SSG model can be reduced to the SLY model. For this reduction to be consistent also in the boundary case it is necessary that at this point the reflection factors for the 1st and the would-be 2nd breather also be equal. This requirement gives functional relations between the two SSG boundary parameters, η and ϑ (first considered in [Nep01a]).

The reflection factors of the boundary SSG model can be found in Appendix A.5. In the $BSSG^+$ case, as it is called in [BPT02], the supersymmetric factor $R_{\mathrm{SUSY}}(\theta)$ (see A.5.8) does not contain the boundary parameters and the only way it depends on the species of the breather is through the parameter ρ which at this special coupling is $\rho_k = \pi - k\frac{2\pi}{3}$. From $\rho_1 = -\rho_2 = \frac{\pi}{3}$ it is obvious that $\mathcal{A}_\pm(\theta)$ are automatically the same for $k = 1, 2$.

Now we turn to the scalar part, i. e. to the SG reflection factors. It turns out that $R^{(1)}(\theta) = R^{(2)}(\theta)$ if

$$\eta = i\vartheta + \frac{2k+1}{2}\pi\,, \qquad\qquad k \in \mathbb{Z}\,. \tag{4.2.8}$$

If $k = 1$, i. e. $\eta = i\vartheta + \frac{3\pi}{2}$ then $R^{(1)} = R^{(2)} = R_0$ where

$$R_0(\theta) = \left(\frac{1}{2}\right)\left(\frac{3}{2}\right)\left(\frac{4}{2}\right)^{-1}, \tag{4.2.9}$$

where we introduced the notation

$$(x) = \frac{\sin(\frac{\theta}{2i} + x\frac{\pi}{6})}{\sin(\frac{\theta}{2i} - x\frac{\pi}{6})}\,.$$

If $k=1$, i. e. $\eta = i\vartheta + \frac{\pi}{2}$ then $R^{(1)} = R^{(2)} = R_I$ with

$$R_I(\theta) = R_0(\theta)\left(\frac{1+b}{2}\right)\left(\frac{1-b}{2}\right)^{-1}\left(\frac{5-b}{2}\right)\left(\frac{5+b}{2}\right)^{-1} = R_0(\theta)\left(S_{\mathrm{LY}}\Big(\theta + i\frac{b+3}{6}\pi\Big)S_{\mathrm{LY}}\Big(\theta - i\frac{b+3}{6}\pi\Big)\right)^{-1}, \quad (4.2.10)$$

where we introduced the parameter $b = \frac{4i}{\pi}\vartheta - 2$. $R_0(\theta)$ and $R_I(\theta)$ are the same reflection factors as those given by Dorey et al. (for example in [DTW99]).

Finally, if $k=-1$, i, e. $\eta = i\vartheta - \frac{\pi}{2}$ then $R^{(1)} = R^{(2)} = R_{II}$ where

$$R_{II}(\theta) = R_0(\theta)\left(\frac{b-1}{2}\right)\left(\frac{b+3}{2}\right)^{-1}\left(\frac{b-3}{2}\right)\left(\frac{5+b}{2}\right)^{-1} = R_0(\theta)\left(S_{\mathrm{LY}}\Big(\theta + i\frac{b+1}{6}\pi\Big)S_{\mathrm{LY}}\Big(\theta - i\frac{b+1}{6}\pi\Big)\right)^{-1}. \quad (4.2.11)$$

The other values of k do not lead to new reflection factors. With the redefinition $b \to b+4$ the factor $R_{II}(\theta)$ becomes

$$R_{II}(\theta) = R_0(\theta)\left(\frac{b+3}{2}\right)\left(\frac{5-b}{2}\right)\left(\frac{b+1}{2}\right)\left(\frac{3-b}{2}\right) = R_0(\theta)\left(S_{\mathrm{LY}}\Big(\theta + i\frac{b+5}{6}\pi\Big)S_{\mathrm{LY}}\Big(\theta - i\frac{b+5}{6}\pi\Big)\right)^{-1}, \quad (4.2.12)$$

which can be identified as the reflection factor for the excited boundary [DTW99]. Thus R_0 and R_I are the two ground state reflection factors for the two boundary conditions of the Lee–Yang model. They satisfy the boundary unitarity and boundary crossing equations (A.6):

$$R(\theta)R(-\theta) = 1\,, \quad (4.2.13)$$

$$R\Big(\frac{i\pi}{2} - \theta\Big) = S_{\mathrm{LY}}(2\theta)R\Big(\frac{i\pi}{2} + \theta\Big)\,. \quad (4.2.14)$$

The SLY reflection factors also satisfy the boundary unitarity equation provided $\mathcal{A}_\pm(\theta)\mathcal{A}_\pm(-\theta) = 1$ and this is indeed true:

$$\mathcal{A}_\pm(\theta)\mathcal{A}_\pm(-\theta) = 2\frac{\cos(\frac{\theta}{2i} \mp \frac{\pi}{4})\cos(-\frac{\theta}{2i} \mp \frac{\pi}{4})}{\cosh(\theta)} = 1\,. \quad (4.2.15)$$

The boundary crossing equations are

$$2^{-\frac{2\theta}{i\pi}}R^\phi_\phi\Big(\frac{i\pi}{2} - \theta\Big) = S^{\phi\phi}_{\phi\phi}(2\theta)R^\phi_\phi\Big(\frac{i\pi}{2} + \theta\Big) + S^{\phi\phi}_{\psi\psi}(2\theta)R^\psi_\psi\Big(\frac{i\pi}{2} + \theta\Big)\,, \quad (4.2.16a)$$

$$2^{-\frac{2\theta}{i\pi}}R^\psi_\psi\Big(\frac{i\pi}{2} - \theta\Big) = S^{\psi\psi}_{\psi\psi}(2\theta)R^\psi_\psi\Big(\frac{i\pi}{2} + \theta\Big) + S^{\psi\psi}_{\phi\phi}(2\theta)R^\phi_\phi\Big(\frac{i\pi}{2} + \theta\Big)\,. \quad (4.2.16b)$$

Since the Lee–Yang parts satisfy the scalar version of the boundary crossing condition we only have to check that the supersymmetric factors S_{SUSY} and R_{SUSY} satisfy (4.2.16). Using the integral representations for them this can be proved analytically. We also checked that the matrix parts satisfy the boundary Yang–Baxter equations as well.

It seems plausible that the two supersymmetric reflection factors, $R_0(\theta)R_{\mathrm{SUSY}}(\theta)$ and $R_I(\theta)R_{\mathrm{SUSY}}(\theta)$ are the reflection factors for the two Neveu–Schwarz boundary conditions of the supersymmetric scaling Lee–Yang model, since for the Ramond type boundary conditions we do not expect diagonal reflection factors (the fermion parity can change). It is also natural to think that R_0R_{SUSY} is for the $(1,1)$ boundary condition, because it does not depend on any boundary parameter. This corresponds to the fact that no boundary field can live on $(1,1)$.

We emphasize that the reflection factors proposed here are different from the non-diagonal one proposed by Ahn and Nepomechie in [AN01]. The $BSSG^-$ reflection factors are non-diagonal [BPT02] and they are likely related to the Ramond boundary states that can change fermion parity.

4.2.2 Relation between the boundary parameter b and the boundary coupling h

Following reference [DPTW98] it is possible to conjecture the relation between b and the coupling constant of the boundary perturbation, h (a similar argument was used also in [BPTT02]). In that paper it was found that the transformation $b \to 4-b$ is a symmetry of the model, since this change of b maps the reflection factors of the ground state and excited boundaries into each other. For $b > 2$ the pole at $\theta = \frac{i(b+1)\pi}{6}$ in R_I, which corresponds to an excited boundary, leaves the physical strip $0 < \mathrm{Im}(\theta) < \pi/2$, but at the same time the pole at $\theta = \frac{i(5-b)\pi}{6}$ in R_{II} enters. Thus for $b > 2$ R_{II} describes the ground state boundary and R_I the excited boundary. Probably a similar phenomenon occurs in our case, but exactly the same thing can not work, since now the excited boundary state is a doublet and R_{II} is a 4x4 matrix, while the boundary ground state is a singlet. However, at the pole $\theta = \frac{i(5-b)\pi}{6}$ R_{II} becomes a 1-dimensional projector. Since the reflection factors are manifestly periodic in b with a period of 12 there is a point ($b = 8$) beyond which the boundary energies swap back and the ground state will be a singlet again. This gives a symmetry $b \to 10 - b$. Together with the trivial symmetry $b \to -6 - b$ of the reflection factors this results in a periodicity of the physical spectrum in b with a period of 16. Similarly to the case in [DPTW98], the value at half way between the fixed points of the two symmetries should correspond to $h = 0$. This leads to the following conjecture for the relation between b and h:

$$h = h_c \sin\left(\frac{(b-1)\pi}{8}\right) \tag{4.2.17}$$

with $h_c = \alpha m^{3/4}$ on dimensional grounds where α is some numeric constant and m is some mass scale of the model, e. g. the mass of the particle.

4.2.3 The massless limit

Now we take the $g \to 0$ ($m \to 0$) limit in order to obtain the reflection factors for our massless theory defined in (4.1.6). It is the supersymmetric part $R_{\rm SUSY}$ for which it is easier to calculate the massless limit since it does not contain boundary parameters. All we have to do is to take the limit $\theta \to \infty$.

$\mathcal{A}_\pm(\theta)$ can be written in the following form:

$$\mathcal{A}_\pm(\theta) = \sqrt{2} 2^{-\frac{\theta}{i\pi}} \frac{\cos(\frac{\theta}{2i} \mp \frac{\pi}{4})}{\sqrt{\cosh(\theta)}} e^{\,I(\theta)}\,, \tag{4.2.18}$$

where

$$I(\theta) = \int_0^\infty \frac{\mathrm{d}t}{t} f(t) \sinh(\frac{\theta}{i\pi} t) = -\frac{1}{2} \int_{-\infty}^\infty \frac{\mathrm{d}t}{t} e^{it\theta} f(t\pi) \tag{4.2.19}$$

with

$$f(t) = -\frac{1}{4} \frac{\cosh(\frac{t}{6}) + \cosh^2(\frac{t}{2})}{\cosh^2(\frac{t}{4}) \cosh^2(\frac{t}{2})}\,. \tag{4.2.20}$$

Now

$$I(\infty) = -\frac{i\pi}{2} f(0) = \frac{1}{4} i\pi \tag{4.2.21}$$

so

$$\lim_{\theta\to\infty} 2^{\frac{\theta}{i\pi}} \mathcal{A}_\pm(\theta) = \sqrt{2}\, \frac{\frac{1}{2}\, e^{\frac{\theta}{2}}\, e^{\mp i\frac{\pi}{4}}}{\sqrt{\frac{1}{2}\, e^{\theta}}}\, e^{\frac{i\pi}{4}} = e^{\frac{i\pi}{4}(1\mp 1)}\,, \tag{4.2.22}$$

which means that

$$R_{\rm SUSY}(\theta) \xrightarrow[\theta\to\infty]{} \begin{pmatrix} 1 & 0 \\ 0 & i \end{pmatrix}\,. \tag{4.2.23}$$

Let us turn to the scalar parts. $R_0(\theta)$ does not depend on the boundary parameters and

$$\lim_{\theta\to\infty} R_0(\theta) = 1\,. \tag{4.2.24}$$

$R_I(\theta)$ does depend on the boundary parameter b. In the massless limit we want to keep h fixed, which means that the sine in (4.2.17) has to go to infinity in a proper way. This can be achieved only if b becomes complex. Setting $b = -3 - i\hat{b}$

$$h = -h_c \cosh(\frac{\hat{b}\pi}{8}) m^{\frac{3}{4}} \longrightarrow -\frac{h_c}{2} (e^{\frac{\hat{b}\pi}{6}} m)^{\frac{3}{4}}\,. \tag{4.2.25}$$

This means that $m\, e^{\frac{\hat{b}\pi}{6}}$ should be kept fixed while $m \to 0$ and $\hat{b} \to \infty$. We also want to keep the physical momentum, $m\cosh(\theta)$ fixed, which implies that me^θ is constant. We conclude that while θ, $b \to \infty$ the combination $\theta - \frac{\hat{b}}{6}\pi$ is fixed. So

$$R_I(\theta) = R_0(\theta) \left(S_{\rm LY}\Big(\theta + \frac{\hat{b}}{6}\pi\Big) S_{\rm LY}\Big(\theta - \frac{\hat{b}}{6}\pi\Big) \right)^{-1} \longrightarrow S_{\rm LY}^{-1}\Big(\theta - \frac{\hat{b}}{6}\pi\Big) = S_{\rm LY}^{-1}(\hat{\theta} - \theta_{\rm B}) \tag{4.2.26}$$

where $\hat{\theta}$ is the pseudo-rapidity and θ_{B} is related to $\hat{b}$.[1]

Therefore the massless reflection factors for the two Neveu–Schwarz boundary conditions of the SLY model are

$$\hat{R}_0 = \begin{pmatrix} 1 & 0 \\ 0 & i \end{pmatrix} \quad \text{and} \quad \hat{R}_I(\hat{\theta}) = S_{\mathrm{LY}}^{-1}(\hat{\theta} - \theta_{\mathrm{B}})\hat{R}_0 \,. \tag{4.2.27}$$

In the following we will omit the hat in the notation for the pseudo-rapidity.

4.3 TCSA results

4.3.1 TCSA fits

The Bethe–Yang equation for a massless particle moving between the boundaries is

$$e^{ip2R}\hat{R}_0\hat{R}_I(\theta) = 1 \,, \tag{4.3.1}$$

that is

$$e^{ip2R}S_{\mathrm{LY}}^{-1}(\theta - \theta_{\mathrm{B}})\hat{R}_0^2(\theta) = 1 \,. \tag{4.3.2}$$

Taking the logarithm we get

$$2pR + \delta(\theta - \theta_B) = 2n\pi \,, \tag{4.3.3}$$

where

$$\delta(\theta) = \frac{1}{i}\log S_{\mathrm{LY}}^{-1}(\theta) \,, \tag{4.3.4}$$

and n can be integer or half-integer for the two eigenvalues of $\hat{R}_0^2$ (1 and -1).

For a massless particle $p = E = \frac{\mu}{2}e^{\theta}$ where μ is some mass scale. A shift in the pseudo-rapidity θ is equivalent with a change in μ. The shift in θ, $\theta - \theta_{\mathrm{B}}$ can be compensated by changing μ which for the TCSA means changing the numeric value of the dimensionless coupling κ.

We should note that the Bethe–Yang equations are not derived rigorously for massless particles. However, experience shows that it works and gives the correct energy levels even for rather small volumes. The massless limit of the massive TBA equations are the same as those derived from the massless Bethe–Yang equation and they work in a lot of cases, which is another reassuring fact. We will see that also in our case it gives consistent energy levels.

Equation (4.3.3) can be solved for r ($pR = ER = \varepsilon r$) for different values of n and we can plot the inverse of the function $r(\varepsilon)$ and compare the lines with the TCSA data, $\varepsilon_{\mathrm{TCSA}}(r)$. For this we have to distinguish the one-particle energy levels. For the multi-particle states we have a coupled system of Bethe–Yang equations that

[1] The method used in [AN01], taking the joint limits $\theta \to \infty$, $m \to 0$ and demanding that the result be finite and unitary, leads to the same result.

contain also the bulk S-matrix, which makes the behaviour of the energy eigenvalues different for finite volumes. In principle this allows us to select the one-particle levels. Furthermore, for large volume (r) the interaction becomes negligible and the asymptotic behaviour of the energies are

$$E_n \sim \frac{\pi}{r} n \tag{4.3.5}$$

for one-particle states and

$$E_{n_1,n_2,\ldots} \sim \frac{\pi}{r} \sum_i n_i \tag{4.3.6}$$

for multi-particle states. Thus the IR behaviour is the same for one-particle and multi-particle states and for a given (half-)integer number n there is precisely one one-particle state and possibly several multi-particle states with asymptotic energy $n\pi/r$. If for a certain value of n there is only one level, one can be sure that it is a one-particle level. For $n = \frac{1}{2}$ there are obviously no multi-particle states and for greater values of n certain multi-particle states may be forbidden by exclusion rules. For example in the $n = 1$ case the two-particle state corresponding to $1 = \frac{1}{2} + \frac{1}{2}$ is excluded, so for $n = 1/2$, 1 there is only one energy level which corresponds to a one-particle state.

For each value of κ we must first find the appropriate value of θ_{B}, for example by fitting the lowest energy level which is a one particle level. After this is done, all the other one-particle energy eigenvalues should automatically fit the other lines. The result of such a fit can be seen in Figure 4.1(a) for the NS-NS case with $\kappa > 0$, when only the integer levels of the module (1,3) are in the Hilbert space (see (4.1.5) and below). As can be seen, the TCSA spectrum possesses the expected features: the lowest energy levels are non-degenerate in the IR and the higher levels are arranged in groups.

In every group there is exactly one level that fits the one-particle Bethe–Yang energy, with integer values n. It is interesting to observe that these levels are always the highest ones in their group, which indicates that the interaction is attractive. The lines of Figure 4.1(a) not fitted by a solid line correspond to multi-particle states. The number of these levels is neither consistent with bosonic nor with fermionic exclusion statistics. This suggests that these particles obey some generalised exclusion statistics, similarly to the ordinary Lee–Yang model [Sch97].

One would expect that the other eigenvalue of the reflection factor corresponds to the reflection of the other member of the superdoublet, that is the energy eigenvalues from the half-integer levels (NS-$\widetilde{\mathrm{NS}}$ case) will fit the lines of half-integer values of n. Surprisingly, this is not the case and it is not clear why it does not happen. However, the lines are consistent with the assumption of a single reflection factor (see below) but we do not know what this reflection factor is.

For $\kappa < 0$ ($h < 0$) the spectrum becomes complex, just like for the ordinary Lee–Yang model [DPTW98].

Another and more precise approach is obtaining the phase shift $\delta(\theta)$ from the various TCSA eigenvalues and comparing it with the exact function (4.3.4). From

(4.3.3) one gets

$$\delta_{\mathrm{TCSA}}(\log\frac{E_{\mathrm{TCSA}}}{\mu}-\theta_{\mathrm{B}})=\delta_{\mathrm{TCSA}}(\log\varepsilon_{\mathrm{TCSA}}-\theta_{\mathrm{B}})=2n\pi-2\varepsilon\, r\,, \tag{4.3.7}$$

It can be seen that our ignorance of the proper mass scale (or the value of θ_{B}) is only a matter of a horizontal shift of the function along the θ-axis while changing the quantum number n shifts the function vertically by $2n\pi$. In Figure 4.1(b) the phase shifts calculated from the lowest integer one-particle eigenvalues are plotted onto each other, which shows that the phase shifts extracted from the different one-particle levels are the same. This shows that the massless Bethe–Yang equation is meaningful and gives consistent results. The difference between the phase shifts for small rapidities is due to the truncation errors of the TCSA in the IR.

In Table 4.1 the phase shift values calculated from the difference of the two lowest TCSA eigenvalues are compared with the theoretical values (4.3.4). In Figures 4.1(c) and 4.1(d) the the TCSA phase shifts obtained from the lowest eigenvalues are plotted together with the proposed phase shift (4.3.4). As it can be seen there is good agreement.

In Figure 4.2 we plotted together the phase shifts extracted from the lowest half-integer levels. They all give the same phase shift, which is a very strong indication for the existence of a reflection factor for these excitations as well, even though we were not able to derive it.

θ_{TCSA}	$\delta(\theta)$	$\delta_{\mathrm{TCSA}}(\theta)$
0.0025	3.1358	3.0401
0.0570	3.0099	2.9276
0.1154	2.8760	2.8076
0.1782	2.7337	2.6796
0.2462	2.5824	2.5426
0.3204	2.4217	2.3961
0.4022	2.2513	2.2391
0.4935	2.0707	2.0707
0.5968	1.8795	1.8898
0.7158	1.6772	1.6953
0.8562	1.4630	1.4860
1.0275	1.2361	1.2606
1.2461	0.9951	1.0179
1.5461	0.7378	0.7567
2.0163	0.4612	0.4765
3.0696	0.1609	0.1765

Table 4.1: The theoretical phase shift (4.3.4) and the TCSA result

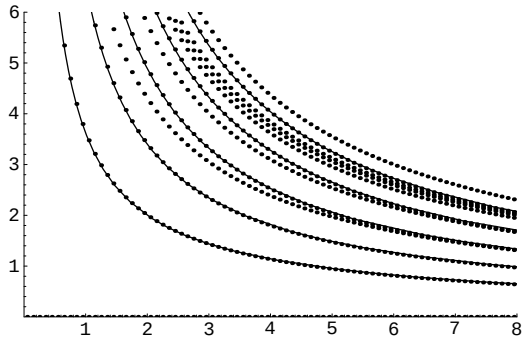

(a) Energy eigenvalues from the integer levels with the theoretical energies from the reflection factor

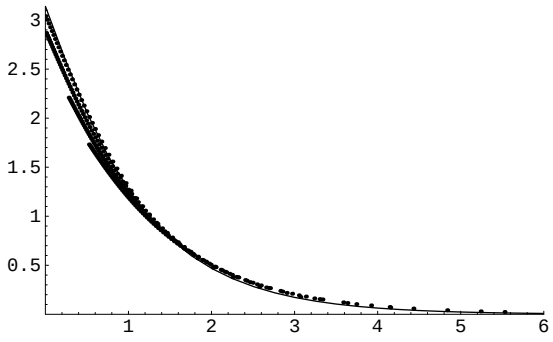

(b) $\delta_{\mathrm{TCSA}}(\theta)$ phase shifts calculated from different TCSA eigenvalues

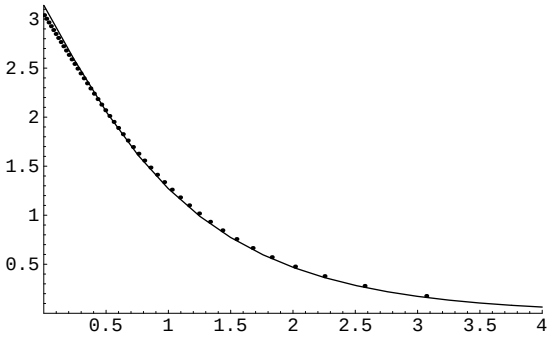

(c) TCSA phase shift from the difference of the first two eigenvalues

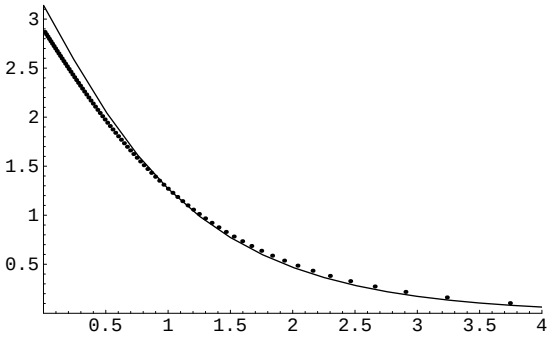

(d) TCSA phase shift from the difference of the 3rd and 1st eigenvalues

Figure 4.1: Reflection factor and TCSA spectrum

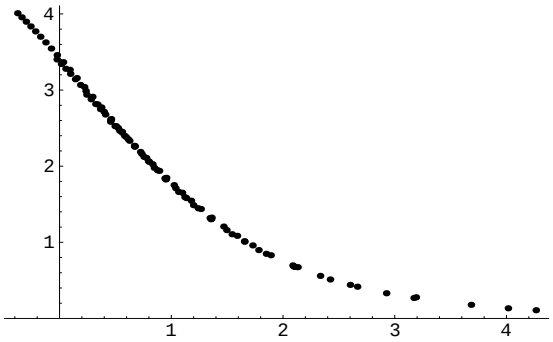

Figure 4.2: TCSA phase shifts from the half-integer energy levels

4.4 TBA for the flow

In this section we apply the Boundary Thermodynamic Bethe Ansatz method, described in section 2.6, to the SLY-model. The S-matrix is non-diagonal, so one has to diagonalise the transfer matrix. In our case the massless reflection factors are diagonal, so the eigenvalues are simply the product of the eigenvalues of the

reflection factors and those of the periodic transfer matrix. The diagonalisation of the latter is based on the remarkable property of the S-matrix that its elements, when interpreted as the Boltzmann-weights of a lattice model, satisfy the so-called free fermion condition. This implies that the corresponding 8-vertex model can be written as an XY model with a magnetic field. Denoting the elements of the matrix part of the S-matrix by

$$\begin{pmatrix} a_+ & 0 & 0 & d \\ 0 & b_+ & c & 0 \\ 0 & c & b_- & 0 \\ d & 0 & 0 & a_- \end{pmatrix}, \tag{4.4.1}$$

the free fermion condition reads

$$a_+a_- + b_+b_- = c^2 + d^2\,. \tag{4.4.2}$$

This relation allows the transfer matrix to be rewritten in another form and then it is possible to find a θ-independent similarity transformation that brings it to a triangular form. Then the N-particle transfer matrix turns out to have the eigenvalues ([Ahn94, MS96])

$$\Lambda(\theta) = \prod_{l=1}^{N} 2\frac{\tilde{Z}(\theta-\theta_l)}{\sinh(\theta-\theta_l)}\lambda(\theta)\,, \tag{4.4.3}$$

where $\tilde{Z}(\theta)$ is defined in (4.2.6) and

$$\lambda_{\{x_m,\epsilon_m\}}(\theta) = \text{const.} \times \prod_m \sinh\left(\frac{\theta-x_m}{2} + i\epsilon_m\frac{\pi}{6}\right)\cosh\left(\frac{\theta-x_m}{2} - i\epsilon_m\frac{\pi}{6}\right)\,. \tag{4.4.4}$$

Here the ϵ_m can take values ±1 and x_m are real solutions of the equation (F is the fermion parity):

$$\prod_{l=1}^{N}\frac{\tanh(\frac{x-\theta_l}{2} - \frac{i\pi}{6})}{\tanh(\frac{x-\theta_l}{2} + \frac{i\pi}{6})} = -F\,. \tag{4.4.5}$$

The massless Bethe–Yang equations take the following form:

$$e^{2i\frac{\mu}{2}e^{\theta}L}\prod_{l=1}^{N} 2\frac{Z(\theta-\theta_l)}{\sinh(\theta-\theta_l)}\lambda_{\{x_m,\epsilon_m\}}\gamma_{\alpha\beta}(\theta-\theta_B) = 1\,, \tag{4.4.6}$$

where $\gamma_{\alpha\beta}$ are the eigenvalues of the product of the reflection factors.

Just like in the diagonal case discussed in section 2.6, we introduce the densities of particles $\rho(\theta)$ and holes $P(\theta)-\rho(\theta)$. After taking the logarithm the product in $\lambda_{\{x_m,\epsilon_m\}}$ becomes a sum which in the continuum limit is substituted by an integral. For this we introduce the densities of the roots x_m: $\rho_0(\theta)$ denotes the density distribution of those for which $\epsilon_m = +1$ and $\bar{\rho}_0(\theta)$ for which $\epsilon_m = -1$.

The following equation obtained from equation (4.4.5) relates $P_0(\theta) = \rho_0(\theta) + \bar{\rho}_0(\theta)$ to the particle distributions:

$$2\pi P_0(\theta) = \int \mathrm{d}\theta' \rho(\theta) \frac{\partial}{\partial\theta} \mathrm{Im} \log \left(\frac{\tanh(\frac{1}{2}(\theta - \theta' - i\frac{\pi}{3}))}{\tanh(\frac{1}{2}(\theta - \theta' + i\frac{\pi}{3}))} \right) . \tag{4.4.7}$$

Since the reflection factors in this model are proportional to a constant diagonal matrix (see (4.2.27)), after deriving the logarithm of equation (4.4.6) only the scalar part survives. Thus we obtain the following equation in terms of the densities:

$$\begin{aligned} 2\pi P(\theta) = \frac{\mu}{2} e^{\theta} + \frac{\Psi(\theta)}{2R} + \int \mathrm{d}\theta' \Big[& \rho(\theta') \Phi_z(\theta - \theta') \\ & + \rho_0(\theta') \frac{1}{2} \Phi(\theta - \theta') + \bar{\rho}_0(\theta') (-\frac{1}{2}) \Phi(\theta - \theta') \Big] , \end{aligned} \tag{4.4.8}$$

with kernel functions

$$\Phi_z(\theta) = \frac{\partial}{\partial\theta} \mathrm{Im} \log \left(\frac{Z(\theta)}{\sinh(\theta)} \right) , \tag{4.4.9a}$$

$$\Phi(\theta) = \frac{\partial}{\partial\theta} \mathrm{Im} \log S_{\mathrm{LY}}(\theta) = -\frac{4\sqrt{3}\cosh(\theta)}{1 + 2\cosh(2\theta)} , \tag{4.4.9b}$$

$$\Psi(\theta) = \frac{\partial}{\partial\theta} \mathrm{Im} \log S_{\mathrm{LY}}^{-1}(\theta - \theta_B) = -\Phi(\theta - \theta_B) , \tag{4.4.9c}$$

where $Z(\theta)$ is the scalar part of $S_{\mathrm{SLY}}(\theta)$ defined in equation (4.2.7). Note that the kernel in (4.4.7) is $-\Phi(\theta - \theta')$.

Using the fact that $P_0(\theta) = \rho_0(\theta) + \bar{\rho}_0(\theta)$ together with equation (4.4.7) we can eliminate $\rho_0(\theta)$ from equation (4.4.8) getting

$$P(\theta) = \frac{\mu}{4\pi} e^{\theta} + \frac{\Psi(\theta)}{4\pi R} + \Big(\rho \star (\Phi_z - \frac{1}{2} \Phi \star \Phi) \Big)(\theta) - (\bar{\rho}_0 \star \Phi)(\theta) , \tag{4.4.10}$$

where we introduced the notation

$$(\phi \star \psi)(\theta) = \int \frac{\mathrm{d}\theta'}{2\pi} \phi(\theta - \theta') \psi(\theta') \tag{4.4.11}$$

for the convolution. It turns out that the following identity holds ([AN01]):

$$(\Phi_z - \frac{1}{2} \Phi \star \Phi)(\theta) = \Phi(\theta) , \tag{4.4.12}$$

giving

$$P(\theta) = \frac{\mu}{4\pi} e^{\theta} + \frac{\Psi(\theta)}{4\pi R} + \big((\rho - \bar{\rho}_0) \star \Phi \big)(\theta) . \tag{4.4.13}$$

The free energy of the system is given by

$$\begin{aligned} f = \int \mathrm{d}\theta \Big\{ & \rho(\theta)\mu e^{\theta} \\ & - T\big[P(\theta)\log P(\theta) - \rho(\theta)\log\rho(\theta) - (P(\theta)-\rho(\theta))\log(P(\theta)-\rho(\theta))\big] \\ & - T\big[P_0(\theta)\log P_0(\theta) - \bar\rho_0(\theta)\log\bar\rho_0(\theta) - (P_0(\theta)-\bar\rho_0(\theta))\log(P_0(\theta)-\bar\rho_0(\theta))\big]\Big\}. \end{aligned} \tag{4.4.14}$$

Now the densities $\rho(\theta)$, $\bar\rho_0(\theta)$ can be varied to minimize the free energy. Using

$$\delta P = \delta\rho \star \Phi - \delta\bar\rho_0 \star \Phi\,, \tag{4.4.15}$$

$$\delta P_0 = -\delta\rho \star \Phi \tag{4.4.16}$$

and introducing the quasi-particle energies

$$\frac{\rho(\theta)}{P(\theta)} = \frac{e^{-\varepsilon(\theta)}}{1+e^{-\varepsilon(\theta)}}\,, \qquad\qquad \frac{\bar\rho_0(\theta)}{P_0(\theta)} = \frac{e^{-\varepsilon_0(\theta)}}{1+e^{-\varepsilon_0(\theta)}} \tag{4.4.17}$$

performing the steps of section 2.6 we arrive at the following TBA equations:

$$\varepsilon(\theta) = \frac{\mu}{T}e^{\theta} - (\Phi \star (L - L_0))(\theta)\,, \tag{4.4.18a}$$

$$\varepsilon_0(\theta) = (\Phi \star L)(\theta)\,, \tag{4.4.18b}$$

where $L(\theta) = \log(1+e^{-\varepsilon(\theta)})$, $L_0(\theta) = \log(1+e^{-\varepsilon_0(\theta)})$. The equation for $\varepsilon_0(\theta)$ is like a TBA equation for a particle with $\mu = 0$.

Using these equations we can write the extremum of the free energy:

$$\frac{F}{T} = -\frac{1}{2\pi}\int \mathrm{d}\theta(\mu e^{\theta}R + \Psi(\theta))L(\theta)\,. \tag{4.4.19}$$

Since the partition function on the cylinder behaves for large R as (2.4.8):

$$\log \mathcal{Z}_{\alpha\beta} = -\frac{F}{T} \approx \log(g_\alpha g_\beta) - RE_0^{\mathrm{circ}} = \log(g_\alpha g_\beta) + \frac{r}{l}\frac{c_{\mathrm{eff}}\,\pi}{6} \tag{4.4.20}$$

we obtain

$$\log(g_\alpha g_\beta) = -\frac{1}{2\pi}\int_{-\infty}^{\infty} \mathrm{d}\theta\,\Phi(\theta-\theta_B)\log(1+e^{-\varepsilon(\theta)})\,. \tag{4.4.21}$$

This formula is the same given in [LMSS95] but it is different from the formula of Ahn and Nepomechie [AN01] in which $L_0(\theta)$ is used instead of $L(\theta)$.

In the UV limit $\theta_{\mathrm{B}} \to -\infty$, the integrand is non-vanishing if $\theta \to -\infty$ and similarly, in the IR limit $\theta_{\mathrm{B}} \to \infty$ the non-zero contribution comes from the $\theta \to \infty$ domain. Using the fact that $\int_{-\infty}^{\infty}\mathrm{d}\theta\,\Phi(\theta) = -2\pi$, it is easy to see from the TBA equations (4.4.18) that

$$\varepsilon(\infty) = \infty \quad \Rightarrow \quad L(\infty) = 0, \quad L_0(\infty) = \sqrt{2}\,. \tag{4.4.22}$$

Finding the values at $-\infty$ amounts to solving the system of equations

$$\left.\begin{aligned} x &= \frac{1+y}{1+x}\,, \\ y &= 1+x \end{aligned}\right\}$$

for $x = e^{-\varepsilon(-\infty)}$, $y = e^{-\varepsilon_0(-\infty)}$. We get

$$L(-\infty) = \log(1+\sqrt{2})\,, \qquad L(\infty) = 0\,, \tag{4.4.23a}$$

$$L_0(-\infty) = \log(2+\sqrt{2})\,, \qquad L_0(\infty) = \log 2\,. \tag{4.4.23b}$$

Using that the factor $g_\beta = g_{1,1}$ cancels we finally obtain

$$\log\left(\frac{g_\alpha^{\mathrm{UV}}}{g_\alpha^{\mathrm{IR}}}\right) = \log(1+\sqrt{2}) = \log\left(\frac{g_{1,3}}{g_{1,1}}\right)\,, \tag{4.4.24}$$

where we used the formula (4.1.4) for the g-factor. Thus TBA predicts the flow $(1,3) \to (1,1)$, which is different from the prediction of [AN01]. We will see that TCSA supports our result.

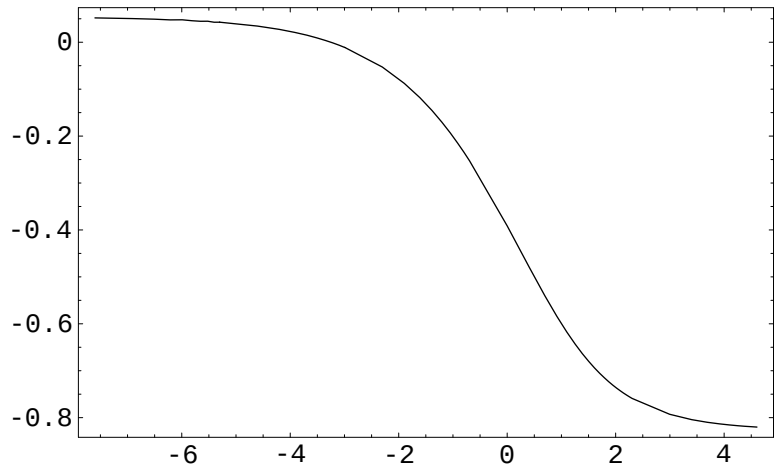

Figure 4.3: TBA: $\log(g)$ along the flow

4.5 Flows with TCSA

The characters of the (1,3) and $(1,1)$ highest weight representations are

$$\chi_{1,3}(q) = 1 + q^{1/2} + q + q^{3/2} + 2q^2 + 2q^{5/2} + 2q^3 + 3q^{7/2} + 4q^4 + 5q^{9/2} + 5q^5 + 6q^{11/2} + 8q^6 + 9q^{13/2} + 10q^7 + \ldots \tag{4.5.1a}$$

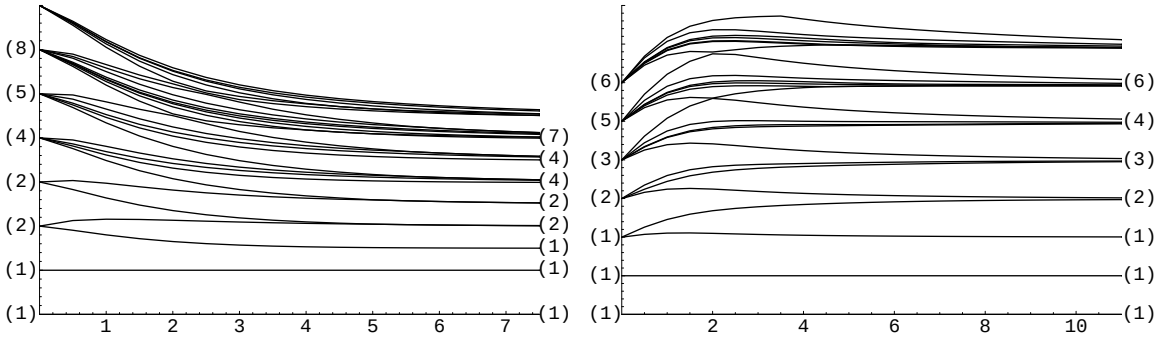

(a) Integer levels (b) Half-integer levels

Figure 4.4: The RG flows starting from the (1,3) NS and $\widetilde{\text{NS}}$ b. c.-s in SM(2,8)

$$\chi_{1,1}(q) = 1 + q^{3/2} + q^2 + q^{5/2} + q^3 + q^{7/2} + 2q^4 + 2q^{9/2} + 2q^5 + 3q^{11/2} + 4q^6 + 4q^{13/2} + 4q^7 + \dots \quad (4.5.1b)$$

In the TCSA calculations the dimension of the Hilbert space was 393 for the integer levels and 344 for the half-integer ones. In Fig. 4.4 the normalised energy differences, $(\varepsilon_i - \varepsilon_0)/(\varepsilon_1 - \varepsilon_0)$ are plotted, and the degeneracies are shown in parentheses. We have found that starting with the integer (half-integer) levels of the module (1,3) the flow tends to a degeneracy pattern corresponding to the integer (half-integer) levels of the module (1,1). Since we did not perturb the (1,1) boundary we can assume that this boundary condition remained the same during the flow. Taking into account that (1,1) is bosonic and (1,3) fermionic, this – keeping in mind the conclusions after equation (4.1.5) – leads to the conclusion that the flows are

$$(1,3)_{\text{NS}} \longrightarrow (1,1)_{\widetilde{\text{NS}}}\,, \quad (4.5.2a)$$

$$(1,3)_{\widetilde{\text{NS}}} \longrightarrow (1,1)_{\text{NS}} \quad (4.5.2b)$$

in perfect agreement with the results of the TBA analysis based on our proposed reflection factor.

The flow of the boundary entropy, $\log(g)$ can also be explored numerically using TCSA [DRTW00]. The trace in the partition function (4.1.5) can be approximated by the finite sum over the TCSA eigenvalues. For each value of l one must find the scaling region, the domain in r for which $\log \mathcal{Z}$ behaves as in (4.4.20). The volume r should be great enough for this scaling behaviour, but for too large values the truncation errors start to dominate and spoil this simple linear form. In Figure 4.5(a) it can be seen that the scaling region is centered around $r/l = 3$ and in Figure 4.5(b) the logarithm of the partition function is plotted.

The partition function depends only on the combination $x = hL^{1/2-\Delta_{1,3}} = hL^{3/4} = \kappa l^{3/4}$. After making the linear fit in r/l along the scaling region for different values of x one gets the product of the $\mathcal{G}^{(0)}$-functions (see (2.4.12)) as a function of x. However this function generally contains a linear term in L which corresponds

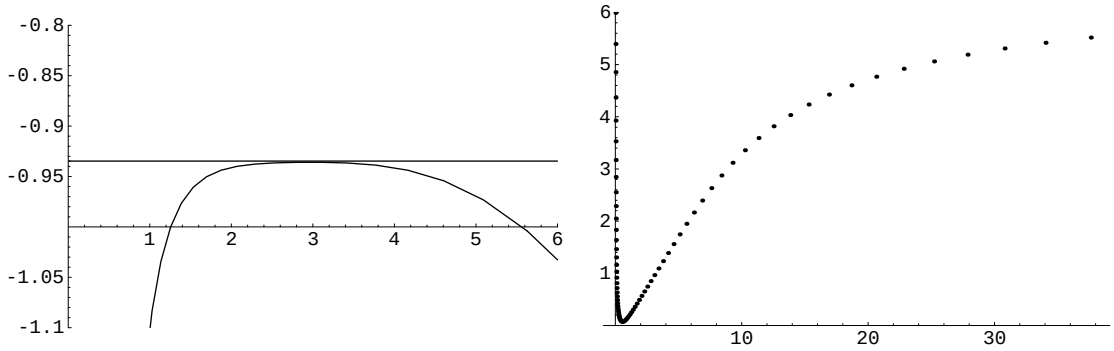

(a) $\mathrm{d}(\log \mathcal{Z})/\mathrm{d}(r/l)$ (b) $\log \mathcal{Z}$ vs. r/l

Figure 4.5: The partition function ($x = 0.1$)

to the free energy density coming from the boundaries (cf. (2.4.14)). In order to get the correct final result this term should be subtracted. We extracted this term numerically from the large L behaviour of the naive fits for the g-function.

The numeric results are compared with the TBA data in Table 4.2 and they are plotted in Figure 4.6 together. Unfortunately there is no systematic method for determining the TCSA errors, but one can make estimates for them. One way is comparing the results obtained at different cuts, i. e. at different dimensions of the Hilbert space, here we found that for $x < 1$ the relative error is 0.5–2%. Another source of error is in the choice of the scaling region, the corresponding error is 0.2–0.7%. Finally, the error of the linear fit itself is about 0.2–0.4%. So our estimate for the relative error in the TCSA results is about 1–3% and the TBA and TCSA values for the g-function agree within this error. Apart from the difference due to the truncation errors in g_{TCSA} at large values of x (as in [DRTW00]) there is an excellent agreement between the two approaches.

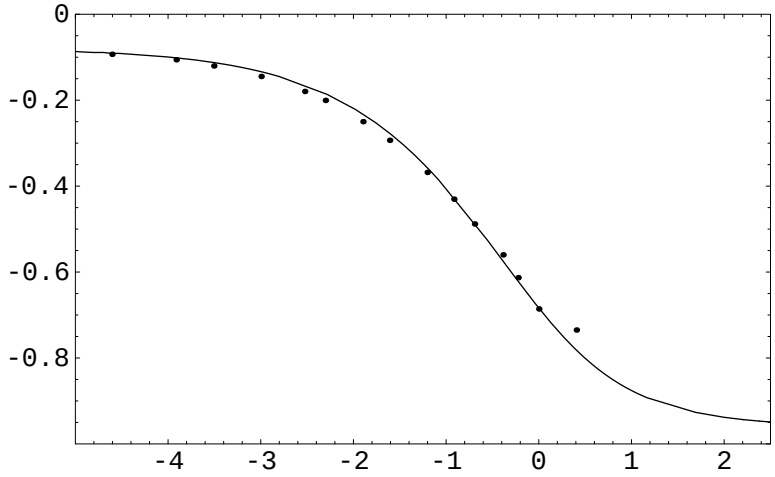

Figure 4.6: $\log(g)$ vs. $\log(x)$ along the flow, TCSA (dots) and TBA (solid line) results

$\log x$	$\log g_{\mathrm{TBA}}$	$\log g_{\mathrm{TCSA}}$
-4.605	-0.0900	-0.0932
-3.912	-0.1013	-0.1059
-3.507	-0.1122	-0.1203
-2.996	-0.1337	-0.1449
-2.302	-0.1846	-0.2008
-1.609	-0.2768	-0.2941
-0.916	-0.4264	-0.4322
-0.693	-0.4864	-0.4906
-0.224	-0.6215	-0.6177
0	-0.6837	-0.6922
0.405	-0.7817	-0.7457
0.693	-0.8347	-0.9015
0.916	-0.8659	-0.9377
1.504	-0.9169	-1.2646

Table 4.2: TBA and TCSA results for $\log g$

4.6 Generalisation to SM$(2, 4n + 4)$

The supersymmetric Lee–Yang model is the first member of the series of superconformal minimal models with $p = 2$, the models SM(2,4n+4). Using TCSA we have found that for $\kappa > 0$ starting from the even (odd) levels of any NS module we end up at the even (odd) levels of the (1,1) module (see Figures 4.7, 4.8). So the IR fixed point seems to be always the (1,1) boundary condition and depending on the fermion parity of the field corresponding to the UV boundary condition the flow is of type NS→NS ($\widetilde{\mathrm{NS}} \to \widetilde{\mathrm{NS}}$) or NS→ $\widetilde{\mathrm{NS}}$ ($\widetilde{\mathrm{NS}}$ →NS):

$$(1,3)_{\mathrm{NS}} \longrightarrow (1,1)_{\widetilde{\mathrm{NS}}}\,, \tag{4.6.1a}$$
$$(1,3)_{\widetilde{\mathrm{NS}}} \longrightarrow (1,1)_{\mathrm{NS}}\,, \tag{4.6.1b}$$

$$(1,5)_{\mathrm{NS}} \longrightarrow (1,1)_{\mathrm{NS}}\,, \tag{4.6.2a}$$
$$(1,5)_{\widetilde{\mathrm{NS}}} \longrightarrow (1,1)_{\widetilde{\mathrm{NS}}}\,, \tag{4.6.2b}$$

$$(1,7)_{\mathrm{NS}} \longrightarrow (1,1)_{\widetilde{\mathrm{NS}}}\,, \tag{4.6.3a}$$
$$(1,7)_{\widetilde{\mathrm{NS}}} \longrightarrow (1,1)_{\mathrm{NS}} \tag{4.6.3b}$$
$$\vdots$$

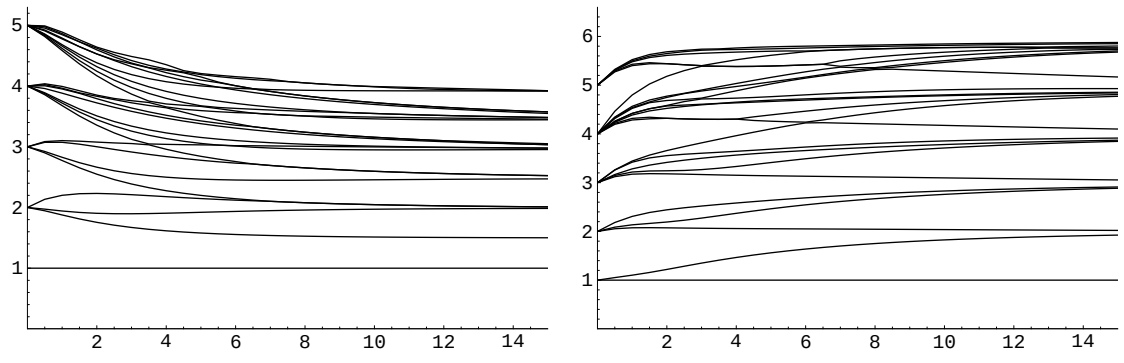

(a) Even levels (b) Odd levels

Figure 4.7: The RG flows starting from b. c. (1,5) in SM(2,12)

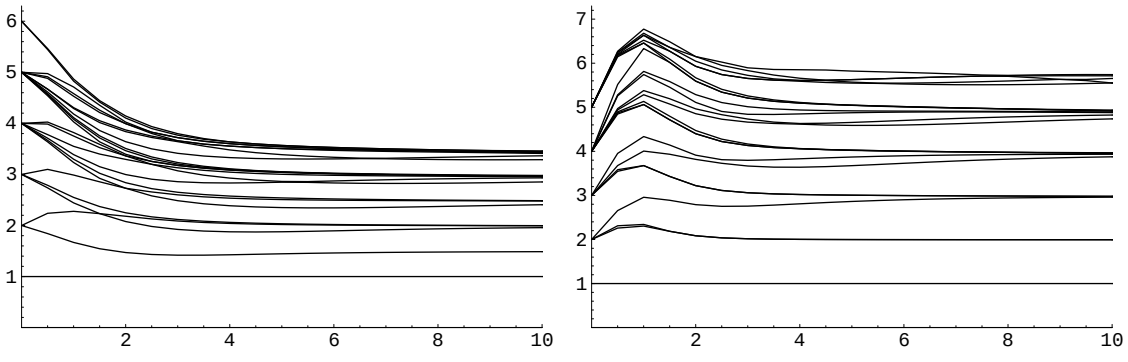

(a) Even levels (b) Odd levels

Figure 4.8: The RG flows starting from b. c. (1,7) in SM(2,16)

Chapter 5

Conclusions

In this thesis we investigated $N = 1$ supersymmetric two-dimensional conformal field theories in the presence of boundaries. Our main subject of interest was the exploration of boundary renormalisation group flows induced by a boundary perturbation.

The first main part of the work dealt with the charting of boundary flows of the unitary $N = 1$ superconformal minimal models triggered by the boundary operator $\hat{G}_{-1/2}\Phi_{1,3}$. For this we used the Truncated Conformal Space Approach that had to be generalised to the supersymmetric minimal models, which is an original result of the author. We found a rather simple rule for the flow pattern that is similar to the rules for the ordinary minimal models. This result is in agreement with former theoretical predictions in their domain of validity, like those of Fredenhagen [Fre03], and we found natural extensions of the rules for the cases that were not covered by them (e.g. models with p even).

In the second part we studied reflection factors and boundary renormalisation group flows of the (non-unitary) supersymmetric Lee–Yang model (SM(2,8) or M(3,8)). First we proposed reflection factors for the NS type boundary conditions by considering our model as a reduction of the supersymmetric sine–Gordon model. After determining the massless limit of the reflection factors we checked them by comparing the energy levels predicted by the Bethe–Yang equation with the numerical spectrum calculated with TCSA. We found very good agreement for the even levels of the super Verma module.

Then we turned to the question of the boundary renormalisation group flows of the SLY model. Based on our reflection factor we determined the flow of the boundary entropy (g-function) using boundary TBA, from which we could determine the fixed points of the boundary flow. We checked the g-function flow and also the fixed points applying the TCSA method and we found perfect agreement with the prediction of the TBA analysis.

The proposed reflection factors differ from earlier conjectures [AN01], but the energy spectrum, the fixed point of the boundary renormalisation group flow and the TBA g-function based on them are in very good agreement with the TCSA results.

In the end we examined with the TCSA method the boundary flows in generalisations of the SLY model, the non-unitary superconformal minimal models SM$(2, 4n + 4)$. We found that every Neveu–Schwarz (NS and $\widetilde{\text{NS}}$) boundary condition flows to the (1,1) boundary condition.

There are several possibilities for continuing this work. One possibility is to consider $N = 2$ models, which have direct relevance in string theory. In the literature there exist theoretical predictions for the flow pattern of these models which could be confirmed or disproved. Using boundary TCSA the off-critical behaviour of the g-function can also be investigated both in the $N = 1$ and $N = 2$ cases.

In order to be able to examine flows triggered by joint bulk and boundary perturbations it is necessary to know the boundary structure constants. For the superconformal minimal models these are not known yet, but following the method applied for the non-supersymmetric minimal models they could be calculated. In the Ramond sector even the bulk structure constants are unknown and determining them would be interesting for string theory as well.

Using recently developed techniques for boundary form factors the non-integrable boundary flows can be handled with form factor perturbation theory. The results can be compared with TCSA and thus a complete charting of both the integrable and non-integrable boundary flows would be possible.

TCSA and the study of truncation effects can be very useful also for a non-perturbative understanding of the renormalisation group [Tot06, FGP$^+$06].

Theories with defects are also of great interest. Their study is highly motivated by condensed matter physics and it is now a quickly developing area of research. Conformal defects can be regarded as generalisations of conformal boundaries and they can connect different conformal field theories. Moreover, applying a folding trick it can be shown that defect theories are equivalent to certain boundary theories [BG06]. The TCSA method could be extended to defects and the numerical results could help in answering many open questions, e. g. the proposed transmission and reflection amplitudes could be checked. The boundary form factor programme can also be extended to defects and similarly to the case of boundaries, their non-integrable perturbations could be investigated using form factor perturbation theory and defect TCSA.

Appendix A

Appendix

A.1 Superconformal characters

The Neveu–Schwarz characters are given by

$$\chi^{\mathrm{NS}}_{r,s}(q) = e^{-i\pi/24}\frac{\eta(-q^{1/2})}{\eta(q)^2}\left[\Theta(q^{1/2}, pr-qs, pq) - \Theta(q^{1/2}, pr+qs, pq)\right] , \qquad \text{(A.1.1)}$$

where $\eta(q)$ denotes the Dedekind function:

$$\eta(q) = q^{1/24}\prod_{n=1}^{\infty}(1-q^n) \qquad \text{(A.1.2)}$$

and

$$\Theta(q,\lambda,k) = \sum_{n=-\infty}^{\infty} q^{\frac{(2kn+\lambda)^2}{4k}} . \qquad \text{(A.1.3)}$$

The formula for the Ramond characters is

$$\chi^{\mathrm{R}}_{r,s}(q) = \frac{\eta(q^2)}{\eta(q)^2}(1-\frac{1}{2}\delta_{r,\frac{q}{2}}\delta_{s,\frac{p}{2}})\left[\Theta(q^{1/2}, pr-qs, pq) - \Theta(q^{1/2}, pr+qs, pq)\right] . \qquad \text{(A.1.4)}$$

A.2 Superconformal generalisations of the Verlinde formula

Cardy found that for extremal solutions of his equations the numbers $n^i_{\alpha\beta}$ of the irreducible representation i in the Hilbert space with the boundary conditions α and β are related to the fusion coefficients. The corresponding relations for the $N = 1$ superconformal minimal models are [Nep01b]:

$$n^i_{\mathbf{k}^{NS}\mathbf{l}^{NS}} = n^i_{\mathbf{k}^{\widetilde{NS}}\mathbf{l}^{NS}} = n^i_{\mathbf{k}^{\widetilde{NS}}\mathbf{l}^{\widetilde{NS}}} = \sum_{j\in\Delta_{NS}} \frac{S^{[NS,NS]}_{kj} S^{[NS,NS]}_{lj} (S^{[NS,NS]})^{-1}_{ji}}{S^{[NS,NS]}_{0j}}\,, \quad \text{(A.2.1a)}$$

$$\widetilde{n}^i_{\mathbf{k}^{NS}\mathbf{l}^{NS}} = -\widetilde{n}^i_{\mathbf{k}^{\widetilde{NS}}\mathbf{l}^{NS}} = \widetilde{n}^i_{\mathbf{k}^{\widetilde{NS}}\mathbf{l}^{\widetilde{NS}}} = \sum_{j\in\Delta_{R}} \frac{S^{[\widetilde{NS},R]}_{kj} S^{[\widetilde{NS},R]}_{lj} (S^{[\widetilde{NS},R]})^{-1}_{ji}}{S^{[\widetilde{NS},R]}_{0j}}\,, \quad \text{(A.2.1b)}$$

$$n^i_{\mathbf{k}^{R}\mathbf{l}^{R}} = 2\sum_{j\in\Delta_{NS}} \frac{S^{[R,\widetilde{NS}]}_{kj} S^{[R,\widetilde{NS}]}_{lj} (S^{[NS,NS]})^{-1}_{ji}}{S^{[NS,NS]}_{0j}}\,, \quad \text{(A.2.1c)}$$

$$m^i_{\mathbf{k}^{NS}\mathbf{l}^{R}} = 2\sum_{j\in\Delta_{NS}} \frac{S^{[NS,NS]}_{kj} S^{[R,\widetilde{NS}]}_{lj} (S^{[R,\widetilde{NS}]})^{-1}_{ji}}{S^{[NS,NS]}_{0j}}\,, \quad \text{(A.2.1d)}$$

$$n^i_{\mathbf{k}^{NS}\mathbf{l}^{R}} = \widetilde{n}^i_{\mathbf{k}^{NS}\mathbf{l}^{R}} = \widetilde{n}^i_{\mathbf{k}^{R}\mathbf{l}^{R}} = m^i_{\mathbf{k}^{NS}\mathbf{l}^{NS}} = m^i_{\mathbf{k}^{R}\mathbf{l}^{R}} = 0\,. \quad \text{(A.2.1e)}$$

A.3 Figures

In the figures below we plotted the normalized energy levels $((\varepsilon - \varepsilon_0)/(\varepsilon_i - \varepsilon_0)$ for some appropriate i, usually 1) against the dimensionless coupling parameter κ. The starting boundary condition is unprojected for the Neveu–Schwarz ones (i.e. $\mathrm{NS} \oplus \widetilde{\mathrm{NS}}$), so these flows go to unprojected NS or R boundary conditions.

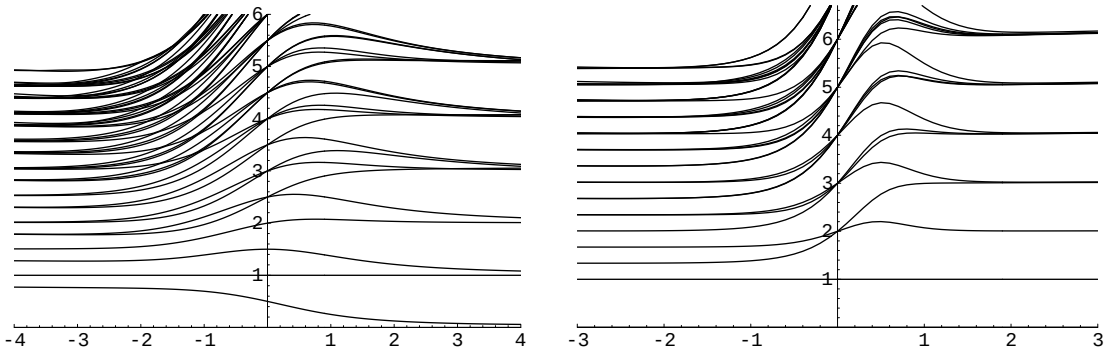

(a) Flows starting from b.c. $(1,3)$ in SM(3,5) (b) Flows starting from b.c. $(1,2)$ in SM(3,5)

Figure A.1: Flows in SM(3,5)

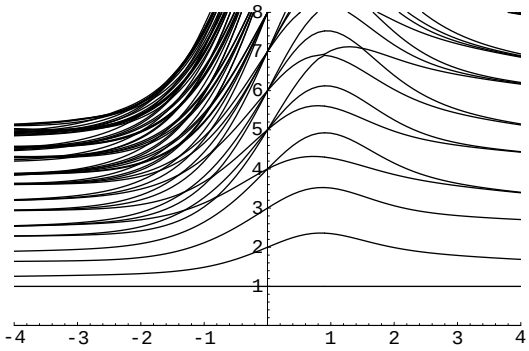

(a) Flows starting from b.c. $(1, 3)$ in SM(4,6)

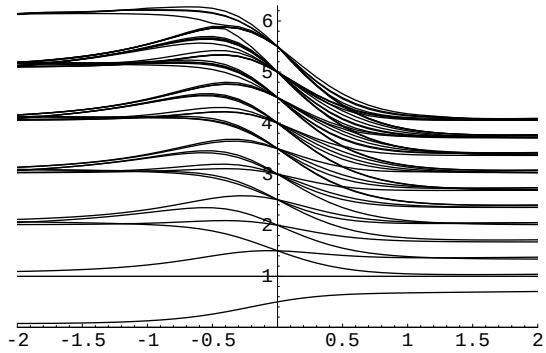

(b) Flows starting from b.c. $(2, 2)$ in SM(4,6)

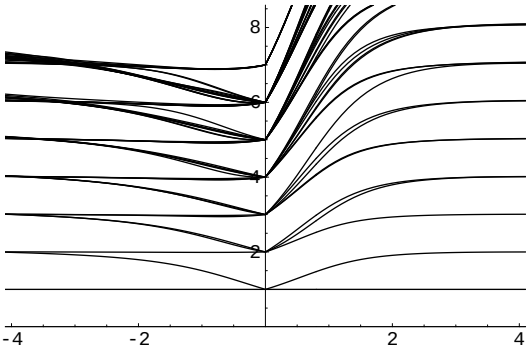

(c) Flows starting from b.c. $(1, 4)$ in SM(4,6)

Figure A.2: Flows in SM(4,6)

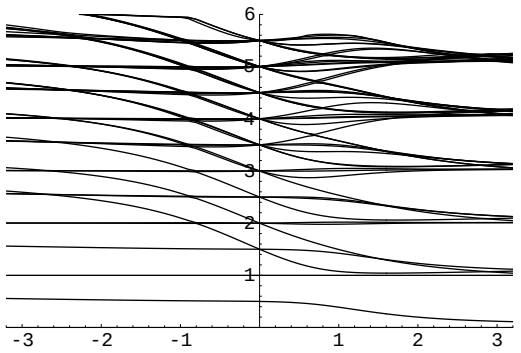

(a) Flows starting from b.c. $(1,5)$ in SM(5,7)

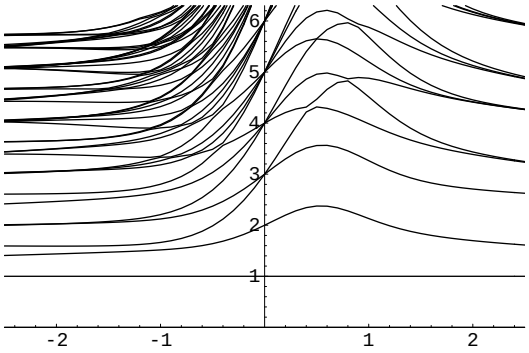

(b) Flows starting from b.c. $(2,4)$ in SM(5,7)

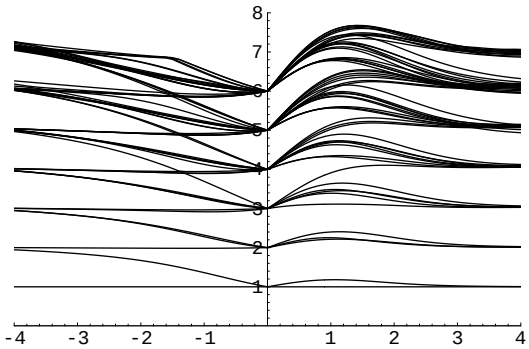

(c) Flows starting from b.c. $(1,4)$ in SM(5,7)

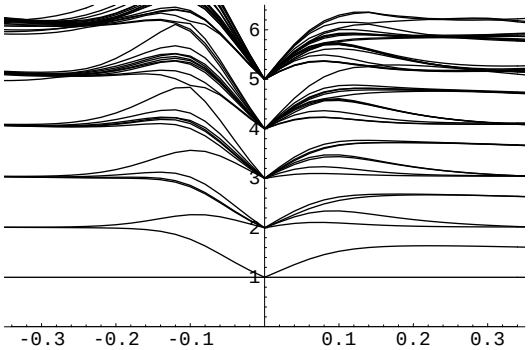

(d) Flows starting from b.c. $(2,3)$ in SM(5,7)

Figure A.3: Flows in SM(5,7)

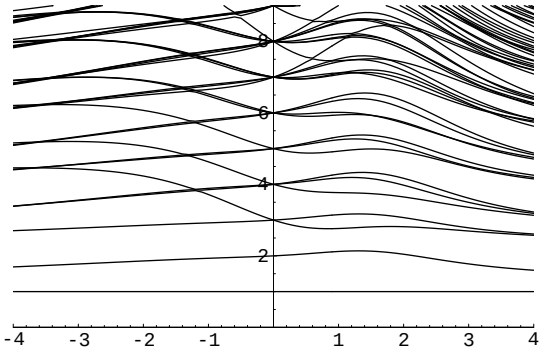

(a) Flows starting from b.c. $(1,5)$ in SM(6,8)

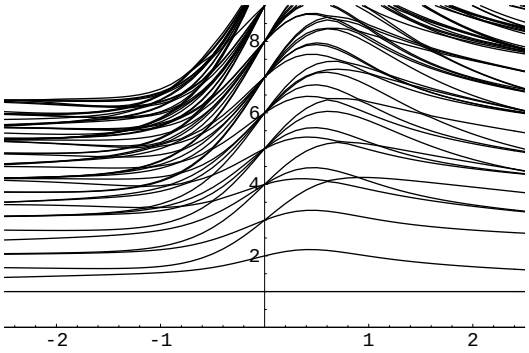

(b) Flows starting from b.c. $(2,4)$ in SM(6,8)

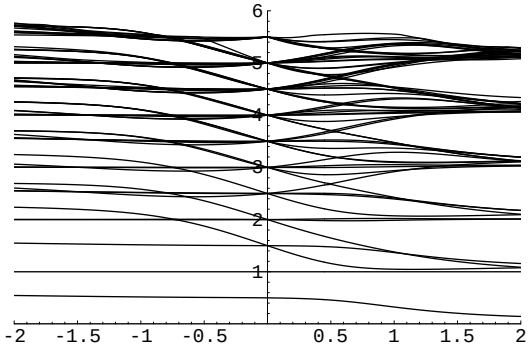

(c) Flows starting from b.c. $(2,6)$ in SM(6,8)

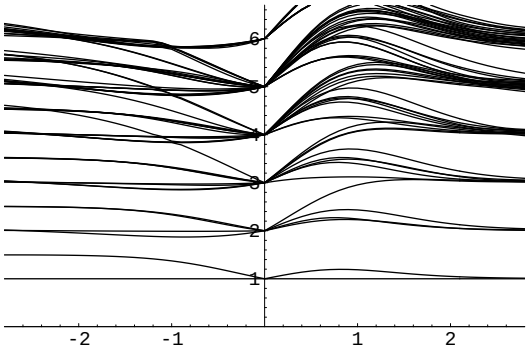

(d) Flows starting from b.c. $(2,5)$ in SM(6,8)

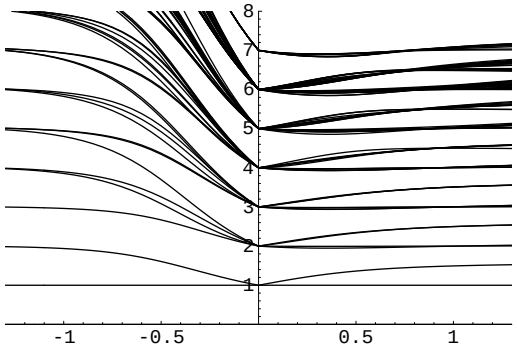

(e) Flows starting from b.c. $(3,2)$ in SM(6,8)

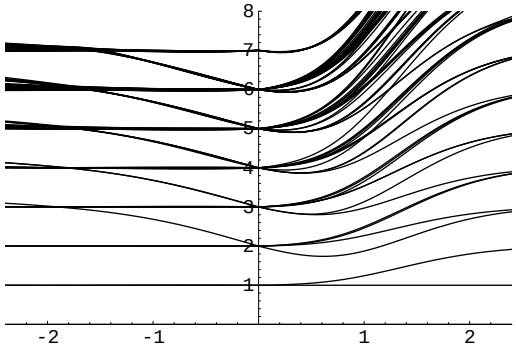

(f) Flows starting from b.c. $(1,6)$ in SM(6,8)

Figure A.4: Flows in SM(6,8)

A.4 The SSG S-matrix

The nth breather in the supersymmetric sine–Gordon model has mass

$$m_n = 2m \sin\left(\frac{n\pi}{2\lambda}\right) . \tag{A.4.1}$$

The SSG breather S-matrix can be written in the form

$$S^{(i,j)}_{\mathrm{SSG}}(\theta) = S^{(i,j)}_{\mathrm{SG}}(\theta) S^{(i,j)}_{\mathrm{SUSY}}(\theta) . \tag{A.4.2}$$

Here [Ahn91]

$$S^{(i,j)}_{\mathrm{SG}}(\theta) = \frac{\sinh(\theta) + i\sin(\frac{i+j}{2\lambda}\pi)}{\sinh(\theta) - i\sin(\frac{i+j}{2\lambda}\pi)} \frac{\sinh(\theta) + i\sin(\frac{i-j}{2\lambda}\pi)}{\sinh(\theta) - i\sin(\frac{i-j}{2\lambda}\pi)} \times \prod_{k=1}^{j-1} \frac{\sin^2(\frac{i-j-2k}{4\lambda}\pi + i\frac{\theta}{2})}{\sin^2(\frac{i-j-2k}{4\lambda}\pi - i\frac{\theta}{2})} \frac{\cos^2(\frac{i+j-2k}{4\lambda}\pi + i\frac{\theta}{2})}{\cos^2(\frac{i+j-2k}{4\lambda}\pi - i\frac{\theta}{2})} \tag{A.4.3}$$

is the sine–Gordon S-matrix and the supersymmetric factor is

$$S^{(i,j)}_{\mathrm{SUSY}}(\theta) = M^{(i,j)}(\theta) G^{(i,j)}(\theta) \tag{A.4.4}$$

with

$$M^{(n,m)}(\theta) = \begin{pmatrix} 1 + i\frac{\sin(\frac{n\pi}{2\lambda})+\sin(\frac{m\pi}{2\lambda})}{\sinh(\theta)} & 0 & 0 & \frac{\sqrt{\sin(\frac{n\pi}{2\lambda})\sin(\frac{m\pi}{2\lambda})}}{\cosh(\frac{\theta}{2})} \\ 0 & 1 - i\frac{\sin(\frac{n\pi}{2\lambda})-\sin(\frac{m\pi}{2\lambda})}{\sinh(\theta)} & i\frac{\sqrt{\sin(\frac{n\pi}{2\lambda})\sin(\frac{m\pi}{2\lambda})}}{\sinh(\frac{\theta}{2})} & 0 \\ 0 & i\frac{\sqrt{\sin(\frac{n\pi}{2\lambda})\sin(\frac{m\pi}{2\lambda})}}{\sinh(\frac{\theta}{2})} & 1 + i\frac{\sin(\frac{n\pi}{2\lambda})-\sin(\frac{m\pi}{2\lambda})}{\sinh(\theta)} & 0 \\ \frac{\sqrt{\sin(\frac{n\pi}{2\lambda})\sin(\frac{m\pi}{2\lambda})}}{\cosh(\frac{\theta}{2})} & 0 & 0 & -1 + i\frac{\sin(\frac{n\pi}{2\lambda})+\sin(\frac{m\pi}{2\lambda})}{\sinh(\theta)} \end{pmatrix} \tag{A.4.5}$$

and

$$G^{(n,m)}(\theta) = \frac{g(\frac{n+m}{4\lambda})g(\frac{1}{2} - \frac{n-m}{4\lambda})}{g(\frac{1}{2})} , \tag{A.4.6}$$

$$g(\Delta) = \frac{\sinh(\frac{\theta}{2})}{\sinh(\frac{\theta}{2}) + i\sin(\Delta\pi)} \exp\left\{ \int_0^\infty \frac{\mathrm{d}t}{t} \frac{\sinh(\Delta t)\sinh((1-\Delta)t)}{\cosh^2(\frac{t}{2})\cosh(t)} \sinh\left(\frac{it\theta}{\pi}\right) \right\} . \tag{A.4.7}$$

A.5 SSG reflection factors

The sine–Gordon reflection factor for the nth breather is ([Gho94])

$$R_{\mathrm{SG}}^{(n)}(\theta) = R_0^{(n)}(\theta) R_1^{(n)}(\theta)\,, \tag{A.5.1}$$

where

$$R_0^{(n)}(\theta) = (-1)^{n+1} \frac{\cos(\frac{\theta}{2i} + \frac{n\pi}{4\lambda}) \cos(\frac{\theta}{2i} - \frac{\pi}{4} - \frac{n\pi}{4\lambda}) \sin(\frac{\theta}{2i} + \frac{\pi}{4})}{\cos(\frac{\theta}{2i} - \frac{n\pi}{4\lambda}) \cos(\frac{\theta}{2i} + \frac{\pi}{4} + \frac{n\pi}{4\lambda}) \sin(\frac{\theta}{2i} - \frac{\pi}{4})} \times \prod_{l=1}^{n-1} \frac{\sin(\frac{\theta}{i} + \frac{l\pi}{2\lambda}) \cos^2(\frac{\theta}{2i} - \frac{\pi}{4} - \frac{l\pi}{4\lambda})}{\sin(\frac{\theta}{i} - \frac{l\pi}{2\lambda}) \cos^2(\frac{\theta}{2i} + \frac{\pi}{4} + \frac{l\pi}{4\lambda})}\,. \tag{A.5.2}$$

$R_1^{(n)}(\theta)$, which contains the boundary parameters η and ϑ is different depending on whether n is even or odd:

$$R_1^{(2n)}(\theta) = S^{(2n)}(\eta, \theta) S^{(2n)}(i\vartheta, \theta)\,, \tag{A.5.3}$$

where

$$S^{(2n)}(x, \theta) = \prod_{l=1}^{n} \frac{\sin(\frac{\theta}{i}) - \cos(\frac{x}{\lambda} - (l - \frac{1}{2})\frac{\pi}{\lambda})}{\sin(\frac{\theta}{i}) + \cos(\frac{x}{\lambda} - (l - \frac{1}{2})\frac{\pi}{\lambda})} \frac{\sin(\frac{\theta}{i}) - \cos(\frac{x}{\lambda} + (l - \frac{1}{2})\frac{\pi}{\lambda})}{\sin(\frac{\theta}{i}) + \cos(\frac{x}{\lambda} + (l - \frac{1}{2})\frac{\pi}{\lambda})} \tag{A.5.4}$$

and

$$R_1^{(2n-1)}(\theta) = S^{(2n-1)}(\eta, \theta) S^{(2n-1)}(i\vartheta, \theta) \tag{A.5.5}$$

with

$$S^{(2n-1)}(x, \theta) = \frac{\cos(\frac{x}{\lambda}) - \sin(\frac{\theta}{i})}{\cos(\frac{x}{\lambda}) + \sin(\frac{\theta}{i})} \prod_{l=1}^{n-1} \frac{\sin(\frac{\theta}{i}) - \cos(\frac{x}{\lambda} - \frac{l\pi}{\lambda})}{\sin(\frac{\theta}{i}) + \cos(\frac{x}{\lambda} - \frac{l\pi}{\lambda})} \frac{\sin(\frac{\theta}{i}) - \cos(\frac{x}{\lambda} + \frac{l\pi}{\lambda})}{\sin(\frac{\theta}{i}) + \cos(\frac{x}{\lambda} + \frac{l\pi}{\lambda})}\,. \tag{A.5.6}$$

In the supersymmetric sine–Gordon model the reflection factors are of the form ([Nep01a, BPT02])

$$R_{\mathrm{SSG}}^{(n)}(\theta) = R_{\mathrm{SG}}^{(n)}(\theta) \otimes R_{\mathrm{SUSY}}(\theta)\,. \tag{A.5.7}$$

In the so-called $BSSG^+$ case, in which the fermion parity is conserved during the reflection

$$R_{\mathrm{SUSY}}(\theta) = \begin{pmatrix} \mathcal{A}_+ & 0 \\ 0 & \mathcal{A}_- \end{pmatrix} \tag{A.5.8}$$

with

$$\mathcal{A}_\pm(\theta) = P\Big(\theta + i\frac{\rho}{2}\Big) P\Big(\theta - i\frac{\rho}{2}\Big) \sqrt{2} K(2\theta) 2^{-\frac{\theta}{i\pi}} \cos\Big(\frac{\theta}{2i} \mp \frac{\pi}{4}\Big)\,, \tag{A.5.9}$$

where for the kth breather $\rho_k = \pi - k\frac{\pi}{\lambda}$. The functions $K(\theta)$, $P(\theta)$ are defined as

$$K(\theta) = \frac{1}{\sqrt{\pi}} \prod_{k=1}^{\infty} \frac{\Gamma(k - \frac{1}{2} + \frac{\theta}{2\pi i})\Gamma(k - \frac{\theta}{2\pi i})}{\Gamma(k + \frac{1}{2} - \frac{\theta}{2\pi i})\Gamma(k + \frac{\theta}{2\pi i})}\,, \tag{A.5.10}$$

$$P(\theta) = \prod_{k=1}^{\infty} \frac{\Gamma^2(k - \frac{\theta}{2\pi i})}{\Gamma(k - \frac{1}{4} - \frac{\theta}{2\pi i})\Gamma(k + \frac{1}{4} - \frac{\theta}{2\pi i})} / \{\theta \to -\theta\}\,. \tag{A.5.11}$$

They have the following integral representations:

$$P(\theta) = \exp\left\{ -\frac{1}{8} \int_0^{\infty} \frac{\mathrm{d}t}{t} \frac{\sinh(\frac{\theta t}{2\pi i})}{\cosh^2(\frac{t}{8})\cosh^2(\frac{t}{4})} \right\}, \tag{A.5.12}$$

$$K(\theta) = \frac{1}{\sqrt{\cosh(\frac{\theta}{2})}} \exp\left\{ -\frac{1}{4} \int_0^{\infty} \frac{\mathrm{d}t}{t} \frac{\sinh(\frac{\theta t}{2\pi i})}{\cosh^2(\frac{t}{4})} \right\}. \tag{A.5.13}$$

Then $R_{\mathrm{SUSY}}(\theta)$ can be written as

$$R_{\mathrm{SUSY}}(\theta) = \frac{\sqrt{2}2^{-\frac{\theta}{i\pi}}}{\sqrt{\cosh(\theta)}} \exp\left\{ -\frac{1}{4} \int_0^{\infty} \frac{\mathrm{d}t}{t} \frac{\cosh(\frac{\rho t}{2\pi}) + \cosh^2(\frac{t}{2})}{\cosh^2(\frac{t}{4})\cosh^2(\frac{t}{2})} \sinh\left(\frac{\theta t}{i\pi}\right) \right\} \times \begin{pmatrix} \cos(\frac{\theta}{2i} - \frac{\pi}{4}) & 0 \\ 0 & \cos(\frac{\theta}{2i} + \frac{\pi}{4}) \end{pmatrix}. \tag{A.5.14}$$

A.6 Bootstrap axioms

The analytic S-matrix in an integrable theory has to satisfy the following conditions [ZZ79]:

- Unitarity
$$S_{a_1 a_2}^{c_1 c_2}(\theta) S_{c_1 c_2}^{b_1 b_2}(-\theta) = \delta_{a_1}^{b_1} \delta_{a_2}^{b_2}\,, \tag{A.6.1}$$
- Crossing symmetry
$$S_{a_1 a_2}^{b_1 b_2}(\theta) = S_{a_2 \bar{b}_1}^{b_2 \bar{a}_1}(i\pi - \theta)\,, \tag{A.6.2}$$
- Yang–Baxter equation (factorisation)
$$S_{a_1 a_2}^{c_1 c_2}(\theta) S_{c_1 a_3}^{b_1 c_3}(\theta + \theta') S_{c_2 c_3}^{b_2 b_3}(\theta') = S_{a_2 a_3}^{c_2 c_3}(\theta) S_{a_1 c_3}^{c_1 b_3}(\theta + \theta') S_{c 1 2 c_1}^{b_1 b_2}(\theta')\,. \tag{A.6.3}$$

The reflection matrix or R-matrix must satisfy the following constraints [GZ94]:

- Boundary unitarity
$$R_a^c(\theta) R_c^b(-\theta) = \delta_a^b\,, \tag{A.6.4}$$

- Boundary crossing

$$R^{b}_{\bar{a}}(\frac{i\pi}{2}-\theta) = S^{ab}_{a'b'}(2\theta)R^{a'}_{\bar{b}'}(\frac{i\pi}{2}+\theta)\,, \tag{A.6.5}$$

- Boundary Yang–Baxter equation

$$\begin{aligned} &R^{c_2}_{a_2}(\theta_2)S^{c_1d_2}_{a_1c_2}(\theta_1+\theta_2)R^{d_1}_{c_1}(\theta_1)S^{b_2b_1}_{d_2d_1}(\theta_1-\theta_2) \\ &\qquad = S^{c_1c_2}_{a_1a_2}(\theta_1-\theta_2)R^{d_1}_{c_1}(\theta_1)S^{d_2b_1}_{c_2d_1}(\theta_1+\theta_2)R^{b_2}_{d_2}(\theta_2)\,. \end{aligned} \tag{A.6.6}$$

Bibliography

[Aff95] I. Affleck, *Conformal Field Theory Approach to the Kondo Effect*, Acta Phys. Polon. **B26**, 1869–1932 (1995), cond-mat/9512099.

[Ahn91] C.-r. Ahn, *Complete S matrices of supersymmetric Sine-Gordon theory and perturbed superconformal minimal model*, Nucl. Phys. **B354**, 57–84 (1991).

[Ahn94] C.-r. Ahn, *Thermodynamics and form-factors of supersymmetric integrable field theories*, Nucl. Phys. **B422**, 449–475 (1994), hep-th/9306146.

[AL91] I. Affleck and A. W. W. Ludwig, *Universal noninteger 'ground state degeneracy' in critical quantum systems*, Phys. Rev. Lett. **67**, 161–164 (1991).

[AN01] C.-r. Ahn and R. I. Nepomechie, *The scaling supersymmetric Yang-Lee model with boundary*, Nucl. Phys. **B594**, 660–684 (2001), hep-th/0009250.

[ANS06] C. Ahn, R. I. Nepomechie and J. Suzuki, *Finite size effects in the spin-1 XXZ and supersymmetric sine-Gordon models with Dirichlet boundary conditions*, (2006), hep-th/0611136.

[AR99] C.-r. Ahn and C. Rim, *Boundary flows in the general coset theories*, J. Phys. **A32**, 2509–2525 (1999), hep-th/9805101.

[AS02] C. Angelantonj and A. Sagnotti, *Open strings*, Phys. Rept. **371**, 1–150 (2002), hep-th/0204089.

[BDP+04] Z. Bajnok, C. Dunning, L. Palla, G. Takacs and F. Wagner, *SUSY sine-Gordon theory as a perturbed conformal field theory and finite size effects*, Nucl. Phys. **B679**, 521–544 (2004), hep-th/0309120.

[BG06] Z. Bajnok and A. George, *From defects to boundaries*, Int. J. Mod. Phys. **A21**, 1063–1078 (2006), hep-th/0404199.

[BK03] P. Baseilhac and K. Koizumi, *$N = 2$ boundary supersymmetry in integrable models and perturbed boundary conformal field theory*, Nucl. Phys. **B669**, 417–434 (2003), hep-th/0304120.

[BPPZ00] R. E. Behrend, P. A. Pearce, V. B. Petkova and J.-B. Zuber, *Boundary conditions in rational conformal field theories*, Nucl. Phys. **B570**, 525–589 (2000), hep-th/9908036.

[BPT02] Z. Bajnok, L. Palla and G. Takacs, *Spectrum of boundary states in $N = 1$ SUSY sine-Gordon theory*, Nucl. Phys. **B644**, 509–532 (2002), hep-th/0207099.

[BPTT02] Z. Bajnok, L. Palla, G. Takacs and G. Z. Toth, *The spectrum of boundary states in sine-Gordon model with integrable boundary conditions*, Nucl. Phys. **B622**, 548–564 (2002), hep-th/0106070.

[Car84] J. L. Cardy, *Conformal Invariance and Surface Critical Behavior*, Nucl. Phys. **B240**, 514–532 (1984).

[Car89] J. L. Cardy, *Boundary Conditions, Fusion Rules and the Verlinde Formula*, Nucl. Phys. **B324**, 581 (1989).

[CL91] J. L. Cardy and D. C. Lewellen, *Bulk and boundary operators in conformal field theory*, Phys. Lett. **B259**, 274–278 (1991).

[CSS02] J. S. Caux, H. Saleur and F. Siano, *The Josephson current in Luttinger liquid-superconductor junctions*, Phys. Rev. Lett. **88**, 106402 (2002), cond-mat/0109103.

[CSS03] J. S. Caux, H. Saleur and F. Siano, *The two-boundary sine-Gordon model*, Nucl. Phys. **B672**, 411–461 (2003), cond-mat/0306328.

[CT78] S. R. Coleman and H. J. Thun, *On the prosaic origin of the double poles in the sine–Gordon S matrix*, Commun. Math. Phys. **61**, 31 (1978).

[DFRT04] P. Dorey, D. Fioravanti, C. Rim and R. Tateo, *Integrable quantum field theory with boundaries: The exact g-function*, Nucl. Phys. **B696**, 445–467 (2004), hep-th/0404014.

[DPTW98] P. Dorey, A. Pocklington, R. Tateo and G. Watts, *TBA and TCSA with boundaries and excited states*, Nucl. Phys. **B525**, 641–663 (1998), hep-th/9712197.

[DRTW00] P. Dorey, I. Runkel, R. Tateo and G. Watts, *g-function flow in perturbed boundary conformal field theories*, Nucl. Phys. **B578**, 85–122 (2000), hep-th/9909216.

[DTW99] P. Dorey, R. Tateo and G. Watts, *Generalisations of the Coleman-Thun mechanism and boundary reflection factors*, Phys. Lett. **B448**, 249–256 (1999), hep-th/9810098.

[FGP+06] G. Feverati, K. Graham, P. A. Pearce, G. Z. Toth and G. Watts, *A renormalisation group for TCSA*, (2006), hep-th/0612203.

[FK04] D. Friedan and A. Konechny, *On the boundary entropy of one-dimensional quantum systems at low temperature*, Phys. Rev. Lett. **93**, 030402 (2004), hep-th/0312197.

[FLS96] P. Fendley, F. Lesage and H. Saleur, *A unified framework for the Kondo problem and for an impurity in a Luttinger liquid*, J. Statist. Phys. **85**, 211 (1996), cond-mat/9510055.

[FPR03] G. Feverati, P. A. Pearce and F. Ravanini, *Exact phi(1,3) boundary flows in the tricritical Ising model*, Nucl. Phys. **B675**, 469–515 (2003), hep-th/0308075.

[Fre03] S. Fredenhagen, *Organizing boundary RG flows*, Nucl. Phys. **B660**, 436–472 (2003), hep-th/0301229.

[Gho94] S. Ghoshal, *Bound state boundary S matrix of the Sine-Gordon model*, Int. J. Mod. Phys. **A9**, 4801–4810 (1994), hep-th/9310188.

[GKO86] P. Goddard, A. Kent and D. I. Olive, *Unitary Representations of the Virasoro and Supervirasoro Algebras*, Commun. Math. Phys. **103**, 105–119 (1986).

[GRW00] K. Graham, I. Runkel and G. M. T. Watts, *Renormalisation group flows of boundary theories*, (2000), hep-th/0010082.

[GRW01] K. Graham, I. Runkel and G. M. T. Watts, *Minimal model boundary flows and c = 1 CFT*, Nucl. Phys. **B608**, 527–556 (2001), hep-th/0101187.

[GW04] K. Graham and G. M. T. Watts, *Defect lines and boundary flows*, JHEP **04**, 019 (2004), hep-th/0306167.

[GZ94] S. Ghoshal and A. B. Zamolodchikov, *Boundary S matrix and boundary state in two-dimensional integrable quantum field theory*, Int. J. Mod. Phys. **A9**, 3841–3886 (1994), hep-th/9306002.

[HKM00] J. A. Harvey, D. Kutasov and E. J. Martinec, *On the relevance of tachyons*, (2000), hep-th/0003101.

[Kor06] M. Kormos, *Boundary renormalisation group flows of unitary superconformal minimal models*, Nucl. Phys. **B744**, 358–379 (2006), hep-th/0512085.

[Kor07] M. Kormos, *Boundary renormalisation group flows of the supersymmetric Lee-Yang model and its extensions*, Nucl. Phys. **B772/3**, 227–248 (2007), hep-th/0701061.

[KTW97] H. Kausch, G. Takacs and G. Watts, *On the relation between Phi(1,2) and Phi(1,5) perturbed minimal models and unitarity*, Nucl. Phys. **B489**, 557–579 (1997), hep-th/9605104.

[LMSS95] A. LeClair, G. Mussardo, H. Saleur and S. Skorik, *Boundary energy and boundary states in integrable quantum field theories*, Nucl. Phys. **B453**, 581–618 (1995), hep-th/9503227.

[LSS98] F. Lesage, H. Saleur and P. Simonetti, *Boundary flows in minimal models*, Phys. Lett. **B427**, 85–92 (1998), hep-th/9802061.

[Mat90] P. Mathieu, *Integrability of perturbed superconformal minimal models*, Nucl. Phys. **B336**, 338 (1990).

[MS96] M. Moriconi and K. Schoutens, *Thermodynamic Bethe Ansatz for N = 1 Supersymmetric Theories*, Nucl. Phys. **B464**, 472–491 (1996), hep-th/9511008.

[NA02] R. I. Nepomechie and C. Ahn, *TBA boundary flows in the tricritical Ising field theory*, Nucl. Phys. **B647**, 433–470 (2002), hep-th/0207012.

[Nep01a] R. I. Nepomechie, *The boundary supersymmetric sine-Gordon model revisited*, Phys. Lett. **B509**, 183–188 (2001), hep-th/0103029.

[Nep01b] R. I. Nepomechie, *Consistent superconformal boundary states*, J. Phys. **A34**, 6509–6524 (2001), hep-th/0102010.

[RP02] C. Richard and P. A. Pearce, *Integrable lattice realizations of N = 1 superconformal boundary conditions*, Nucl. Phys. **B631**, 447–470 (2002), hep-th/0109083.

[RRS00] A. Recknagel, D. Roggenkamp and V. Schomerus, *On relevant boundary perturbations of unitary minimal models*, Nucl. Phys. **B588**, 552–564 (2000), hep-th/0003110.

[Sal98] H. Saleur, *Lectures on non perturbative field theory and quantum impurity problems*, (1998), cond-mat/9812110.

[Sal00] H. Saleur, *Lectures on non perturbative field theory and quantum impurity problems. II*, (2000), cond-mat/0007309.

[Sch97] K. Schoutens, *Exclusion statistics in conformal field theory spectra*, Phys. Rev. Lett. **79**, 2608–2611 (1997), cond-mat/9706166.

[Smi90] F. A. Smirnov, *Reductions of the sine-Gordon model as a perturbation of minimal models of conformal field theory*, Nucl. Phys. **B337**, 156–180 (1990).

[Tot04] G. Z. Toth, *$N = 1$ supersymmetric boundary bootstrap*, Nucl. Phys. **B676**, 497–536 (2004), hep-th/0308146.

[Tot06] G. Z. Toth, *A study of truncation effects in boundary flows of the Ising model on a strip*, (2006), hep-th/0612256.

[Ver88] E. P. Verlinde, *Fusion Rules and Modular Transformations in 2D Conformal Field Theory*, Nucl. Phys. **B300**, 360 (1988).

[YZ90] V. P. Yurov and A. B. Zamolodchikov, *Truncated conformal space approach to scaling Lee–Yang model*, Int. J. Mod. Phys. **A5**, 3221–3246 (1990).

[Zam87] A. B. Zamolodchikov, *Renormalization Group and Perturbation Theory Near Fixed Points in Two-Dimensional Field Theory*, Sov. J. Nucl. Phys. **46**, 1090 (1987).

[ZZ79] A. B. Zamolodchikov and A. B. Zamolodchikov, *Factorized S-matrices in two dimensions as the exact solutions of certain relativistic quantum field models*, Annals Phys. **120**, 253–291 (1979).